SIMULATIONS AND FEEDBACK CONTROL OF NON LINEAR COUPLED ELECTROMECHANICAL OSCILLATORS FOR ENERGY CONVERSION APPLICATIONS

By

Dimitrios Psarrou

A Thesis Submitted to the Faculty of

The College of Engineering and Computer Science

in Partial Fulfillment of the Requirements for the Degree of

Master of Science

Florida Atlantic University

Boca Raton, Florida

August 2011

SIMULATIONS AND FEEDBACK CONTROL OF NON LINEAR COUPLED ELECTROMECHANICAL OSCILLATORS FOR ENERGY CONVERSION APPLICATIONS

By
Dimitrios Psarrou

This thesis was prepared under the direction of the candidate's thesis advisors, Dr. Manhar Dhanak, Department of Ocean and Mechanical Engineering and Dr. Nikolaos Xiros, Virginia Tech, and has been approved by the members of his supervisory committee. It was submitted to the faculty of the College of Engineering and Computer Science and was accepted in partial fulfillment of the requirements for the degree of Master of Science.

SUPERVISORY COMMITTEE:

Manhar Dhanak, Ph.D.
Thesis Co-Advisor

Nikolaos Xiros, Ph.D.
Thesis Co-Advisor

Pierre-Philippe Beaujean, Ph.D.

James VanZwieten, Ph.D.

Javad Hashemi, Ph.D.
Chair, Department of Ocean and Mechanical Engineering

Mohammad Ilyas, Ph.D
Interim Dean, College of Engineering and Computer Science

Barry T. Rosson, Ph.D.
Dean, Graduate College

July 22, 2011
Date

ACKNOWLEDGEMENTS

I wish to express my heartfelt thanks to all the people that supported me during the composition of this work. I have learned so many new and exciting things, and for that reason I would like to especially thank Dr Nikolaos Xiros and Dr Manhar Dhanak for being my advisors, guiding and giving me the chance to work on this project. Special thanks to my family for supporting me in pursuing this Masters degree far away from my home country, to all my friends back in Greece who would constantly cheer me up, to Nicolas Gantiva, Armando Sinistera, Nicolas Kouvaras and Georgios Lilas for being great friends and roommates, and to this specific person that I made sad when I decided to pursue my dreams in a foreign country. Lastly I would like to thank Dr, Pierre-Philippe Beaujean for showing me that wonderful mathematics is behind wonderful music.

ABSTRACT

Author: Dimitrios Psarrou

Title: Simulations and feedback control of non linear coupled electromechanical oscillators for energy conversion applications

Institution: Florida Atlantic University

Thesis Advisors: Dr. Nikolaos Xiros, Dr. Manhar Dhanak

Degree: Master of Science

Year: 2011

This thesis discusses the coupling of a mechanical and electrical oscillator, an arrangement that is often encountered in mechatronics actuators and sensors. The dynamics of this coupled system is mathematically modeled and a low pass equivalent model is presented. Numerical simulations are then performed, for various input signals to characterize the nonlinear relationship between the electrical current and the displacement of the mass. Lastly a framework is proposed to estimate the mass position without the use of a position sensor, enabling the sensorless control of the coupled system and additionally providing the ability for the system to act as an actuator or a sensor. This is of value for health monitoring, diagnostics and prognostics, actuation and power transfer of a number of interconnected machines that have more than one electrical system, driving corresponding mechanical subsystems while being driven by the same voltage source and at the same time being spectrally separated and independent.

SIMULATIONS AND FEEDBACK CONTROL OF NON LINEAR COUPLED ELECTROMECHANICAL OSCILLATORS FOR ENERGY CONVERSION APPLICATIONS

LIST OF TABLES

TABLE OF FIGURES

1. INTRODUCTION

1.1 Overview

The aim of this section is to provide a brief introduction to the subject of this thesis, modeling and analysis of coupled electromechanical systems. Common applications and uses of such systems will be discussed and the case studied in this document will be presented.

1.2 Electromechanical System Analysis

The developments in the fields of mechatronics and micro-electromechanical systems (MEMS)/ nano-electromechanical systems (NEMS) as well as in telecommunications have made electromechanical system analysis gain significant attention. This is due to the need for integrated devices that will be used as tiny actuators or sensors to control and monitor other systems and processes such as ships, cars, aircrafts and power plants. Such devices in a typical scenario can be small mechanical systems like a resonator, that is coupled and driven by analog electronics, amplifiers, voltage sources and more that are in turn controlled by a digital signal processing (DSP) system or a FPGA field programmable gate array[1].

1.3 Case studied

A typical small scale arrangement often encountered in mechatronics actuators or sensors is a second order mass-spring-damper system coupled to a resistor-inductor-capacitor electrical circuit. The voltage source is the source that makes the mechanical system to oscillate and serves as the information signal that drives the mass to the desired position. As it can be seen in figure 1.1, the inductor's inductance L is a function of the mass position making the subsystems coupled and at the same time nonlinear by introducing a nonlinear magnetic force to the mass-spring-damper system. In addition, the motion of the mass changes the value of the inductance making it possible to establish a feedback path that with appropriate control will increase the system performance and stability even when random outer forces and disturbances act on the system[2]. The analysis of such systems is of great interest mostly due to the nonlinear terms that appear with the coupling of the subsystems. Advanced mathematical tools are required to proceed with analyzing the dynamics and the behavior of the system, such as Volterra series theory, Hilbert transform, perturbation theory, and more.

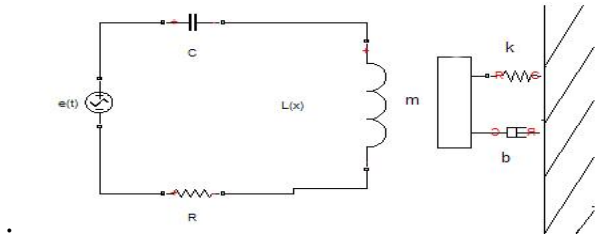

Figure 1.1 Electromechanical System

1.4 Applications and uses of electromechanical systems

1.4.1 Energy conversion

The electromechanical system considered in this thesis is in many aspects the fundamental setup for any electromechanical conversion device. Indeed, there is a magnetic circuit through which magnetic flux is applied to the rotor by the stator (the RLC circuit with the voltage source). The rotor includes inertial load (payload mass), velocity-dependent friction and position-dependent restoring force while the effect of exogenous excitation (in form of a disturbance force is also considered).

In this respect, this “bare-bones” version of an electromechanical energy conversion system is a fundamental testing platform of control strategies and algorithms applicable to both rotary and rectilinear electric machinery running in both motor or generator (including brake and regeneration) mode. The fundamental difference from the approaches encountered in literature is the addition of a capacitance in series with the resistance and the inductance of the electromagnet. This makes the stator circuit band-pass instead of low-pass. In effect, for energy transfer to take place between the voltage source and the stator circuit, source’s voltage needs to be amplitude modulated at a carrier frequency equal or in the vicinity of the resonance frequency of the stator circuit. Furthermore, the interaction between the stator and the rotor becomes non-trivially nonlinear and in effect the introduction of tools like the Hilbert Transform and Nonlinear System Theory becomes necessary.

This investigation was carried out in the framework and with the invaluable support of the Southeast National Marine Renewable Energy Center at Florida Atlantic

University (SNMREC @ FAU). They are in train of developing systems and concepts to harvest hydrokinetic energy and convert it to electric power through arrangements of underwater turbines and directly coupled generators. Research in the field of electromechanical energy conversion becomes a core field in this effort. The work done, even if the machines to be used by SNMREC are rotary, reveals the fundamental interactions between the electrical and mechanical parts of machinery and provide with a framework to have more than one electrical systems, driving corresponding mechanical subsystems, driven by the same voltage source and at the same time be spectrally separated and therefore independent. This can be of value for sensing (and in effect health monitoring, diagnostics and prognostics), actuation and power transfer of a number of interconnected machines.

Additionally in many processes that involve environmental monitoring, there is need for self-powered systems. This power can be produced by conventional electrochemical batteries, or by scavenging energy from ambient sources such as heat, light, acoustic noise and vibrations [10].

1.4.2 Acoustic Vibrations

Acoustic vibrations are very interesting because they appear at very low frequencies (ranging from about 1 to 10 Hz) that are very close to a “normal” mechanical system’s resonance frequency. By vibrating the mass of the mechanical subsystem, a change in the inductance of the electrical system is induced, converting in that way the mechanical energy to electrical.

1.4.3 Actuators and force sensors

This mutual “communication” of the electrical and mechanical subsystem enables the overall system to also operate as an actuator, by appropriately modifying the voltage source signal to move the mass to the desired position, or as a sensor, where the position of the mass can be identified by the change in the inductance that eventually will lead to a change in the circuit’s current. Therefore from this relationship the force applied to the mechanical system can be identified, making the overall system act as a force sensor.

1.4.4 Vibration Damping

A problem appearing in many applications in the engineering field is the vibration damping of mechanical structures [12]. A classic solution to this problem is the coupling of an electrical circuit to the mechanical structure. By effectively controlling the magnetic force generated by a typical RLC system, one can provide vibration damping in a more customizable, efficient and up to date manner.

1.4.5 Vortex Induced Vibrations

Vortex induced vibrations are the vibrations induced on an object, produced by the periodical irregularities of the flow the object is facing. A typical example is when we position a cylindrical object into sea (or regular) water, and move it in a perpendicular to its axis direction. A layer of water known as boundary layer will be formed at the surface of the object because of the water’s viscosity by which the flow will be slowed down when it contacts the surface. This layer can separate from the body mostly because of its curvature, allowing the formulation of vortices that will change the pressure distribution along the surface. In effect different lifting forces will appear and act on the object that

will make it move in a traversal to the flow way motion. This phenomenon is very common to offshore structures, bridges and marine cables. In that way one can transform the mechanical energy produced by those vibrations to electrical energy using the electromechanical system presented in this text.

1.5 Problem Statement

The second order electrical oscillator is a band pass system; that is the system's resonance frequency maintains high values. A second order mass spring damper system's resonance frequency is defined by the mass of the object and the constant of the spring, usually exhibiting low values making the system low pass. When someone attempts to model and simulate the dynamics of the coupling of the two systems using computer aided design software, the sampling frequency (or time step) needs to be set to at least twice the value of the higher present frequency, the frequency of the electrical circuit. In this thesis a low pass equivalent model of the band pass coupled system is presented where the signals will retain full information while the resonance frequency of the equivalent system will be brought down to around the mechanical subsystem's resonance frequency. This will effectively speed up simulation times and provide an additional method for analyzing the dynamics of the two subsystems. Moreover, lower sampling rates make better use of the limited bandwidth integrated devices have allowing for faster responses.

The low pass equivalent model will be validated against the band pass model and a framework will be proposed to estimate the mass position without the use of a position sensor, enabling the sensorless control of the coupled system and additionally providing the ability to act as an actuator or a sensor.

1.6 Thesis Outline

The first step to implement the solution is to accurately model the dynamics of the electromechanical system using the simulation software Matlab Simulink. A band pass and a low pass equivalent simulation model will be created and then compared with each other for validation. Chapter 2 focuses in a literature review presenting basic knowledge needed for the reader to follow this text. In Chapter 3 the mathematical models describing the dynamics of the coupled system will be formed. In addition the various parameters that characterize the system, such as the natural frequencies for each sub system will be defined. Chapter 4 focuses in the formulation of the Simulink models for the band pass and the low pass equivalent system respectively. After the models are validated and compared with each other they are tested for different input signals and frequencies and their behavior is recorded and studied in chapter 5. The nonlinear relationships connecting the displacement of the mass with the changes in amplitude of the current, the voltage signal and the exogenous disturbance force are investigated. Finally in Chapter 6, a framework will be presented to obtain an estimation of the position of the mass without using any position or additional sensor other than a simple ammeter to measure the current through the resistor in the electrical circuit.

2. LITERATURE REVIEW

2.1 Overview

To better aid the reader in understanding the concept of analysis of the dynamics of electromechanical systems, this section will provide important definitions and some background information about the dynamics of mechanical and electrical systems.

2.2 Signals

In the electrical engineering field a signal can be any function that is time varying, meaning that it contains time as an independent variable, or space-varying. A typical example of a signal is the position of a moving mass on a mass-spring-damper system, or its velocity [5]. A distributed signal is the signal that contains more than one independent variable. Signals can be divided into two categories, analog and digital signals. An analog signal is a continuous signal that is defined for all time in an interval (that is an infinite interval). Temperature is such a continuous signal. A digital signal is a discrete signal where its quantities are described on a discrete set of time and most of the time is quantized, with its values being restricted to a finite set. Typical example of a discrete and quantized signal is the input of a digital signal processing system (DSP) where the analog signal is sampled over a finite time interval using an analog to digital converter (ADC) and then fed to the DSP system for further processing.

2.3 LTI and Non-Linear TI systems

An electric network, a marine engine, or a turbine constitutes a system. Therefore a system can be defined as any confined space that if disturbed by an input signal, will produce an output signal often called response. Systems can be divided into various categories, but on this document I will present only 2 district categories: Linear (LTI) and Non-linear (Non-Linear TI) Time Invariant systems. Time Invariant systems are the systems in which time is an independent variable. A Linear Time-Invariant system is described by differential equations that have constant coefficients and satisfy the superposition principle, where any linear combination of independent solutions of the differential equation constitutes a solution to the equation. A non linear system on the other hand, does not satisfy this principle, or less technically we could say that its output is **not** directly proportional to its input. A typical second order mass-spring-dumper or a Resistor-Inductor-Capacitor system constitutes a LTI system. However the coupling of these two LTI systems constitutes a Non-Linear system as it is going to be presented later.

2.4 Dynamic analysis

2.4.1 Mechanical system

The transfer function of an LTI system represents the relation of its input and its output after applying the Laplace transform assuming zero initial conditions. For example consider the following mass-spring-damper system described by the second order differential equation:

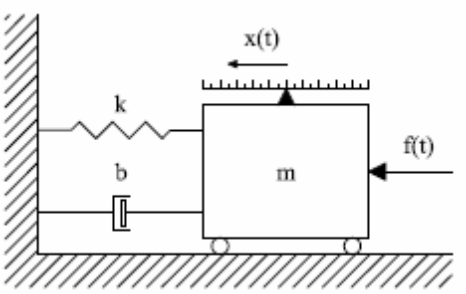

Figure 2.1 A typical mass-spring-damper system [3]

$$m\ddot{x} + b\dot{x} + kx = f(t) \quad (2.1)$$

Where:

m: represents the mass of the object.

b: is the damping coefficient.

k: is the spring constant.

f(t) is the excitation force.

After applying the Laplace Transform assuming zero initial conditions the equation becomes:

$$ms^2X(s) + bsX(s) + kX(s) = F(s) \Leftrightarrow (ms^2 + bs + k)X(s) = F(s) \quad (2.2)$$

Dividing by F(s) we get:

$$H(s) = \frac{X(s)}{F(s)} = \frac{1}{ms^2 + bs + k} \quad (2.3)$$

Where:

H(s): is the transfer function of the system.

($ms^2 + bs + k$): the characteristic polynomial.

2.4.2 Impulse Response

The impulse response of a system is the response produced when excited by a brief or sudden input signal, more specifically a Dirac delta function.

$$\int_{-\infty}^{\infty} \delta(t)dt = 1,\ \delta(t) = \begin{cases} 0, t \neq 0 \\ undefined, t = 0 \end{cases} \quad (2.4)$$

The impulse response of the above system for some random value of m, b, k, is presented in figure 2.2.

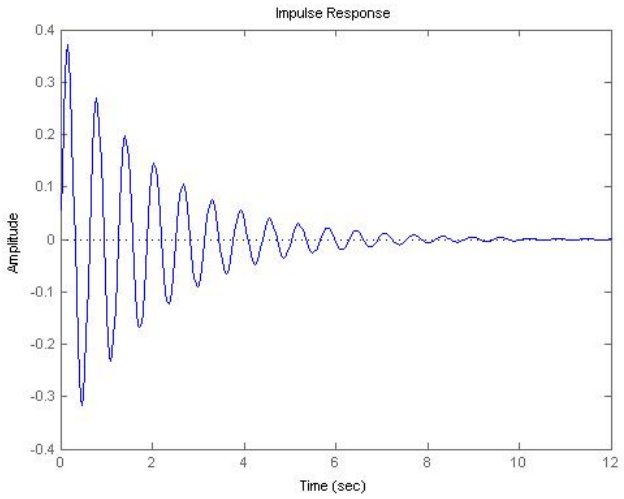

Figure 2.2 Impulse response of the mechanical system

By applying the inverse Laplace transform to the transfer function, we can obtain the impulse response of the system.

$$h(t) = L^{-1}\{H(s)\} \Leftrightarrow h(t) = L^{-1}\left\{\frac{1}{ms^2 + bs + k}\right\} \quad (2.5)$$

By finding the two roots s_1, s_2 of the characteristic polynomial and doing partial fraction expansion, we obtain:

$$h(t) = \frac{1}{s_1 - s_2}(e^{s_1 t} - e^{s_2 t}) \quad (2.6)$$

The convolution of the impulse response of the system with the excitation force f(t) gives the actual response of the system. Indeed:

$$x(t) = h(t) * f(t) \quad (2.7)$$

2.4.3 Step Response

An alternative way to study the behavior of the system avoiding some problems that arise with the implementation of a Dirac delta signal, a unit step signal, also known as Heaviside Step Function signal is used as an input, and the output of the system is then called step response.

$$u_{step}(t) = \begin{cases} 1, t > 0 \\ 0, t \le 0 \end{cases} \quad (2.8)$$

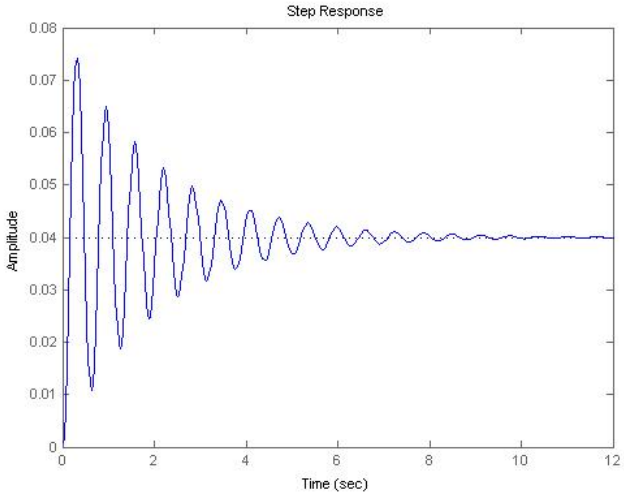

Figure 2.3 Step response of the mechanical system

The natural (resonance) frequency of the above system is given by

$$\omega_m = \sqrt{\frac{k}{m}} \quad (2.9)$$

2.4.4 Electrical System

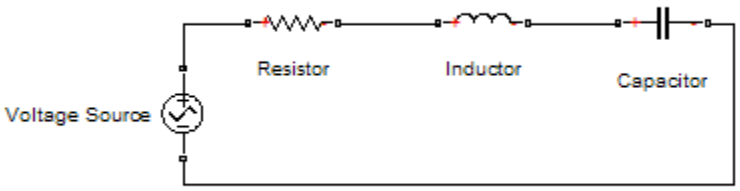

Figure 2.4 A typical RLC system

In the same respect as presented above, an electrical circuit that consists of a voltage source, a resistor, inductor and capacitor also known as RLC system, is described by the following differential equation:

$$e(t) = r\dot{q} + L\ddot{q} + \frac{q}{c} \quad (2.10)$$

Where:

r: is the resistor's resistance

L:is the inductor's inductance

c: is the capacitor's capacitance

q: is the electric charge

e(t):is the excitation voltage.

After applying the Laplace transform we obtain the following transfer function:

$$H(s) = \frac{Q(s)}{E(s)} = \frac{1}{Ls^2 + rs + \frac{1}{c}} \quad (2.11)$$

The natural frequency of the system is found by the following equation:

$$\omega_e = \sqrt{\frac{1}{Lc}} \quad (2.12)$$

2.4.5 System stability

Stability is a very important characteristic of a system and is the property that will define the need of control in order to stabilize an unstable system. Stability can be defined as the ability of a system to produce a bounded output when excited by a bounded input. In the following figure we can see the trajectories of two stable systems. The first system represented by the blue curve is asymptotically stable since its state vector's norm converges to zero, while the second system represented with the red curve is critically stable since its state vector's norm never decreases to zero. There exists a criterion that allows us to characterize a system as unstable by simple inspection. If the

coefficients of the characteristic polynomial are real and exhibit at least one sign change, then the system is guaranteed to be unstable, that is to obtain at least one root in the right-hand complex plane. In addition, if each and every one of the poles of the system (the roots of the characteristic polynomial) has a negative real part, then the system is guaranteed to be critically stable.

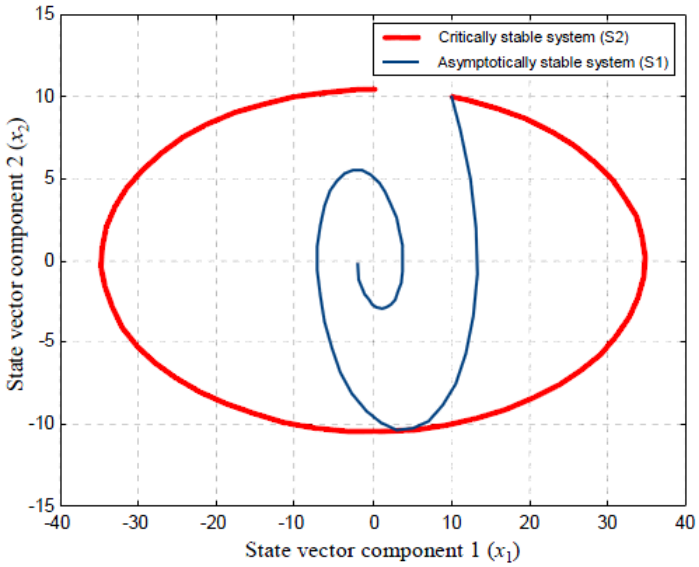

Figure 2.5 Stability graph [3]

2.4.6 Control of LTI systems

In order to bind the output of a system to a desirable value or to adjust the behavior of the system with respect to a reference signal, a control system (controller) is inserted to the process. As depicted in the following figure, a reference point r is set that when combined with the output of the process (feedback) will produce an error e. This error is then fed to the controller that will try to reduce it and appropriately process it in order to generate a control signal u that will compensate for the effect of the disturbance force d.

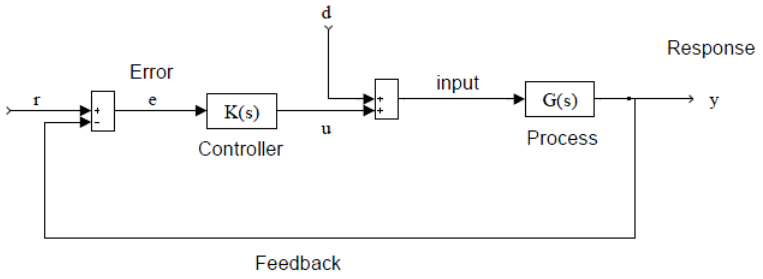

Figure 2.6 A typical control system [3]

Two widely used methods of control are the ON/OFF control and Proportional-Integral-Differential control (PID).

2.4.6.1 ON/OFF control

The ON/OFF control is one of the simplest methods used for control, often found in thermostats. The relationship that connects the error (input) to the control signal (output) also known as control law [3], is:

$$u = \begin{cases} A\,\mathrm{sgn}(e), |e| \geq Z_d \\ 0, |e| \geq Z_d \end{cases} \text{ or } u = \begin{cases} +A, e \geq +Z_d \\ 0, |e| < Z_d \\ -A, e \leq -Z_d \end{cases} \quad (2.13)$$

Where

Z: is a threshold value for which the control signal is activated.

2.4.6.2 PID control

The PID control method consists of a proportional gain part, an integral gain part and an differential gain part, and deals with control issues in a more improved manner than simple ON/OFF control. In time domain, the control law [3] of a PID controller is as follows:

$$u(t) = K_p e(t) + K_i \int_0^t e(\xi) d\xi + K_d \frac{d}{dt} e(t) \quad (2.14)$$

Where:

K_p: constant that refers to proportional gain

K_i: constant that refers to integral gain

K_d: constant that refers to differential gain.

When K_i and K_d constants are equal to zero, then the controller is only a proportional gain controller acting very similar to the ON/OFF control. However this type of controller shows a major drawback during steady state, in which the error cannot be made zero. For this reason the Proportional-Integral controller is used (with K_d constant equal to zero). The PI controllers are widely used for speed regulation of engines, turbines etc. There is also a drawback associated with this kind of controllers, as they exhibit high overshoot above the set point, as we can see on the following figure. To eliminate this problem the full form of the PID control relationship is used.

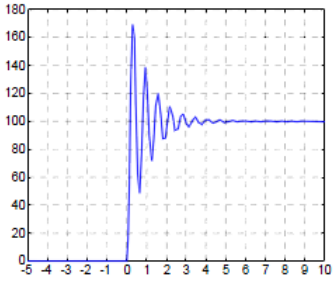

Figure 2.7 Overshoot problem of a PI controller [3]

3. MODELLING THE COUPLED SYSTEM DYNAMICS

3.1 Overview

This section will attempt to model the dynamics of the coupling of the electrical and mechanical system by appropriate handling of the governing equations describing each subsystem. The system equations will then be formulated in state-space form and the parameters that describe the system will be defined. Four criterions are established in order to define the system's parameters. according to the goal of this study.

3.2 Modeling the band pass system dynamics

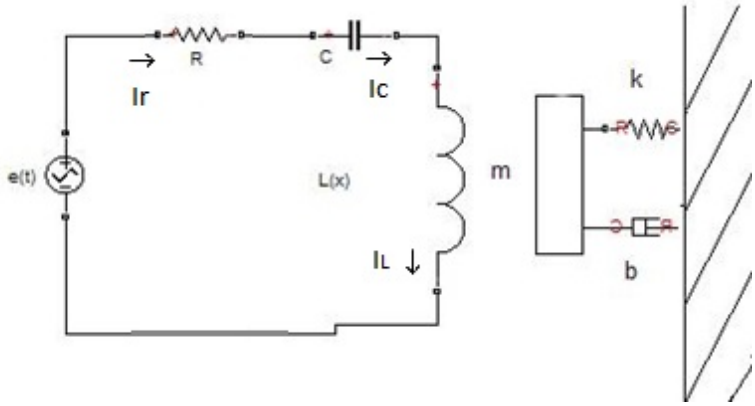

Figure 3.1 Coupled Electromechanical system

The coupled system consists of two second order oscillators, a RLC electrical circuit in series, and a mass-spring-damper mechanical system. By applying Kirchhoff's voltage

law in the electrical circuit and Newton's second law of motion, the governing equations for each subsystem are:

$$m\ddot{x} + b\dot{x} + kx = d(t) \quad (3.1)$$

for the mechanical subsystem where D is an exogenous disturbance force, and

$$e(t) = Ri_R + \frac{q}{c} + \frac{d}{dt}(Li_L) \quad (3.2)$$

for the electrical circuit where $\frac{d}{dt}(Li_L)$ is the magnetic flux through the inductor's coil and is often denoted as Ψ_M. However since the electric circuit is in series, it holds that

$$i = i_R = i_c = i_L = \dot{q} \quad (3.3)$$

The above equations describe the two subsystems when they are uncoupled. The interesting part of this study comes when coupling occurs, where two non linear terms appear in the governing equations. The inductance L of the inductor becomes depended on the displacement of the mass. One would expect the inductance to increase when the metallic mass moves closer to the inductor, and to decrease when the mass moves away. When the mass is far away enough, the inductance L would be characterized only by the coil of the inductor. Therefore if we define x=0 the position point where no force acts on the mechanical system (ie the only forces appearing are the weight of the mass that is negated by the force of the spring) then the inductance can be represented by the following relationship:

$$L(x) = L_0 + L_1 x \quad (3.4)$$

Where:

x: is the position of the mass, acquiring values from 0 to X_{max} being the point where the mass is contacting the inductor.

L_0: inductance constant that depends on the inductor's coil.

L_1: a constant defining the relationship of the mass to the inductance.

In the same respect, a non linear electromagnetic force produced by the inductor will appear to the mechanical subsystem's governing equation. By using standard electro mechanics analysis [2] it can be found that the electromagnetic force is equal to:

$$F_{em} = \frac{L_1}{2} i^2 \quad (3.5)$$

Therefore by substituting and rearranging the system of equations becomes:

$$m\ddot{x} + b\dot{x} + kx = \frac{L_1}{2} i^2 + d(t) \quad (3.6)$$

$$e(t) = (L_0 + L_1 x)\ddot{q} + (R + L_1 \dot{x})\dot{q} + \frac{q}{c} \quad (3.7)$$

Or in state space form:

$$\begin{bmatrix} x \\ \dot{x} \end{bmatrix} = \begin{bmatrix} 0 & 1 \\ -\frac{k}{m} & -\frac{b}{m} \end{bmatrix} \begin{bmatrix} x \\ \dot{x} \end{bmatrix} + \begin{bmatrix} 0 \\ \frac{L_1}{2m} \end{bmatrix} i^2 \quad (3.8)$$

$$\begin{bmatrix} q \\ \dot{q} \end{bmatrix} = \begin{bmatrix} 0 & 1 \\ -\frac{1}{(L_0 + L_1 x)c} & -\frac{R + L_1 x}{L_0 + L_1 x} \end{bmatrix} \begin{bmatrix} q \\ \dot{q} \end{bmatrix} + \begin{bmatrix} 0 \\ \frac{1}{L_0 + L_1 x} \end{bmatrix} e \quad (3.9)$$

When L_1 is equal to 0 it is easy to verify that the two subsystems become decoupled.

The coupled system is band pass, since the frequency of the carrier signal in the electrical subsystem is very high, much higher than the natural frequency of the mechanical subsystem. In reality, the voltage input signal of the RLC system contains a low pass and a band pass part. This voltage signal e(t) can be represented by the relationship:

$$e(t) = v(t)cos(\omega_\varepsilon t) \quad (3.10)$$

Where:

v(t): is the information signal that is going to drive the mass and has the form $v(t) = 2Acos(\omega_m t)$.

ω_ε: is the natural frequency of the electrical circuit.

ω_m:is the natural frequency of the mechanical system

From the above it is easy to see that v(t) is the low pass control signal that will define the displacement of the mass and $cos(\omega_\varepsilon t)$ is the carrier signal. For the coupling to work, $\omega_m << \omega_\varepsilon$ needs to hold true.

3.3 Modeling the low pass equivalent system dynamics

By separating the state vector of the system into a band pass and a low pass part one can obtain a low pass equivalent model retaining all the important information found in the band pass system. Using advanced mathematical tools such as Hilbert transform it is possible to analyze the dynamics of spectrally decoupled non linear systems that interact through amplitude or frequency modulation. In doing so, the low pass equivalent of a band pass system, will allow much faster simulation times, much lower sampling rates, and the signals will be “carrier free” [2].

3.3.1 Hilbert Transform

The Hilbert transform does not map a function to another domain as Laplace or other transforms do, but its output is on the time domain. It is often seen as a phase shift of $\pm\frac{\pi}{2}$. However the formal definition of Hilbert transform is presented below [2]:

$$\hat{x}(t) = \frac{1}{\pi}\int_{-\infty}^{\infty}\frac{1}{t-\tau}x(\tau)d\tau = \frac{1}{\pi t} * x(t) \quad (3.11)$$

$$\hat{x}(f) = -j\,\mathrm{sgn}(f)x(f) \quad (3.12)$$

The inverse Hilbert transform:

$$x(t) = -\frac{1}{\pi}\int_{-\infty}^{\infty}\frac{1}{t-\tau}\hat{x}(\tau)d\tau \quad (3.13)$$

Some important properties of the Hilbert transform that are associated to the product of a band pass and a low pass signal:

$$x(t) = x_1(t)x_2(t) \Rightarrow \hat{x}(t) = x_1(t)\hat{x}_2(t) \quad (3.14)$$

where $x_1(t)$is real and low pass and $x_2(t)$ is also real and band pass.

For a sinusoidal signal :

$$\begin{aligned} x(t) &= \cos(2\pi f_0 t) \Rightarrow \hat{x}(t) = \sin(2\pi f_0 t) \\ x(t) &= \sin(2\pi f_0 t) \Rightarrow \hat{x}(t) = -\cos(2\pi f_0 t) \end{aligned} \quad (3.15)$$

3.3.2 Formulating the LP equivalent model

Using the Hilbert transform it can be seen that the complex envelope $\tilde{x}(t)$ of a band pass signal $x(t)$ is actually a low pass signal that contains all the information of the original information signal. The pre-envelope of a signal is defined as:

$$x_+(t) = x(t) + j\hat{x}(t) \tag{3.16}$$

The complex envelope of the signal is found by:

$$x_+(t) = \tilde{x}(t)e^{j2\pi f_c t} \Leftrightarrow \tilde{x}(t) = x_+(t)e^{-j2\pi f_c t} \tag{3.17}$$

According to the work of N.Xiros and I. Georgiou [2] after the transformations of the input voltage signal $e(t)$ and the current signal $i(t) = \dot{q}(t)$ the low pass equivalent system that is obtained will be having the following state-space representation form:

$$\begin{bmatrix} \dot{\tilde{q}} \\ \ddot{\tilde{q}} \end{bmatrix} = \begin{bmatrix} -j\omega_\varepsilon & 1 \\ -\dfrac{1}{c(L_0 + L_1 x)} & -\dfrac{R + L_1\dot{x}}{(L_0 + L_1 x)} - j\omega_\varepsilon \end{bmatrix} \begin{bmatrix} \tilde{q} \\ \dot{\tilde{q}} \end{bmatrix} + \begin{bmatrix} 0 \\ \dfrac{1}{(L_0 + L_1 x)} \end{bmatrix} \tilde{e} \tag{3.18}$$

$$\begin{bmatrix} \dot{x} \\ \ddot{x} \end{bmatrix} = \begin{bmatrix} 0 & 1 \\ -\dfrac{k}{m} & -\dfrac{b}{m} \end{bmatrix} \begin{bmatrix} x \\ \dot{x} \end{bmatrix} + \begin{bmatrix} 0 \\ \dfrac{1}{m} \end{bmatrix} d + \begin{bmatrix} 0 \\ \dfrac{L_1}{2m} \end{bmatrix} \left|\dot{\tilde{q}}\right|^2 \tag{3.19}$$

Both signals e(t) and q(t) are now low pass, but at the same time they can be complex. To simulate this system in Simulink, the equations for the electrical band pass system must be manipulated in such way that the real and imaginary parts are separated:

$$\begin{aligned} \mathrm{Re}\left(\dot{\tilde{q}}\right) &= \mathrm{Re}\left(-j\omega_\varepsilon\right)\mathrm{Re}\left(\tilde{q}\right) - \mathrm{Im}(-j\omega_\varepsilon)\,\mathrm{Im}(\tilde{q}) + \mathrm{Re}(1)\,\mathrm{Re}(\dot{\tilde{q}}) - \mathrm{Im}(1)\,\mathrm{Im}(\dot{\tilde{q}}) \\ &= \omega_\varepsilon\,\mathrm{Im}(\tilde{q}) + \mathrm{Re}(\dot{\tilde{q}}) \end{aligned} \tag{3.20}$$

$$\begin{aligned} \mathrm{Im}\left(\dot{\tilde{q}}\right) &= \mathrm{Re}\left(-j\omega_\varepsilon\right)\mathrm{Im}\left(\tilde{q}\right) + \mathrm{Im}(-j\omega_\varepsilon)\,\mathrm{Re}(\tilde{q}) + \mathrm{Re}(1)\,\mathrm{Im}(\dot{\tilde{q}}) + \mathrm{Im}(1)\,\mathrm{Re}(\dot{\tilde{q}}) \\ &= -\omega_\varepsilon\,\mathrm{Re}(\tilde{q}) + \mathrm{Im}(\dot{\tilde{q}}) \end{aligned} \tag{3.21}$$

$$\mathrm{Re}\left(\ddot{\tilde{q}}\right)=\mathrm{Re}\left(-\frac{1}{c(L_0+L_1x)}\right)\mathrm{Re}\left(\tilde{q}\right)-\mathrm{Im}(-\frac{1}{c(L_0+L_1x)})\,\mathrm{Im}(\tilde{q})+\mathrm{Re}(-\frac{R+L_1\dot{x}}{L_0+L_1x})\,\mathrm{Re}(\dot{\tilde{q}})-\mathrm{Im}(-\frac{R+L_1\dot{x}}{L_0+L_1x})\,\mathrm{Im}(\dot{\tilde{q}})$$
$$+\mathrm{Re}(-j\omega_\varepsilon)\,\mathrm{Re}(\dot{\tilde{q}})-\mathrm{Im}(-j\omega_\varepsilon)\,\mathrm{Im}(\dot{\tilde{q}})+\mathrm{Re}(\frac{1}{L_0+L_1x})\,\mathrm{Re}(\tilde{e})-\mathrm{Im}(\frac{1}{L_0+L_1x})\,\mathrm{Im}(\tilde{e})$$

$$\mathrm{Re}(\ddot{\tilde{q}})=-\frac{\mathrm{Re}\left(\tilde{q}\right)}{c(L_0+L_1x)}-(\frac{R+L_1\dot{x}}{L_0+L_1x})\,\mathrm{Re}(\dot{\tilde{q}})+\omega_\varepsilon\,\mathrm{Im}(\dot{\tilde{q}})+\frac{\mathrm{Re}(\tilde{e})}{L_0+L_1x} \quad (3.22)$$

$$\mathrm{Im}\left(\ddot{\tilde{q}}\right)=\mathrm{Re}\left(-\frac{1}{c(L_0+L_1x)}\right)\mathrm{Im}\left(\tilde{q}\right)+\mathrm{Im}(-\frac{1}{c(L_0+L_1x)})\,\mathrm{Re}(\tilde{q})+\mathrm{Re}(-\frac{R+L_1\dot{x}}{L_0+L_1x})\,\mathrm{Im}(\dot{\tilde{q}})+\mathrm{Im}(-\frac{R+L_1\dot{x}}{L_0+L_1x})\,\mathrm{Re}(\dot{\tilde{q}})$$
$$+\mathrm{Re}(-j\omega_\varepsilon)\,\mathrm{Im}(\dot{\tilde{q}})+\mathrm{Im}(-j\omega_\varepsilon)\,\mathrm{Re}(\dot{\tilde{q}})+\mathrm{Re}(\frac{1}{L_0+L_1x})\,\mathrm{Im}(\tilde{e})+\mathrm{Im}(\frac{1}{L_0+L_1x})\,\mathrm{Re}(\tilde{e})$$
$$=-\frac{\mathrm{Im}\left(\tilde{q}\right)}{c(L_0+L_1x)}-(\frac{R+L_1\dot{x}}{L_0+L_1x})\,\mathrm{Im}(\dot{\tilde{q}})-\omega_\varepsilon\,\mathrm{Re}(\dot{\tilde{q}})+\frac{\mathrm{Im}(\tilde{e})}{L_0+L_1x} \quad (3.23)$$

By defining:

$$\tilde{q}=z$$
$$\dot{\tilde{q}}=\dot{z}$$

it is finally obtained:

$$\mathrm{Re}\left(\dot{\tilde{q}}\right)=\omega_\varepsilon\,\mathrm{Im}(z)+\mathrm{Re}(\dot{z}) \quad (3.24)$$

$$\mathrm{Im}\left(\dot{\tilde{q}}\right)=-\omega_\varepsilon\,\mathrm{Re}(z)+\mathrm{Im}(\dot{z}) \quad (3.25)$$

$$\mathrm{Re}(\ddot{\tilde{q}})=-\frac{\mathrm{Re}(z)}{c(L_0+L_1x)}-(\frac{R+L_1\dot{x}}{L_0+L_1x})\,\mathrm{Re}(\dot{z})+\omega_\varepsilon\,\mathrm{Im}(\dot{z})+\frac{\mathrm{Re}(\tilde{e})}{L_0+L_1x} \quad (3.26)$$

$$\mathrm{Im}(\ddot{\tilde{q}})=-\frac{\mathrm{Im}(z)}{c(L_0+L_1x)}-(\frac{R+L_1\dot{x}}{L_0+L_1x})\,\mathrm{Im}(\dot{z})-\omega_\varepsilon\,\mathrm{Re}(\dot{z})+\frac{\mathrm{Im}(\tilde{e})}{L_0+L_1x} \quad (3.27)$$

3.4 System Dimensionalization

Now that the mathematical models describing the dynamics of both band pass and low pass equivalent system are formulated, it is required to define each variable that parameterizes the system. Those values are presented on the following table:

Table 3.1 Parameter values

k	**b**	**m**	**L_0**	**L_1**	**c**	**R**
25kg/s^2	0.5kg/s	0.25kg	0.05H	0.5H/m	0.00002F	10Ω

Where:

k: is the spring constant.

b: is the damping coefficient for the mechanical system.

m: is the mass of the object.

L_0: is the inductance of the inductors coil.

L1:is the inductance constant required for the coupling of the system.

For this to be achieved, four criterions were established:

Criterion 1: maintaining $\omega_m << \omega_\varepsilon$

As discussed before, in order for the two coupled subsystems to communicate, the carrier frequency, that is the natural frequency of the electrical subsystem must be much higher than the natural frequency of the mechanical system. For that reason it was decided that carrier frequency will be larger than the mechanical system's resonance frequency by 2 orders of magnitude. Thus:

Table 3.2 Natural frequencies table (in rad/sec)

ω_m	ω_ε
10rad/s	1000rad/s

Table 3.3 Natural frequencies table (in Hz)

ω_m	ω_ε
1.5915Hz	159.15Hz

With that in mind, by setting one variable and using

$$\omega_\varepsilon = \sqrt{\frac{1}{Lc}}, \quad \omega_m = \sqrt{\frac{k}{m}}$$

the parameters k, m, L_0, L_1, c were calculated as found on table 1.

Criterion 2: damping

One important value that must be considered is the damping ratio of the mechanical and the electrical system. The damping ratio is defined as the ratio of the damping coefficient of a system to its critical damping coefficient. That is b for the mechanical and R for the electrical system in our case. It is often denoted as:

$$\zeta = \frac{b}{c_c} \quad (3.28)$$

Where:

b: is the damping coefficient of the system

c_c: is found from $c_c = 2\sqrt{km}$ and is the critical damping coefficient of the system.

The damping ratio is important since it defines the system behavior, especially during the transients. According to the value of the damping ratio, a system is characterized undamped, under damped, critically damped and over damped.

Undamped case

When a system is undamped, the damping ratio and more over the system's damping coefficient is equal to zero. Without something to damp the oscillation, the system will constantly oscillate around its natural frequency.

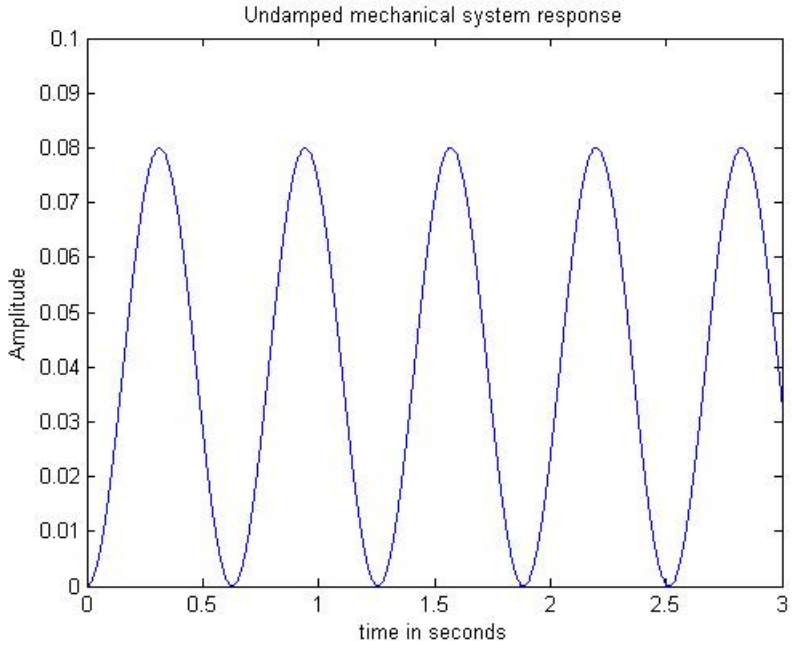

Figure 3.2 Undamped mechanical system response

Under damped and over damped case

In the under damped case, the damping ratio ζ is lower than 1. That will cause the system's oscillations to slowly fade away to rest position. Each oscillation will gradually lose power till the system reaches the steady state. The under damped case is pictured in

figure 3.3 with the red line. When the damping ratio is higher than 1, the system is over damped and it will reach the rest position very slowly, without any oscillations to occur.

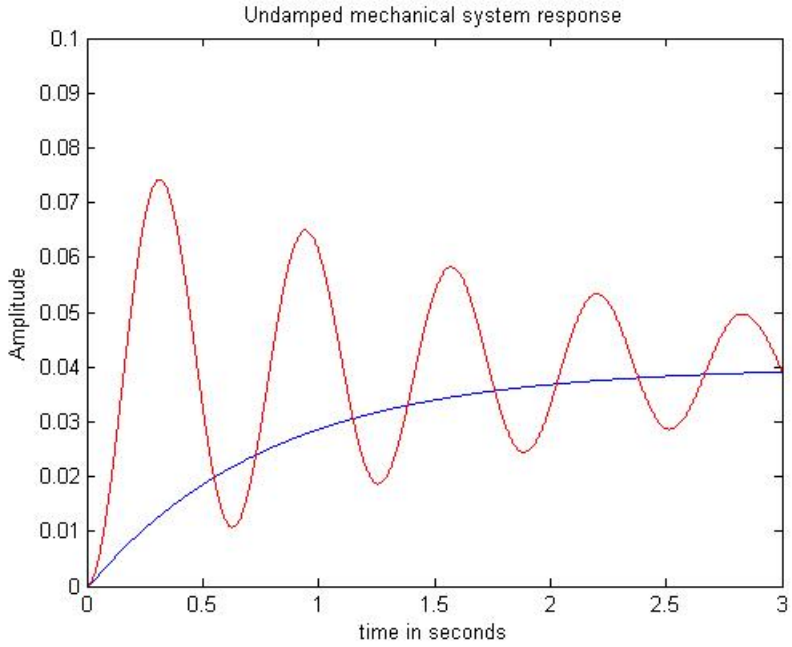

Figure 3.3 In red: under damped system, in blue: over damped system

Critically damped case

This is a special case where the damping ratio is equal to 1. When the system is critically damped it will not oscillate, in a similar way like the under damped case. The key difference between the two cases is that in the critically damped scenario the system will return to rest position in the slowest amount of time. This effectively reduces the effects of the transients on the system.

The transients though are an important part to study in the dynamics of coupled electromechanical systems. In order to preserve the dynamics of the system as much as possible but at the same time control them so that they don't muddle too much with the effects of the exogenous disturbance and the electromagnetic force, a damping ratio of 10 percent (0.1) was decided.

According to the damping ratio formula for the mechanical system:

$$\zeta = \frac{b}{c_c} => b = \frac{1}{2\sqrt{km}} \quad (3.29)$$

This yields a critical damping coefficient of 5kg/s. Thus the damping coefficient for the mechanical subsystem was set to 0.5kg/s.

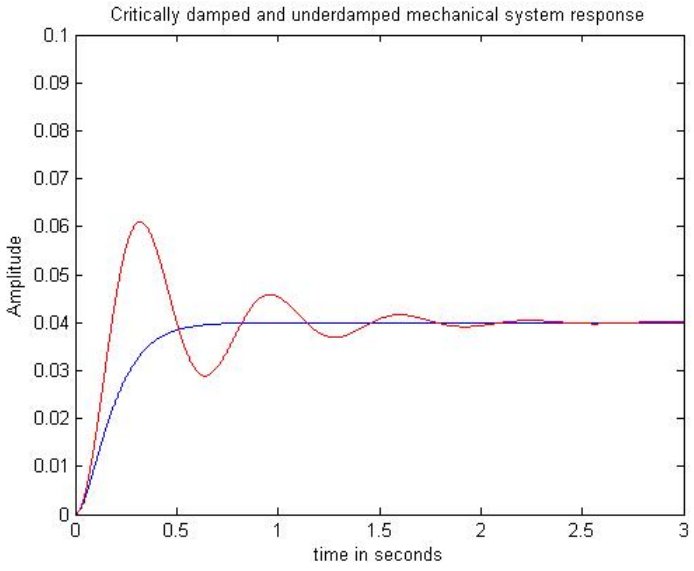

Figure 3.4 Critically damped (b=5.blue) and under damped(b=1, red) mechanical system

For the electrical subsystem, since it is structured in series, the damping coefficient is found by:

$$\zeta = \frac{R}{2}\sqrt{\frac{c}{L_0}} \Rightarrow R = 2\sqrt{\frac{L_0}{c}} \quad (3.30)$$

This would wield a critical damp coefficient for the resistance of 100Ω. However setting a high value of resistance would mean a high value of voltage will be needed for the control signal to have any effect on the mass displacement. Therefore the resistance was set to 10Ω.

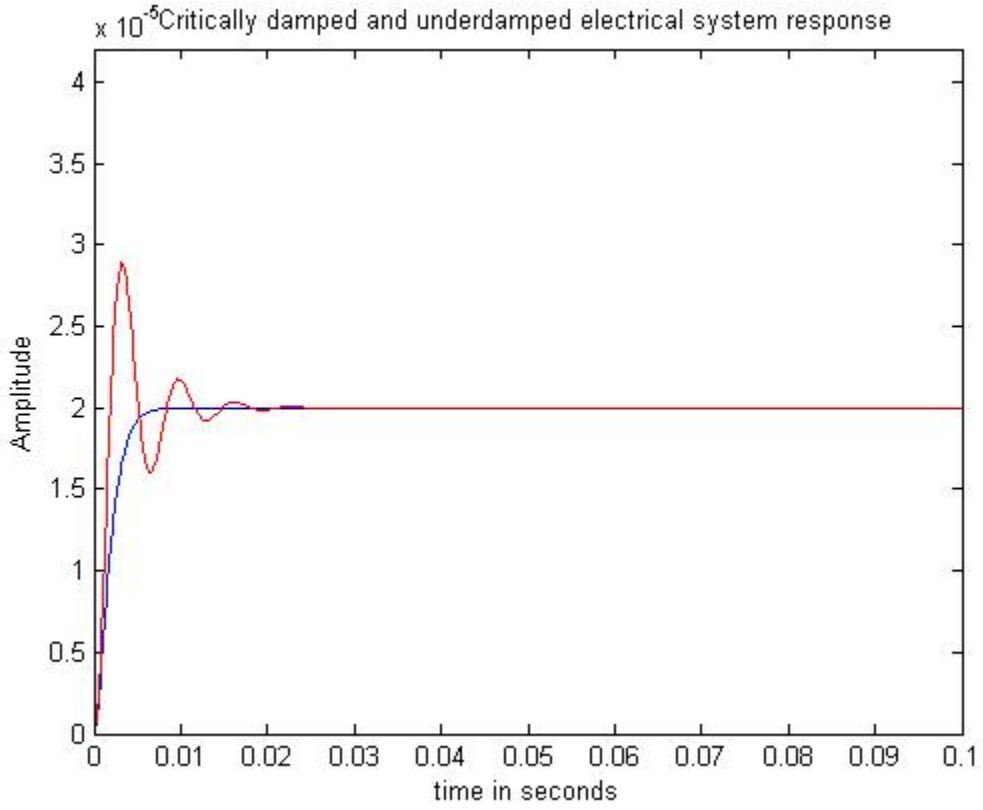

Figure 3.5 Critically damped (R=100Ω, blue) and underdamped (R=25Ω, red) RLC system

Criterion 3: equilibrium point

An important parameter that needs to be defined is the equilibrium point at which the mass of the system will remain still. At this position the nonlinear magnetic force coming

from the electrical system will be negated by the restoring force of the spring, and the actual inductance, current and voltage values can be identified. By selecting an equilibrium point other than zero, we introduce a DC component to the control signal that will maintain the mass to this position. In this study the range of the displacement signal was defined as 0.10m. That is the mass is allowed to move from point 0 to point 0.10m. Therefore the equilibrium point was set to 0.05m.

While the mass stays still at this point, the only forces acting on it are the magnetic force of the inductor and the restoring force of the spring. The two forces must have equal magnitude and opposite direction.

Therefore:

$$\frac{L_1 i_0^{\,2}}{2} = k\frac{x}{2} \Rightarrow i_0^{\,2} = \frac{kx}{L_1} \Rightarrow i_0 = \sqrt{\frac{kx}{L_1}} \quad (3.31)$$

Substituting the values we obtain:

$$i_0 = 2.2361A \quad (3.32)$$

The next step is to find the value of the DC gain of the control signal e(t) that is needed to maintain the mass to point 0.05m. Using the equation of electrical impedance we find:

$$e_0 = \sqrt{R^2 + (\omega_\varepsilon (L_0 + L_1 \frac{u}{2}) - \frac{1}{\omega_\varepsilon c})^2}\,|i_0| \quad (3.33)$$

Solving this equation and substituting the values we get:

$$e_0 = 60.2088V$$

Therefore the input control signal is of the form:

$$e(t) = v(t)\cos\omega_{\varepsilon}t \Rightarrow e(t) = (60.2088 + A\cos\omega_{m}t)\cos\omega_{\varepsilon}t \quad (3.34)$$

Where:

v(t): is the low pass information signal.

A: is the amplitude of the information signal

ω_{ε}: is the carrier frequency

ω_{m}:is the mechanical parts resonance frequency

It is worth to note that the values for the current and the DC envelope in the low pass equivalent system represent RMS values.

Criterion 4: maximum forces applied to the system

Now that we have defined the equilibrium point at 0.05m we have to consider the maximum allowed amplitude for the forces applied to the coupled system. Since the range of the mass displacement is 0.10m and the system will always start from position 0.05m the disturbance force can only move the mass 0.05m upwards or downwards from the equilibrium point. Of course the same holds for the electromagnetic force. Therefore we can calculate the magnitude of the disturbance force based on the spring constant k.

Using Hooke's law:

$$F = -kx \quad (3.35)$$

We find that for a spring constant of 25N/m and distance 0.05m the maximum allowed disturbance force amplitude so that the mass will not move beyond point 0.10m equals

$$D_{max} = 1.25\text{N}.$$

For the electromagnetic force, we have:

$$\frac{L_1}{2} i^2 = -kx \, (3.36)$$

which for the same numbers gives

$$i_{max} = 3.1623A \, (3.37)$$

Likewise we find that the maximum voltage amplitude that corresponds to the max allowed current is

$$e_{0max} = 142.7227 \, (3.38) \text{ (peak value)}$$

Of course the above hold if only each force acts separately on the system and not both of them together. In the cases that both the electromagnetic and the exogenous disturbance force act at the same time, as we will see in the sequel, more voltage and current is needed to overcome the disturbance force and vice versa.

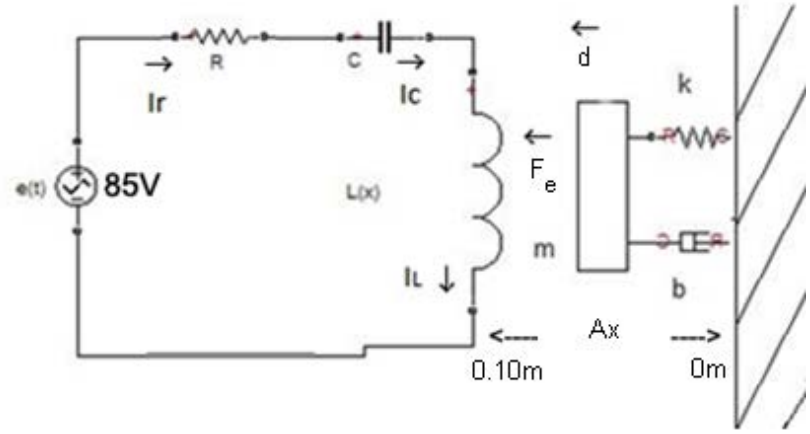

Figure 3.6 System diagram

4. IMPLEMENTING THE MATHEMATICAL MODELS IN SIMULINK

4.1 Overview

In this section the implementation of two Simulink models, one for the band pass system and one for the low pass equivalent system will be presented, to enable further studying and testing of the dynamics. The two models are then to be tested, compared and validates with each other for confirmation of their accuracy and equivalence.

4.2 Input Signals

As discussed in the previous section, the input of the system, which is the voltage control signal, is of the form:

$$e(t) = (60.2088 + A\cos\omega_m t)\cos\omega_\varepsilon t \quad (4.1)$$

However the band pass system works with peak values, rather than RMS values as the low pass equivalent does. Thus the information signal (the low pass voltage signal that is synced to the natural frequency of the mechanical system) has to be multiplied by $\sqrt{2}$. Therefore the input signal for the band pass system is:

$$e(t) = (60.2088 + A\cos\omega_m t)\sqrt{2}\cos\omega_\varepsilon t \quad (4.2)$$

For the low pass equivalent system, we have to consider the complex envelope of the above signal so we can remove high frequency term produced by the carrier signal.

By applying the Hilbert transform in order to obtain the complex envelope $\tilde{e}(t)$

and by using

$$e_0 = 60.2088V$$

it is obtained:

$$e(t) = (e_0 + A\cos\omega_m t)\cos\omega_\varepsilon t = e_0\cos\omega_\varepsilon t + A\cos\omega_m t\cos\omega_\varepsilon t$$

$$\hat{e}(t) = e_0\sin\omega_\varepsilon t + A\cos\omega_m t\sin\omega_\varepsilon t = (e_0 + A\cos\omega_m t)\sin\omega_\varepsilon t$$

$$\begin{aligned} e_+(t) &= e(t) + j\hat{e}(t) = (e_0 + A\cos\omega_m t)\cos\omega_\varepsilon t + j(e_0 + A\cos\omega_m t)\sin\omega_\varepsilon t \\ &= (e_0 + A\cos\omega_m t)(\cos\omega_\varepsilon t + j\sin\omega_\varepsilon t) \\ &= (e_0 + A\cos\omega_m t)e^{j\omega_\varepsilon t} \end{aligned}$$

$$\tilde{e}(t) = e_+(t)e^{-j\omega_\varepsilon t} = 60.2088 + A\cos\omega_m t \quad (4.3)$$

With this it found that the complex envelope of the real input signal that has a low pass part and a band pass part is a real signal equal to the low pass information signal.

4.3 Band pass and low pass equivalent models

Matlab's Simulink was used to run simulations and perform experiments using the mathematical models expressing the dynamics of the electromechanical system. Since we have already formulated the governing equations in state space form, the embedded matlab function blocks were used coupled with some integrators to solve the non linear system.

4.3.1 Band pass model

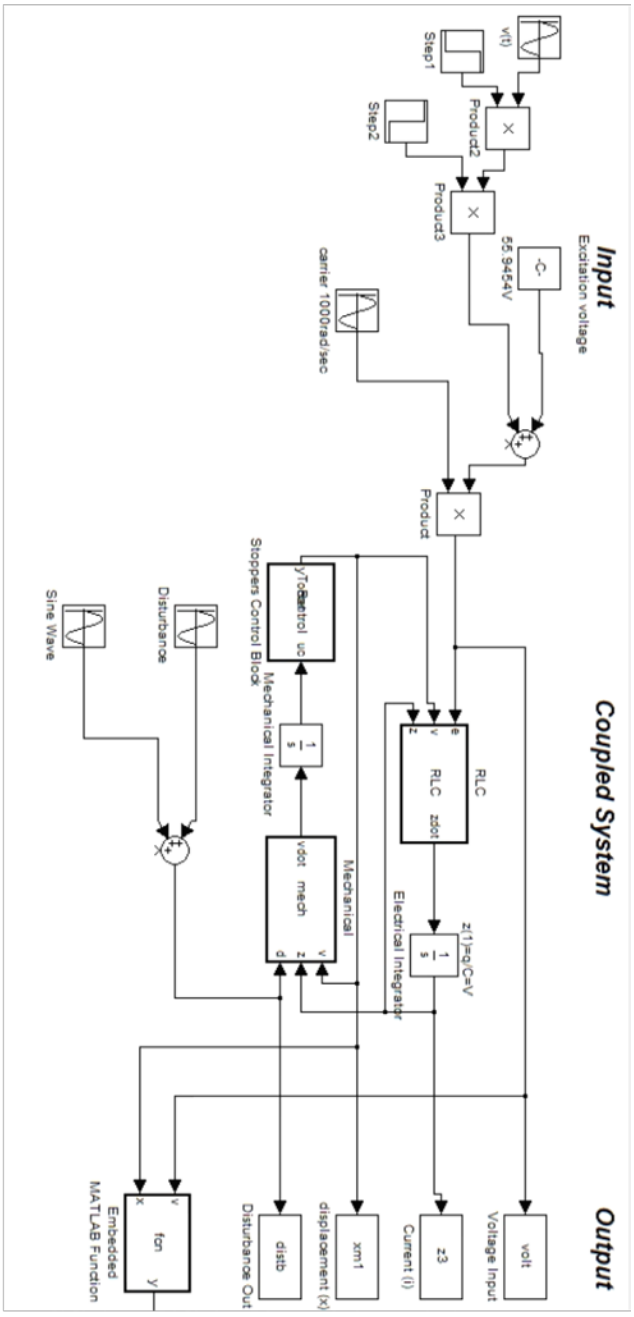

Figure 4.1 Band pass model in Simulink

4.3.2 Low pass equivalent model

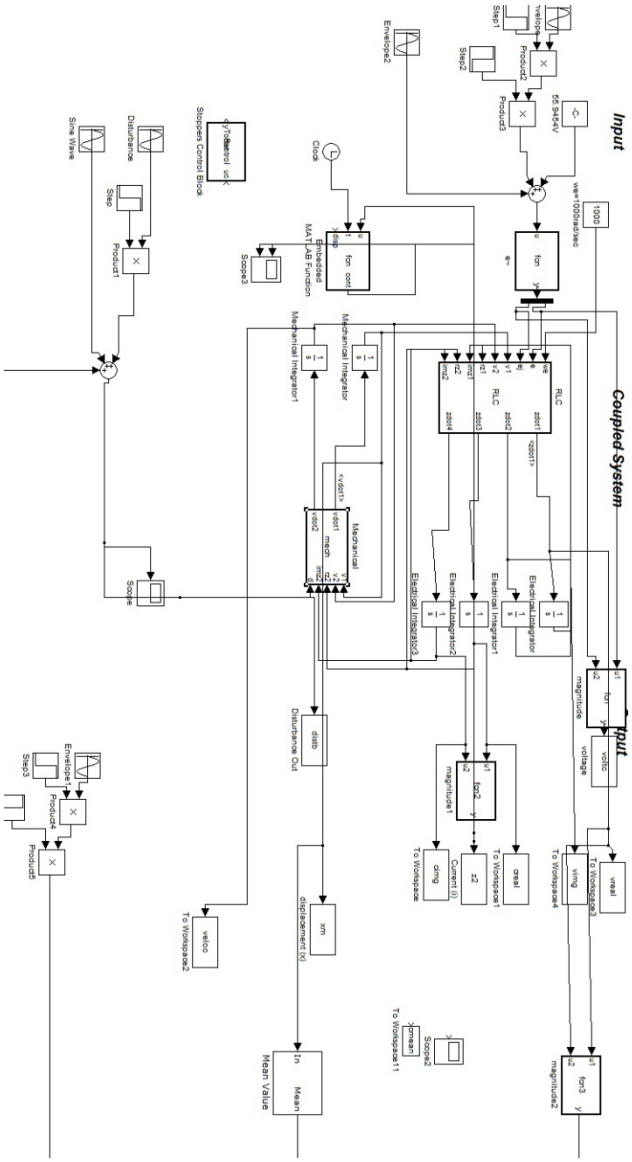

Figure 4.2 Lowpass Equivalent model

4.4 Validation of the models

By setting the DC voltage equal to 60.2088 Volts for the low pass equivalent model and 85.1481 Volts for the band pass model, without having any variable part in the information signal and without any exogenous disturbances we expect the mass to stay still at point 0.05m. Indeed:

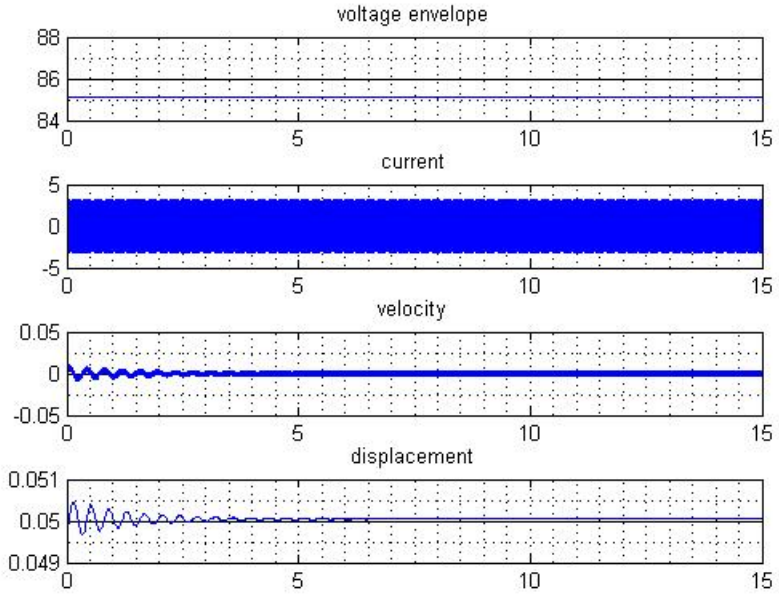

Figure 4.3 Band pass model excited with DC input signal

It is easily seen that both models output almost the same result, as expected from the theoretical work. Moreover the benefits of using the low pass equivalent system are readily seen. The carrier frequency which is very high and obvious in the current signal of the band pass system, does not appear anywhere in the low pass equivalent model.

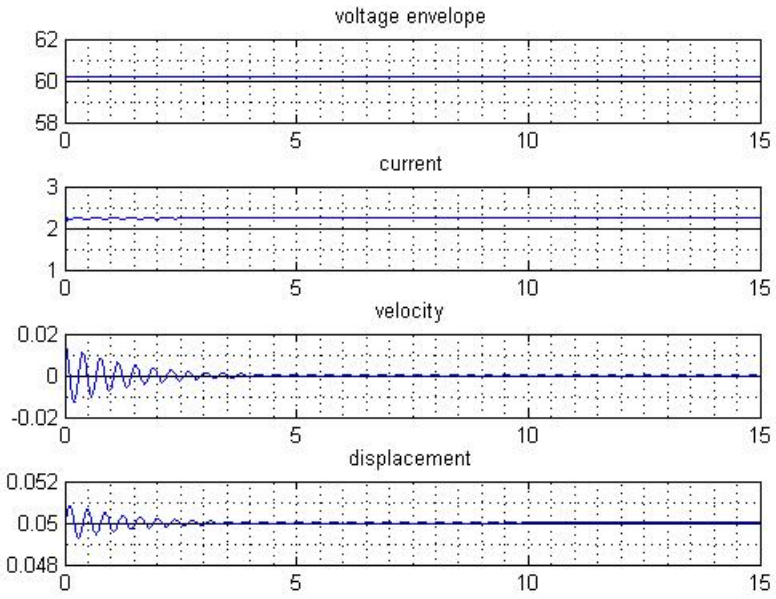

Figure 4.4 Low pass equivalent system excited with DC voltage

Yet all important information, the effect of the inductor to the mass displacement is retained. The time step that is needed in order to simulate the band pass model has to be set at least two times the highest frequency appearing in the system, according to the Nyquist theorem. The low pass system allows for much lower sampling rates since it avoids simulating the carrier signal. Although the highest frequency that it can be seen in this system is the natural frequency of the mechanical part, that is not entirely true. The highest frequency in the system is the frequency of the coupling of both systems, which since they are non linear the frequency can be as high as double mechanical's system natural frequency.

A DC signal holding the mass at the equilibrium point is not enough to prove that both models output the same results. For that reason additional test cases were created to compare both models:

- a negative DC voltage signal that will move the mass below the equilibrium point but above the 0m point
- a positive DC voltage signal that will move the mass above the equilibrium point but below 0.10m point
- a sinusoidal signal of frequency equal to 5rad/s
- a disturbance DC signal of 0.5N
- a sinusoidal disturbance signal
- a filtered white noise disturbance signal.

4.4.1 DC voltage signal

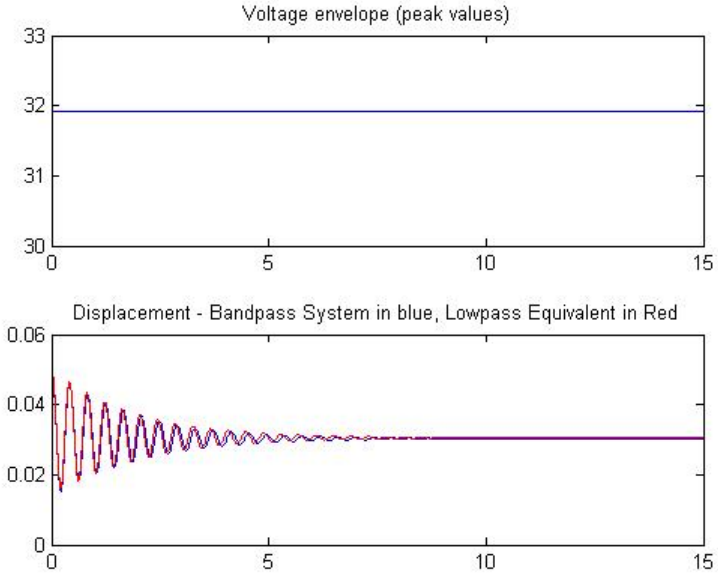

Figure 4.5 BandPass (blue) and Lowpass (red) System excited with -32V DC

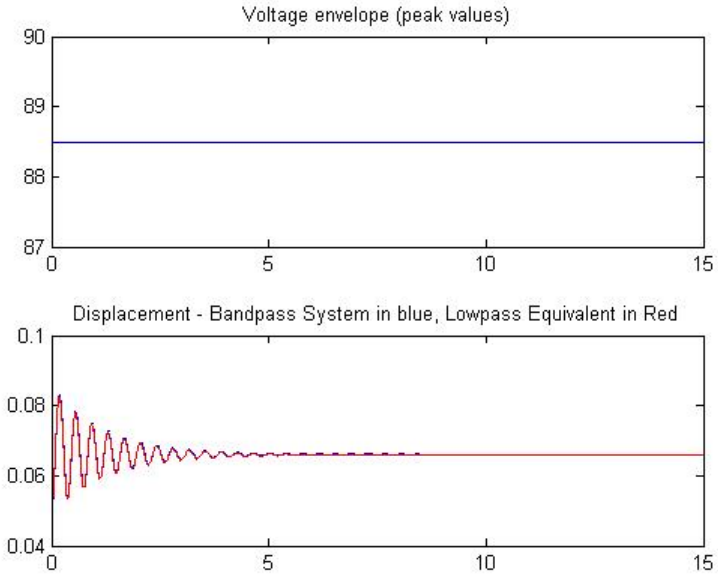

Figure 4.6 BandPass (blue) and Lowpass (red) System excited with 88.5V DC

4.4.2 Sinusoidal voltage signal

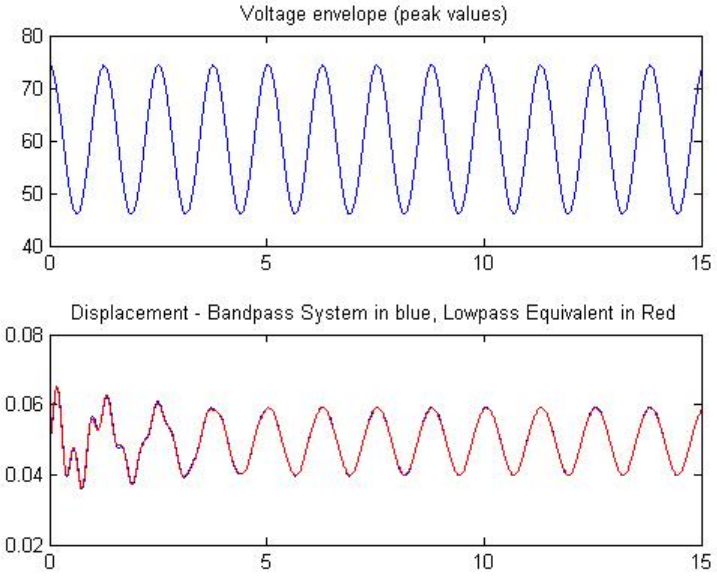

Figure 4.7 Bandpass (blue) and Lowpass (red) model for a 20Volt-5rad/s voltage signal

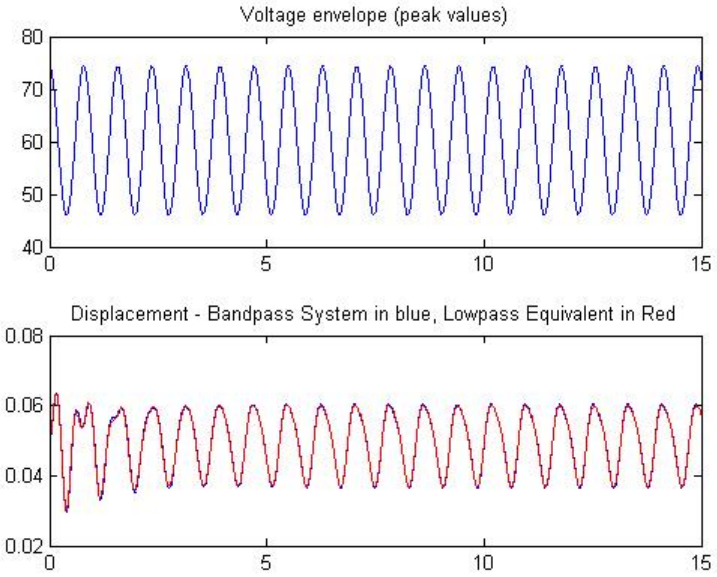

Figure 4.8 Bandpass (blue) and Lowpass (red) for a 20Volt-5rad/s voltage signal

4.4.3 Excitation with disturbance

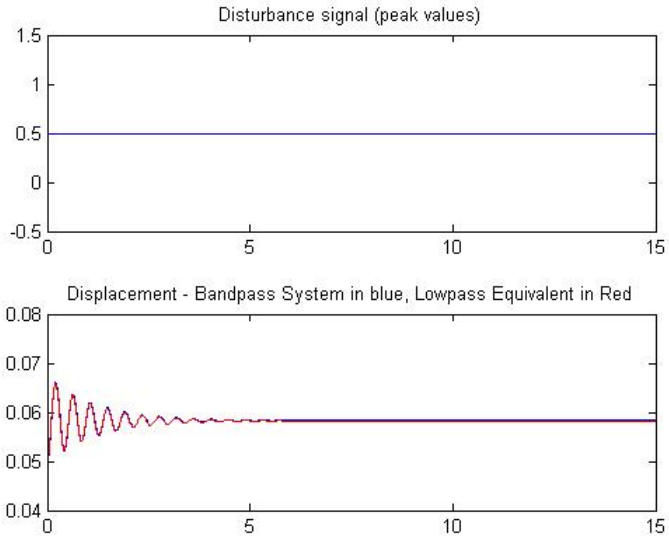

Figure 4.9 Bandpass (blue) and Lowpass (red) for a constant .5N disturbance force

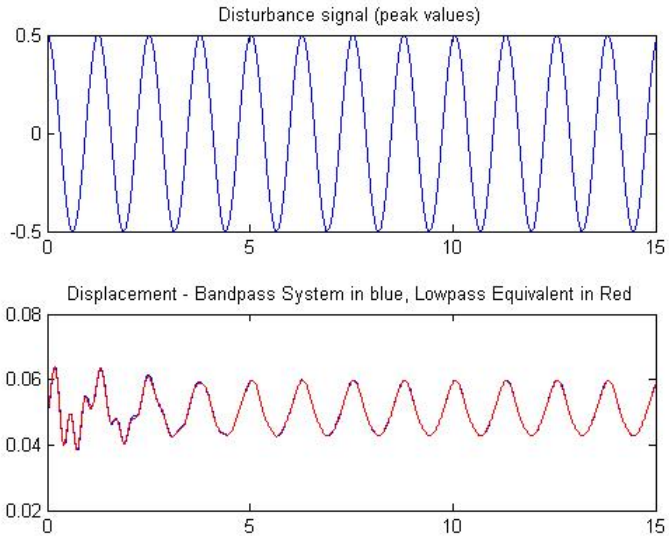

Figure 4.10 Bandpass (blue) and Lowpass (red) for a sinusoidal disturbance force of amplitude .5N and frequency 5rad/s

4.4.4 White Noise Excitation

The coupled electromechanical subsystem was excited with a virtually random disturbance force, in order to simulate a real scenario of random exogenous force acting on the system. white noise was used since it can represent such a random force.

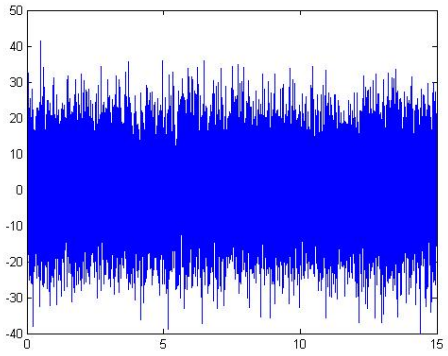

Figure 4.11 White noise

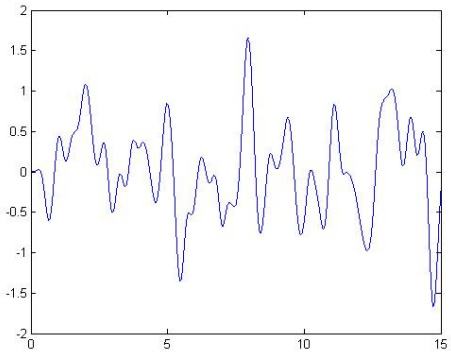

Figure 4.12 Filtered white noise

White noise is an interesting signal in the respect that it contains equal power throughout its bandwidth. In other words its power spectral density is flat. In order to create a white noise signal to excite both low pass and band pass models, the band limited white noise block was used. Since the block is synced to the sampling frequency of the whole system in Simulink, an analog low pass filter was implemented to filter out all higher frequencies other than the mechanical sub system's natural frequency.

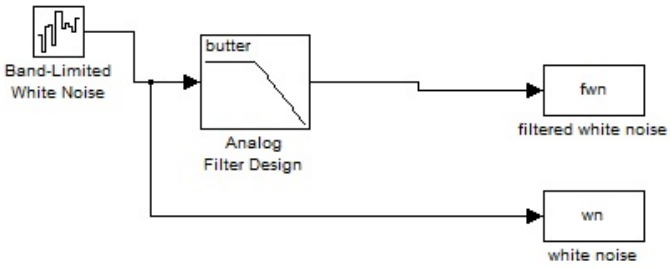

Figure 4.13 Low Band Limited white noise

A simple 6th order low pass Butterworth filter with cutoff frequency 10rad/s was sufficient to allow only the frequencies close to the mechanical system's natural frequency.

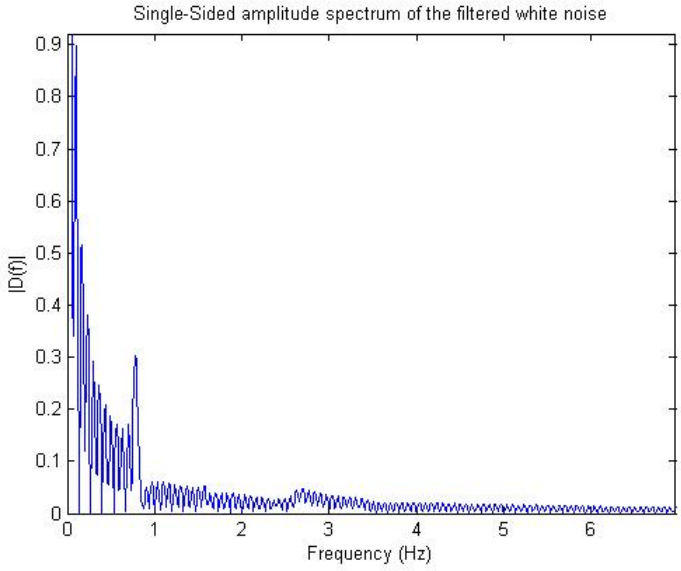

Figure 4.14 Single-sided amplitude spectrum of the filtered noise

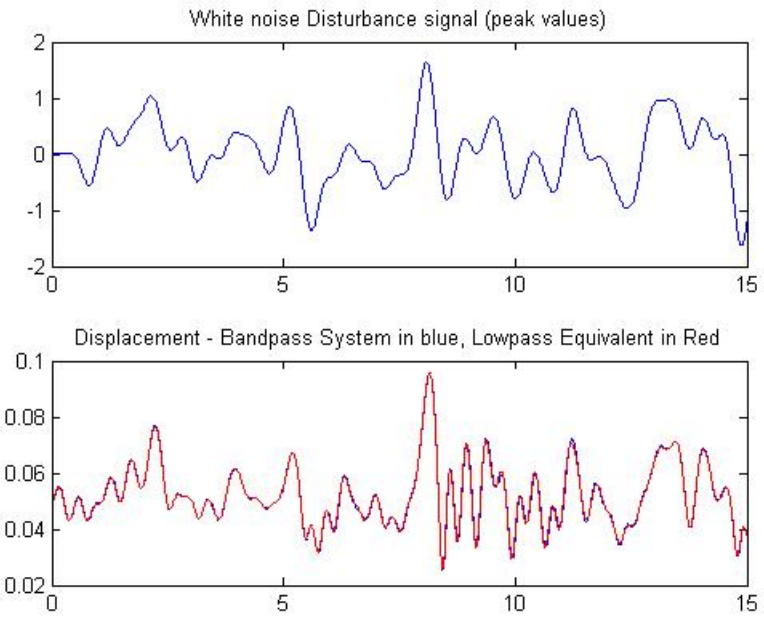

Figure 4.15 Excitation of both system using a white noise disturbance signal

As it is seen from the above results, in every test the models have had similar or almost identical behavior. With this it is proven that the low pass model of the system is actually equivalent to the band pass model and any information that the band pass signals are carrying is fully contained to the low pass complex envelopes of the low pass model.

4.5 Stoppers

In order to keep the displacement of the mass within the wanted space interval [0,0.10]m with 0.05m viewed as the equilibrium point, software "stoppers" were developed that would represent actual physical stoppers. The stoppers will not allow the movement of mass to occur at points greater than 0.10m or lower than 0m. When the mass position exceeds this interval, the stoppers block will correct the displacement and set it equal to the upper or lower limit respectively. In addition the velocity signal will be set equal to 0 each time the mass reaches those limits.

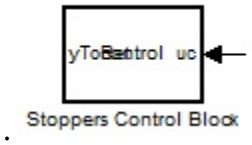

Figure 4.16 Stoppers control block

Mathematically the stoppers are formulated as following:

$$x = \begin{cases} 0, & x < 0 \\ 0.1, & x > 0.1 \end{cases}$$

$$\dot{x} = \begin{cases} 0, & x < 0 \\ 0, & x > 0.1 \end{cases}$$

where x is the displacement of the mass and $\dot{x}$ is the velocity of the mass.

5. TEST CASES AND SIMULATIONS

5.1 Overview

This section will present the results of the test cases run on both low pass and band pass models. The models were excited with single tone and multiple tone signals for the inputs being the disturbance force and the voltage control signal. The system behavior is then identified by determining the effect of the electromagnetic and disturbance force on the displacement of the mass. The change in the displacement amplitude was measured for various frequencies and amplitudes of the excitation/control signals. Using the low pass equivalent system the effect of the disturbance force will be studied as hidden in the imaginary part of the complex envelope of the current.

5.2 Multiple tone signals excitation

A multiple tone signal is a mixture of pure tone signals of different amplitudes and frequencies. These tests are important for studying the behavior of the coupled electromechanical system under specific circumstances. Such a signal was created as a weighted sum of sinusoidal signals with frequency range between 5-20 rad/sec and various amplitude values. In addition a phase term was introduced. The following time series graphs will preview the waveform of the current through the resistor and the displacement of the mass using such a signal in both band pass and low pass equivalent models in a 15 second period.

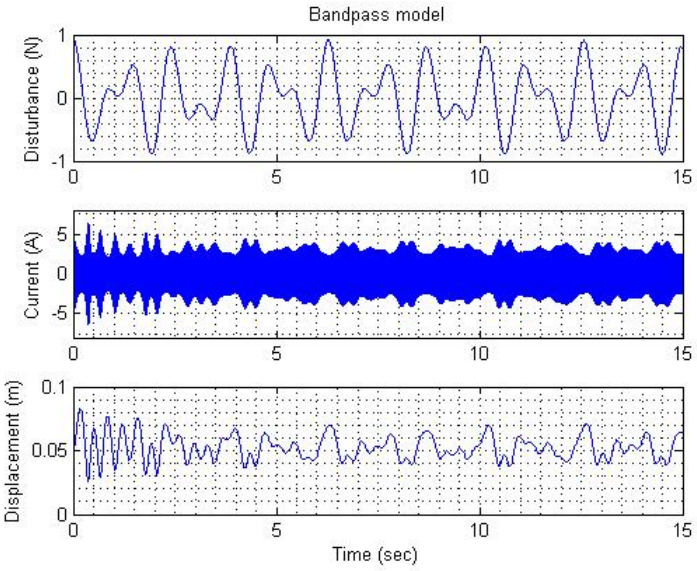

Figure 5.1 Band pass model excited with a disturbance force signal of the form: 0.5035sin(5t+pi/2) + 0.4098sin(8t+pi/2)

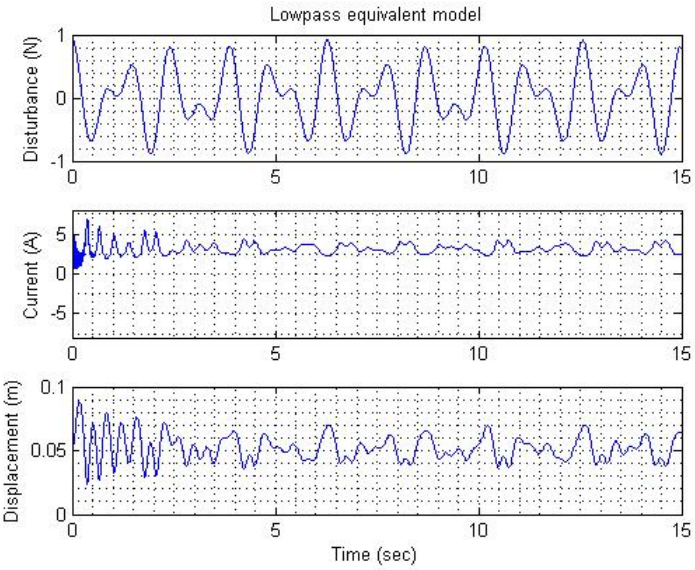

.

Figure 5.2 Low pass equivalent model excited with a disturbance force signal of the form: 0.5035sin(5t+pi/2) + 0.4098sin(8t+pi/2)

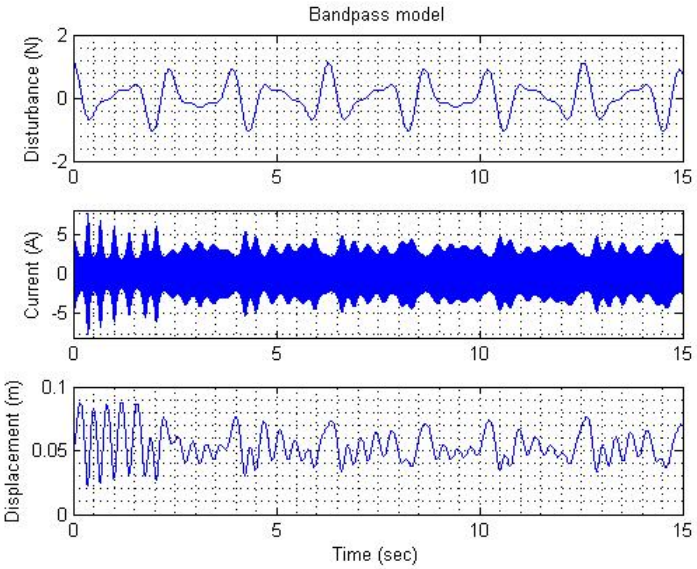

Figure 5.3 Band pass model excited with a three tone disturbance force signal of the form:

0.5035sin(5t+pi/2) + 0.4098sin(8t+pi/2) +0.2sin(11t+pi/2)

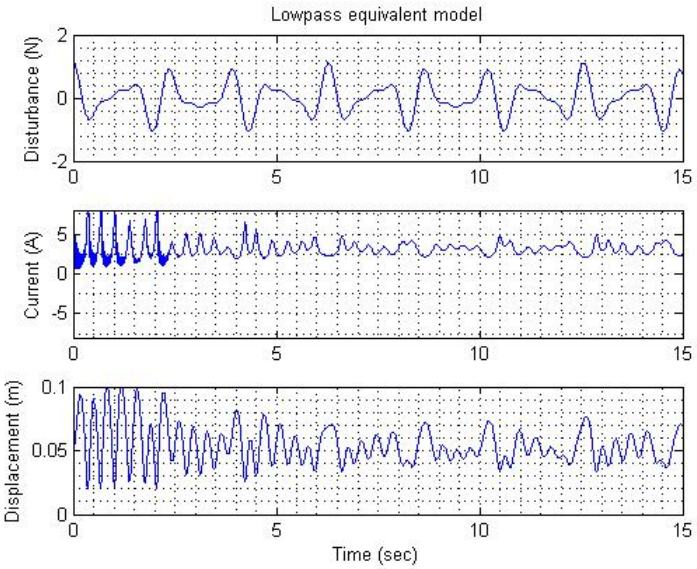

Figure 5.4 Low pass equivalent model excited with a three tone disturbance force signal of the form:

0.5035sin(5t+pi/2) + 0.4098sin(8t+pi/2) +0.2sin(11t+pi/2)

5.3 Imaginary part of the complex envelope of the current

The carrier frequency of the electrical system in the band pass model does not allow us to make accurate assumptions about the coupling effect. The advantage of the low pass complex envelope signals in the low pass equivalent models is obvious. Not only that, by splitting the complex envelope of the current to its real and imaginary part we can investigate for further effects of the excitation force.

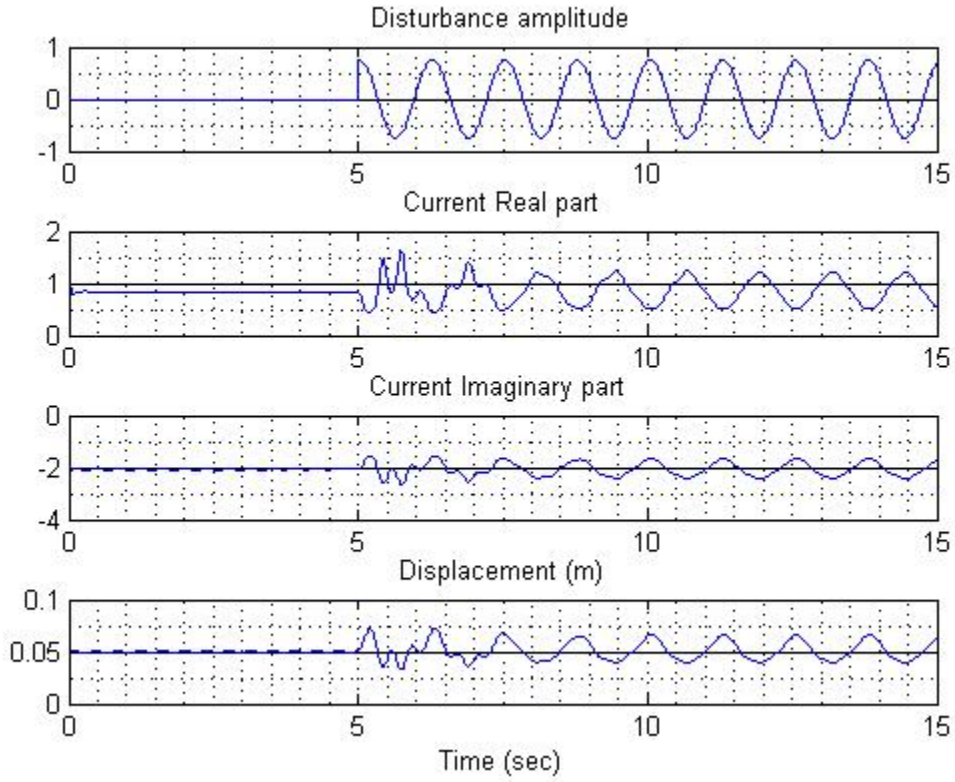

Figure 5.5 Low pass equivalent model - investigating imaginary part of the current complex envelope

In the above figure the low pass model was excited with a disturbance force of amplitude 0.75N and frequency 5 rad/s. The disturbance force is applied after 5 seconds to allow enough time for the system to reach the rest position (steady state). If we pay close

attention to the imaginary part of the complex envelope of the current we can notice many similarities to the waveform of the displacement. The effect is more obvious when multiple tone signals with different frequencies and amplitudes are used for excitation.

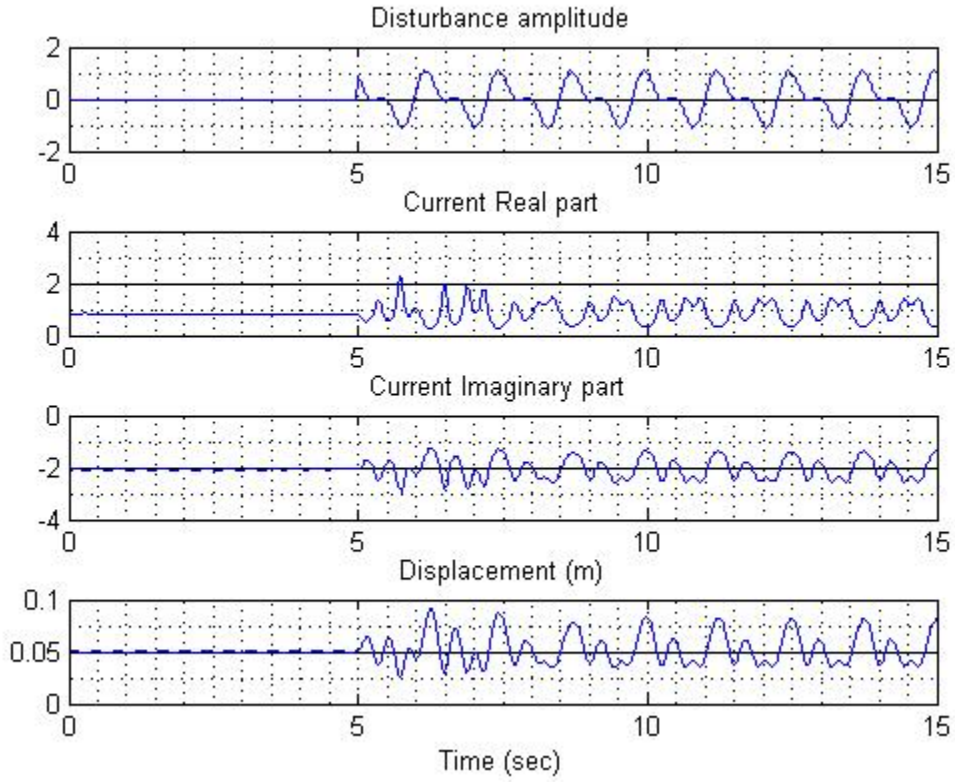

Figure 5.6 Low pass equivalent model - excitation with a disturbance force of the form : 0.75cos(5t) + 0.5cos(10t)

As it can be seen, the information about the mass position is actually translated to the imaginary part of the complex envelope of the current. The waveforms of the two signals might look similar; however non linearity is also apparent. At certain points the peaks and the amplitudes of the two signals are different.

This phenomenon happens only when the system is excited by an exogenous disturbance force but without a control signal being applied other than the DC signal that is required

to keep the mass to the equilibrium point. By using the Fourier transform we can confirm the effect of the disturbance force in the imaginary part of the complex envelope by identifying the dominant frequencies of the disturbance force.

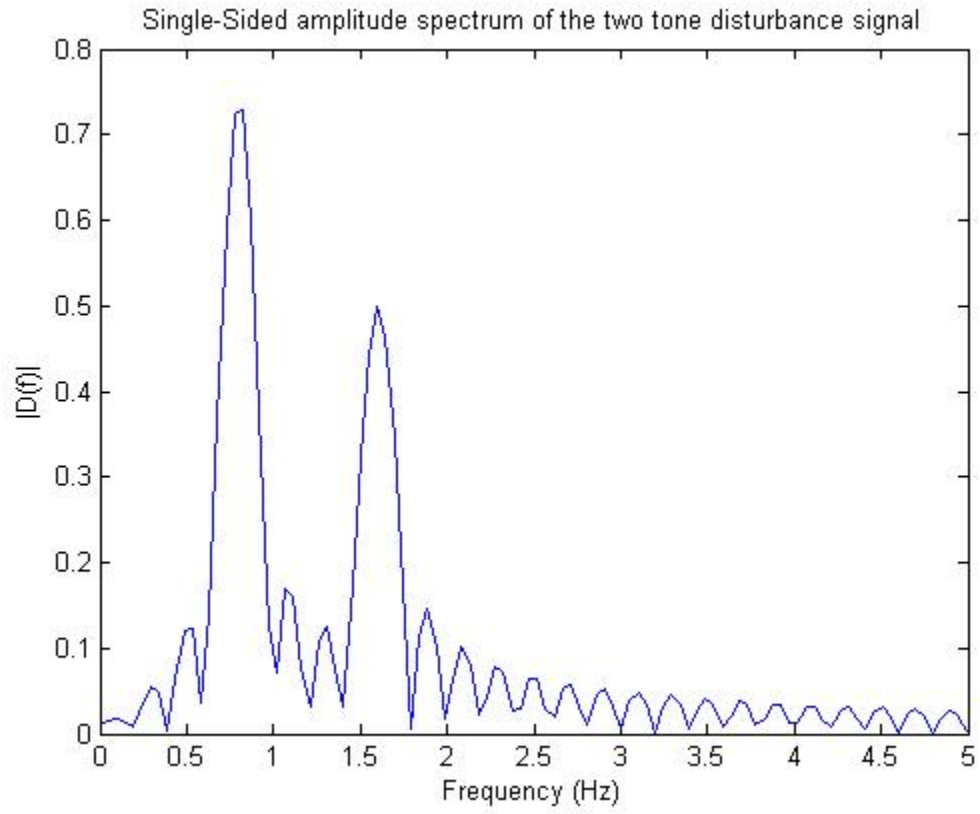

Figure 5.7 Fast Fourier Transform of a disturbance force of the form 0.75cos(5t) + 0.5cos(5t)

Figure 5.7 shows the FFT of the disturbance signal. Since the disturbance force is composed of 2 pure tone sinusoidal signals, the Fourier transform is very accurate. In this graph the magnitude of the sine signals is equal to their amplitude. That's not the case always however. Depending on the time window used, the magnitude values may vary due to averaging.

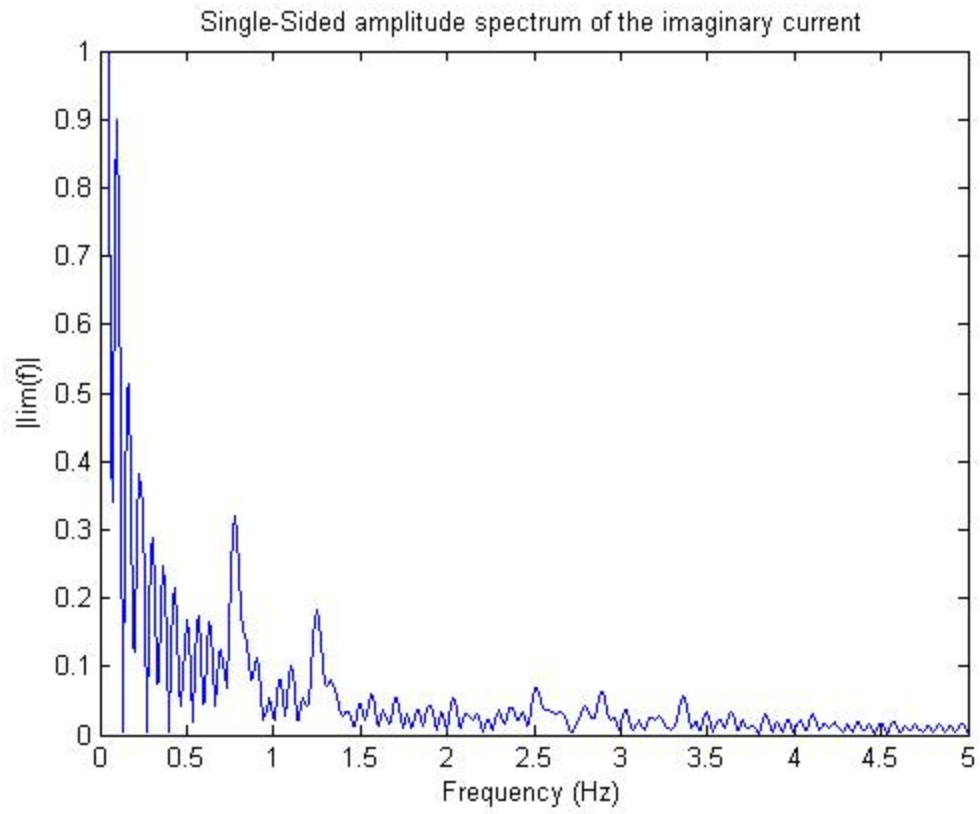

Figure 5.8 Single sided amplitude spectrum of the imaginary part of the complex envelope of the current

The dominant frequencies of the disturbance signal are visible in the single-sided amplitude spectrum of the imaginary part of the current. The zero frequency and its harmonics till 0.5Hz indicate the power of the DC component. In fact the imaginary part of the complex envelope of the current has a value of -1.5811V when the system is at the steady state.

When the system is excited by the voltage signal without any disturbance force present, the imaginary part of the current behaves differently. The waveform seems to be the inverse of the displacement waveform, as figure 5.9 shows.

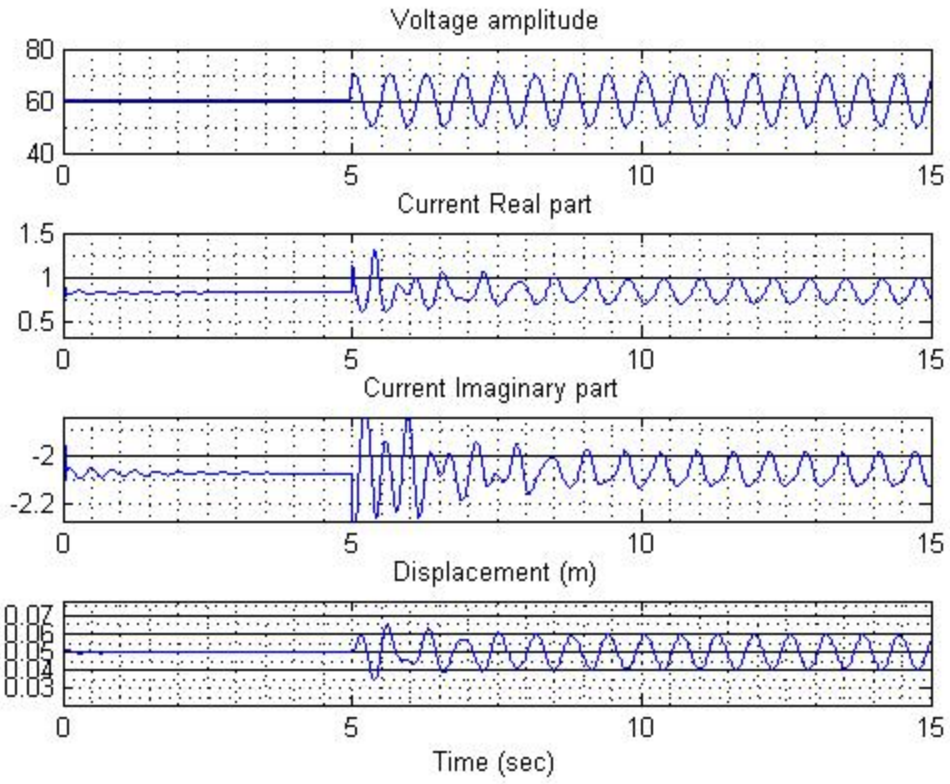

Figure 5.9 Low pass equivalent model excited with a voltage signal of amplitude 10 and frequency 5rad/s.

5.3.1 Correlation

By experimentation and quick calculations it is easy to appropriately adjust the amplitude of the displacement signal in order to match the amplitude of the imaginary part of the current envelope signal. Then by removing their DC component we can present them graphically:

Starting from 5 seconds where a disturbance force is applied we can see the waveform of the current follow the waveform of the displacement. By calculating the correlation coefficient we can characterize how strong the correlation is between the two signals. A correlation coefficient value closer to 1 indicates strong relationship while a value closer

to 0 indicates no relationship. The results however will not be accurate in the case of the electromechanical system studied here.

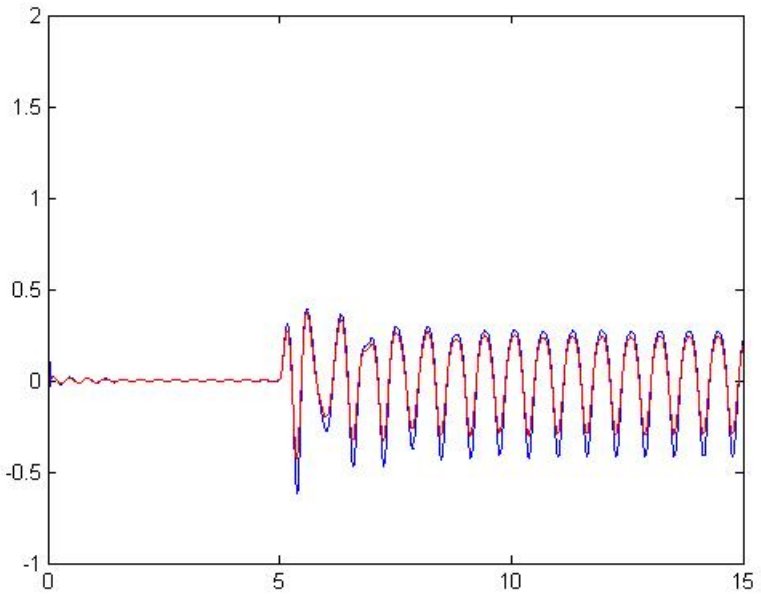

Figure 5.10 (Blue) Imaginary part of the complex envelope of the current. (RED) Displacement signal.

The correlation coefficient is a statistical way to indicate the possibility of a linear relationship between the signals. The signals in the system do not have linear relationships, because of the coupling. Indeed the correlation matrix is found to be

$$r = \begin{bmatrix} 0.0042 & -0.0025 \\ -0.0025 & 0.0132 \end{bmatrix}$$

for a sinusoidal disturbance signal indicating no correlation.

5.4 Excitation using three tone signals with phase difference

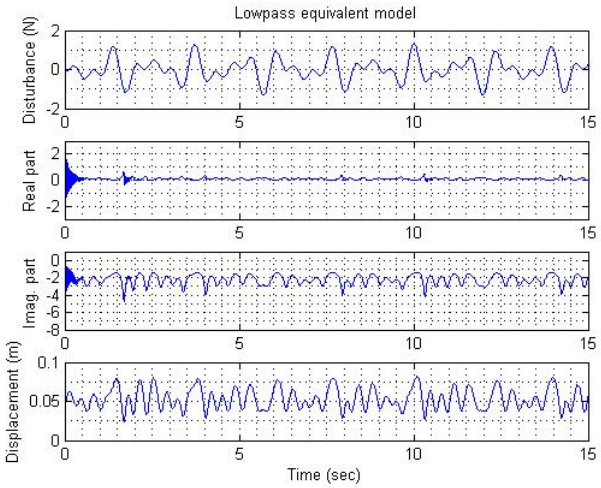

Figure 5.11 Low pass equivalent model excited with a disturbance force of the form 0.5035sin(5t+pi/2) + 0.4098sin(8t+pi) + 0.4075sin(11t+3pi/2)

The low pass equivalent model was excited with a disturbance force signal composed of 3 sinusoidal signals of different frequency, different amplitude and different phase between them.

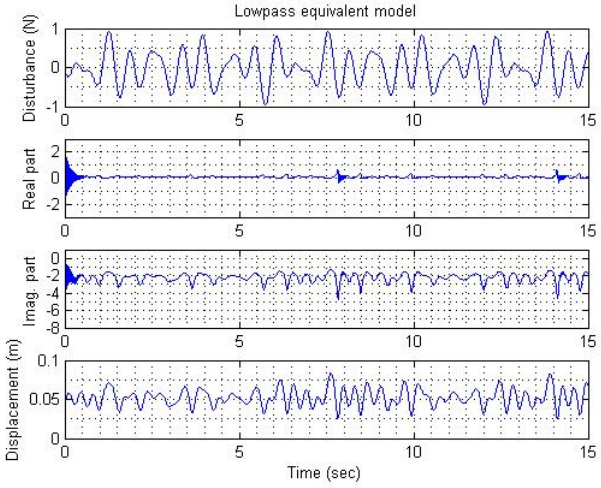

Figure 5.12 Low pass equivalent model excited with a disturbance force of the form 0.4098sin(8t+pi/2) + 0.2313sin(10t+pi) + 0.4075sin(11t+3pi/2).

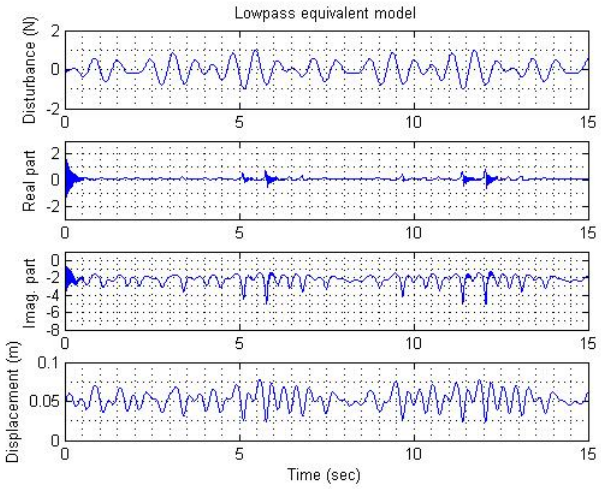

Figure 5.13 Low pass equivalent model excited with a disturbance force of the form 0.4098sin(8t+pi/2) + 0.2313sin(10t+pi) + 0.4075sin(11t+3pi/2)

5.5 Determining the effect of the voltage signal on the mass

As the coupled system is excited with voltage signals of various frequencies, the effect the electromagnetic force has on the mass varies too. The closer we get to the coupled system's natural frequency, the less voltage amplitude is needed to move the mass. For that reason an algorithm was created in order to determine the maximum allowed voltage amplitude so that the mass displacement is always constrained within the preset limits.

The program would then constantly perform simulations on the system changing the amplitude of the voltage signal $v(t)=A\cos(\omega t)$ with a step of 0.2V and changing the frequencies from zero frequency (DC) to 25 rad/s with a step of 1. The simulations stop when a voltage signal is found with such amplitude as the mass would not be moved beyond point x=0.0925m or below x=0.0005m.

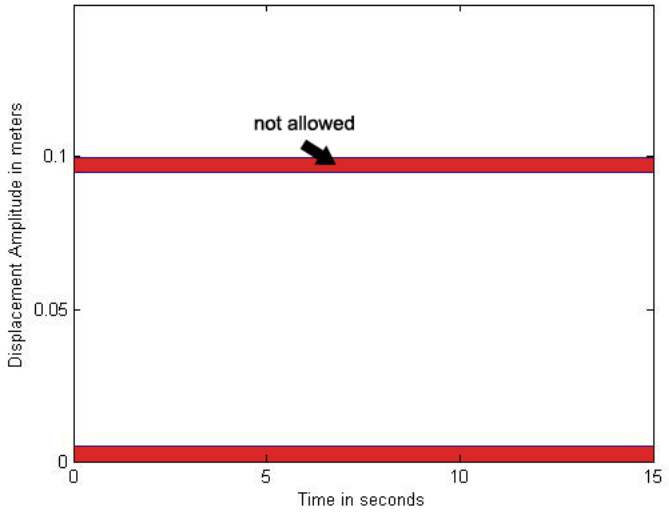

Figure 5.14 Constrained zones of the mass displacement amplitude

This was decided so that coupled system's transients are preserved as much as possible without being attenuated and trimmed by the stoppers.

The following tables were created, showing the values of the maximum voltage amplitude that can be applied to the control signal before the mass goes into the not-allowed zones for the defined coupled electromechanical system.

Table 5.1 Maximum values of voltage amplitude for frequency 0-7rad/s

Ω(rad/s)	**0**	**1**	**2**	**3**	**4**	**5**	**6**	**7**
A_ε (V)	120	70.4	70.8	67.4	67.4	59.6	64.2	55.8
X_{upper}(m)	.099738	.077123	.078031	.078769	.083978	.08193	.076093	.074196
X_{low} (m)	.099225	.007599	.005401	.005385	.006551	.00559	.007596	.005419
A_x (m)	.000513	.069524	.07263	.073384	.077427	.07634	.068497	.068778

Table 5.2 Maximum values of voltage amplitude for frequency 8-15rad/s

Ω(rad/s)	**8**	**9**	**10**	**11**	**12**	**13**	**14**	**15**
A_ε (V)	43.8	52.8	54.4	49	42.6	34.8	26	16.8
X_{upper}(m)	.092963	.092292	.09459	.095223	.094516	.094145	.093426	.092829
X_{low} (m)	.006043	.018429	.011524	.008861	.00836	.009692	.012389	.015464
A_x (m)	.08692	.073864	.083066	.086362	.086155	.084452	.081037	.077366

Table 5.3 Maximum values of voltage amplitude for frequency 16-23rad/s

Ω(rad/s)	**16**	**17**	**18**	**19**	**20**	**21**	**22**	**23**
A_ε (V)	7.8	6.6	16.6	28.2	40.4	53.4	66.4	7.8
X_{upper}(m)	.091602	.091412	.092325	.09207	.092077	.092307	.092372	.091602
X_{low} (m)	.019089	.022448	.025119	.028604	.032043	.035509	.038972	.019089
A_x (m)	.072513	.068964	.067206	.063466	.060034	.056798	.0534	.072513

Where:

A_ε: is the amplitude of the voltage signal (peak value)

X_{upper}: is the maximum point the mass reached when excited by Aε

X_{low}: is the minimum point the mass reached when excited by the Aε

A_x: is the range of the oscillation ($|X_{upper} - X_{low}|$).

These tables are but a short version of the table presenting the simulation results. At the appendix the full form of this table can be found containing the results of other variables as well. Information is presented about the peak-to-peak of the current, its complex envelope (both imaginary and real part),and velocity, when excited by the sinusoidal voltage signal of amplitude A_ε and frequency Ω, and a sinusoidal signal of half the amplitude A_ε for both the low pass equivalent and the band pass models.

By plotting the voltage amplitude against the different frequencies the system was tested:

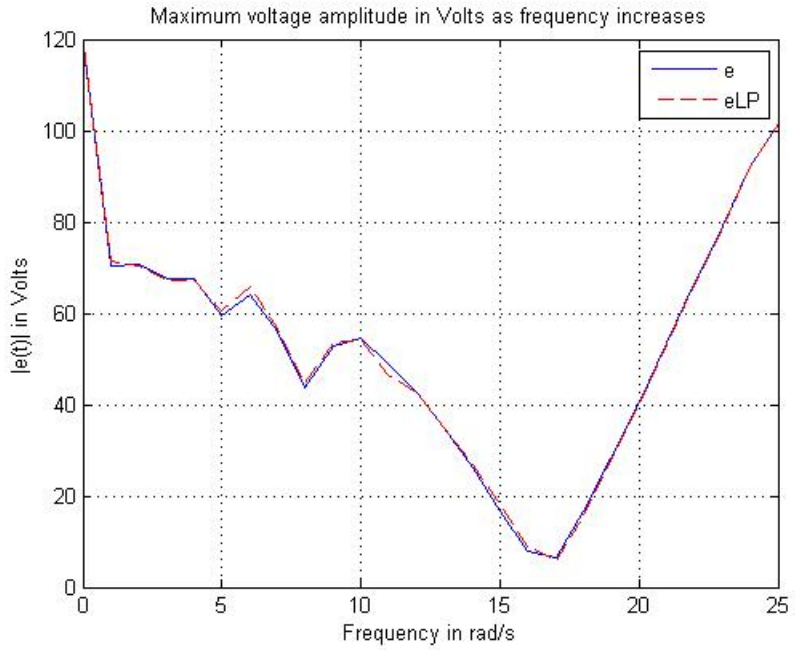

Figure 5.15 Amplitude of a sinusoidal voltage signal such as the displacement is limited below 0.095m and above 0.0005m over frequency.

It can be seen that the electromagnetic force is most effective at frequencies close to 16 rad/s. The low pass equivalent voltage signal (after appropriately divided by sqrt(2) to become a peak value) is represented in red, while the band pass voltage signal appears in blue. According to figure 5.15, it is directly seen that approximately 120Volts are needed to move the mass from point 0.05 to 0.095m for a signal at zero frequency (DC). However at frequency 17rad/s only 9 volts are needed for the same amount of displacement. This frequency requires the lowest amount of energy for a displacement of the mass to occur. As the frequencies increase, the voltage needed is increasing almost linearly; and the voltage signal effect becomes less apparent. The lowest the amplitude of

the voltage signal however, the more precision is needed for the controller in the DSP unit to perform calculations. To demonstrate this with some random numbers, let's suppose that 40volts are needed at frequency 5rad/sec for a change in the position of the mass of about 0.03m. For the same change, only 3volts are needed at frequency 16rad/s. The DSP controller would now need higher accuracy for the calculations, using floating point numbers with a lot of decimal digits to create such a small control signal and its response speed would be reduced a lot. In addition more expensive DSP units will be needed to be able to handle the signals at higher speeds with high accuracy.

The effect of the electromagnetic force is also visible when plotting the peak-to-peak values of the displacement signal versus the frequencies tested.

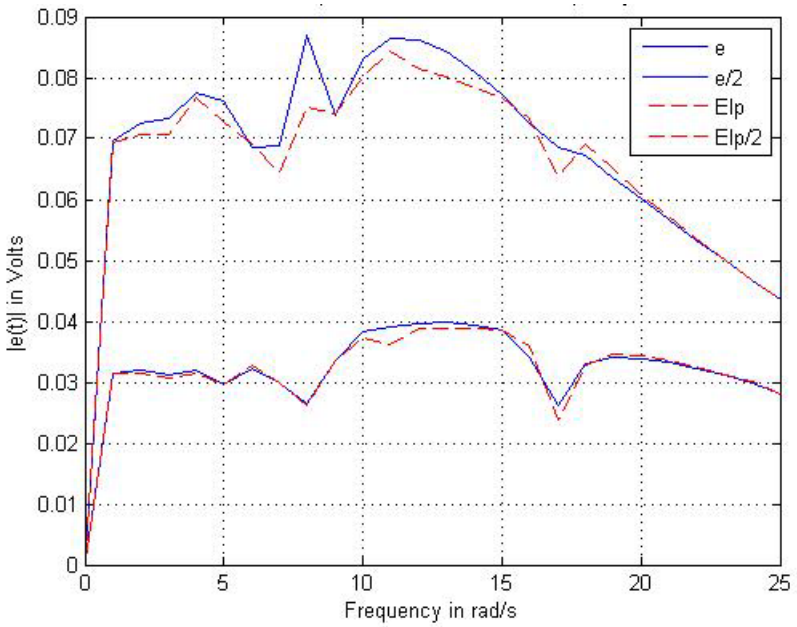

Figure 5.16 Range of the displacement when excited with a variable frequency and amplitude sinusoidal voltage signal

In those figures the behavior of the both band pass and low pass equivalent model is depicted when excited by two sinusoidal voltage signals of varying frequency, one with amplitude Aε and one with amplitude half as the first.

As the frequency grows larger, after about 15 rad/sec the range of the displacement (that is the maximum peak value minus the lowest peak value) grows smaller. This is also proven by the theory this study is based on, as the mechanical system is not affected by the higher frequencies of the carrier of signal of the electric circuit.

Slight differences can be noted between the values of the amplitude of the equivalent low pass voltage signal and the band pass signal. This is due to the fact that the transients in the low pass equivalent model peak slightly higher than those in the band pass model. As a result the averaging window that calculated those values in the algorithm would have caught those peaks and accordingly reduce the voltage excitation to avoid them. When the systems are excited by half the voltage it is seen that the response of the models is almost identical, with small variations that are acceptable since they are minimal. It is seen that the area from 8rad/s to 15rad/s provides the highest peak-to-peak values with of course the value of excitation voltage decreasing as the frequency increases till 16rad/s. Figure 5.17 presents the changes in the amplitude of the current. Having in mind that about 9 volts are required for an efficient electromagnetic force at frequency 17 rad/sec, we can easily see that only 36 Watts of power are needed to move the mass to the limits, in comparison with the 100 Watts that are needed if the system is excited at frequency 10rad/s.

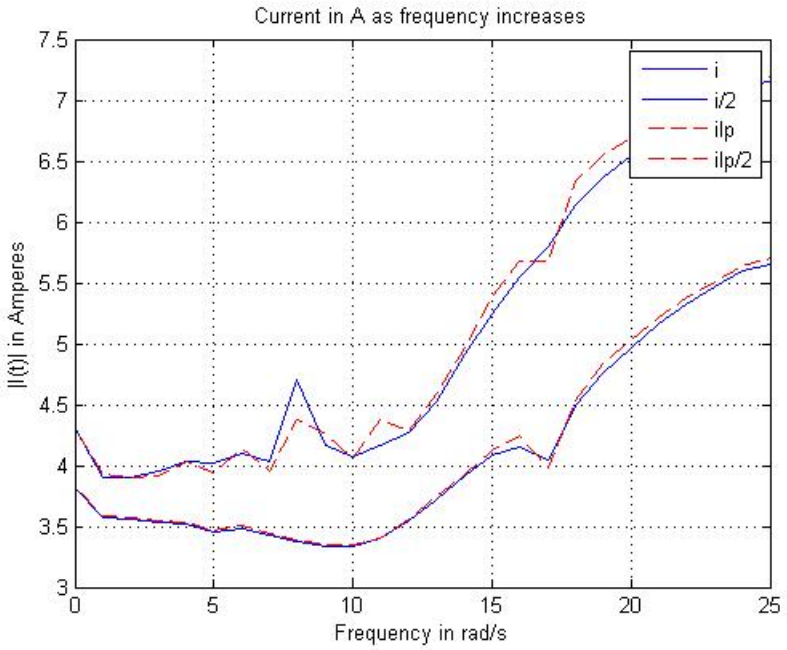

Figure 5.17 Amplitude of current for both systems as frequency increases

5.5 Determining the effect of the disturbance signal on the mass

Following the same test procedure, the coupled system was excited with a sinusoidal disturbance signal with frequency spanning the range 0-25radians/second and with such amplitude as the mass position would be constrained in the limits discussed before. No excitation voltage signal was present, other than the DC voltage required to hold the mass to point x=0.05m. The following tables demonstrate the effect the disturbance force has on the mass:

Table 5.4 Maximum amplitudes of the disturbance signal for frequencies 0-7rad/s

Ω(rad/s)	**0**	**1**	**2**	**3**	**4**	**5**	**6**	**7**
A_D (N)	1.97	1.95	1.9	1.81	1.64	1.58	1.82	1.52
X_{upper}(m)	.094495	.094382	.094472	.094325	.094297	.094432	.089437	.094678
X_{low} (m)	.094495	.030087	.030382	.030558	.029967	.02757	.015746	.025647
A_x (m)	0	.064295	.06409	.063766	.06433	.066862	.073691	.06903

Table 5.5 Maximum amplitudes of the disturbance signal for frequencies 8-15rad/s

Ω(rad/s)	8	9	10	11	12	13	14	15
A_D (N)	.97	1.5	1.72	1.41	1.38	1.1	0.79	0.5
X_{upper}(m)	.094306	.08637	.087215	.086336	.093173	.093802	0.093846	.093244
X_{low} (m)	.023922	.007853	.007613	.013487	.012916	.015032	.017179	.018603
A_x (m)	.070385	.078517	.079602	.072848	.080257	.078769	.076667	.07464

Table 5.6 Maximum amplitudes of the disturbance signal for frequencies 16-23rad/s

Ω(rad/s)	16	17	18	19	20	21	22	23
A_D (N)	.23	.19	.46	.78	1.11	1.46	1.84	2.22
X_{upper}(m)	.092216	.091334	.091826	.091946	.092052	.091894	.092003	.092089
X_{low} (m)	.020028	.021096	.021346	.021667	.022046	.022243	.022442	.022592
A_x (m)	.072188	.070238	.07048	.070279	.070006	.06965	.069561	.069496

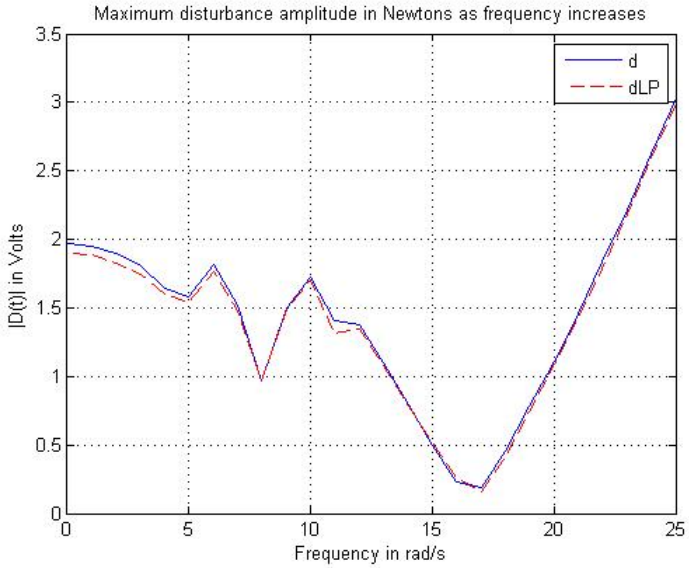

Figure 5.18 Maximum allowed amplitude for the disturbance force over frequency

Again it is directly seen that the curve of the disturbance force follows the same behavior as the curve of the voltage signal. At frequency 16rad/s the least amount of exogenous force is needed to move the mass between the defined space limits. As the frequencies

increase, the effect of the disturbance becomes less apparent till the point the mechanical system becomes immune to high frequency disturbances. The low pass equivalent model behavior is represented with the red line and again slight variations can be noted when compared to the band pass model result. This is accepted as discussed before, due to the dynamics of the low pass system. Those variations will become more apparent at higher amplitudes that push the mass displacement to the limits and are highly depended on the increment step the amplitude of the disturbance force is changed. The algorithm will select the smaller amplitude so that the mass position will not exceed the predefined limits.

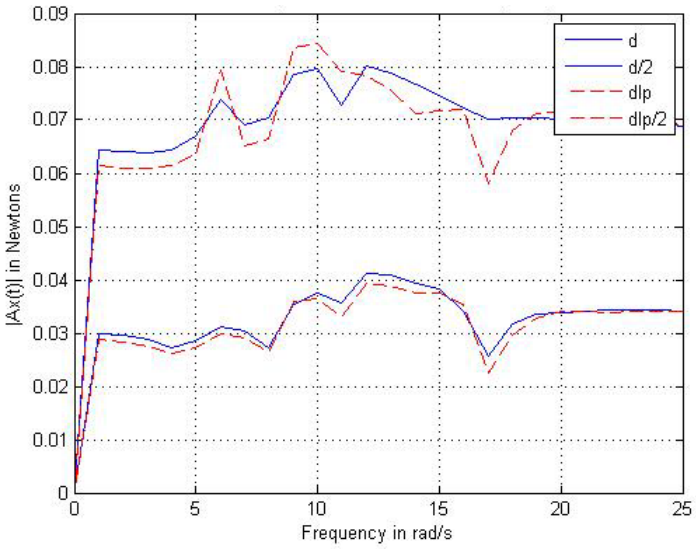

Figure 5.19 Range of the displacement when excited with a variable frequency and amplitude disturbance signal

But as the effect of the force on the mass increases and the amplitude of the disturbance force decreases, higher precision is needed since a slight change on the amplitude will result in a strong change in the displacement of the mass. The increment step that was used to find the maximum amplitudes for the exogenous disturbance force is 0.01N.

Therefore with a smaller increment step we would expect more accurate results at the system's limits.

When the systems are excited with half as much the disturbance force the effects of the saturation of the algorithm disappear, as it is seen at figure 5.19. Therefore we can use the half amplitude signals for further study and for making accurate conclusions for the effect of the disturbance force and the system behavior in general.

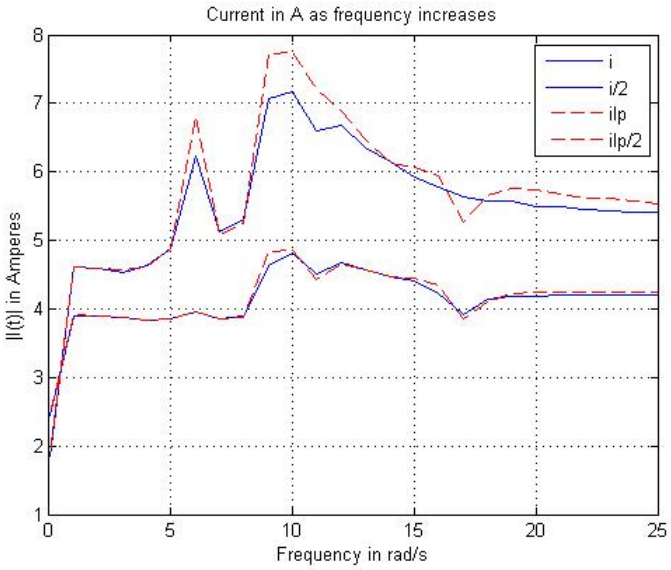

Figure 5.20 Amplitude of current for a sinusoidal disturbance force in both systems as frequency increases.

In figure 5.20 the maximum recorded amplitudes of the current are presented. Using the information of this graph along as figure 5.19, we can see the following effect that is expected theoretically and also proven practically:

The change in the displacement on the mass will be translated in a change in the inductance L of the inductor, that would be translated in a change in the amplitude of the current signal. The current however is inversely proportional to the inductance L which is given by:

$$L = L_0 + L_1 x$$

The inductance tries to oppose the rise of the current, and the maximum value of L is acquired when the mass is close to the inductor, that is at the point x=0.1m. When the mass moves away from the electromagnet, the inductance value is lowered and as a result the current will acquire greater values. In other words high values of the current as presented in figure 5.20 indicate that the mass has moved further away.

The exact opposite effect is demonstrated when the system is excited with a sinusoidal voltage signal instead of a disturbance signal. The voltage signal needs more power in order to increase the electromagnetic force and as a result to move the mass further away. Of course the relationship between the mass position and the inductance is still there. This time not so obvious however, since the inductor will still oppose the rate the current changes by lowering the current amplitude value when the mass is close to the electromagnet, but this change will be harder to notice. This is due to the fact that when the mass is moved by a voltage excitation signal, higher amounts of voltage are required to displace the mass closer to the system limits, effectively increasing the values of the current.

5.6 RMS errors

In order to quantify the differences of the bandpass and lowpass signals presented in the above figures, the root-mean-squared error function was used:

$$RMSE = \sqrt{\frac{\sum_{i=0}^{n} (x_{BP_i} - x_{LP_i})^2}{n}} \quad (5.1)$$

where:

n: is the number of samples

x_{bp}: is range of the displacement signal for the bandpass model

x_{lp}: is the range of the displacement signal for the lowpass model

Table 5.7 RMS error values for the voltage excitation tests

RMSE of the current for e	0.1158
RMSE of current (for e/2)	0.0402
RMSE of displacement for e	0.0032
RMSE of displacement for e/2	9.3174e-004

Table 5.8 RMS error values for the disturbance excitation tests

RMSE of the current for d	0.2755
RMSE of current (for d/2)	0.0581
RMSE of displacement for d	0.0039
RMSE of displacement for d/2	0.0014

The above tables present the RMS error values between the band pass and the low pass equivalent model current and displacement signals. The current amplitude and the range of the mass displacement of the both models were recorded when excited by:

- the maximum allowed control voltage amplitude e
- half the maximum allowed control voltage amplitude e/2
- the maximum allowed disturbance force amplitude d
- half the maximum allowed disturbance force amplitude d/2

Again it is directly seen that for half the amplitude of the input signal excitation, the models produce almost identical results, with very small variations. The following plots

indicate the RMS error for the distinct frequency range of 0-25rad/sec that the system was put under excitation test.

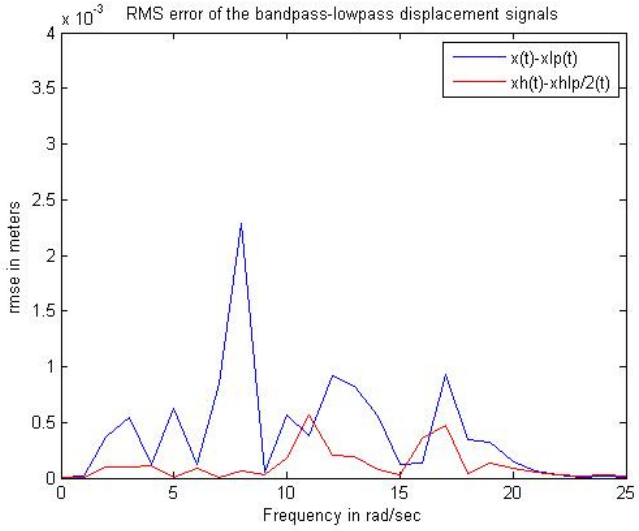

Figure 5.21 RMS error between the band pass and the lowpass displacement signal for a control voltage excitation

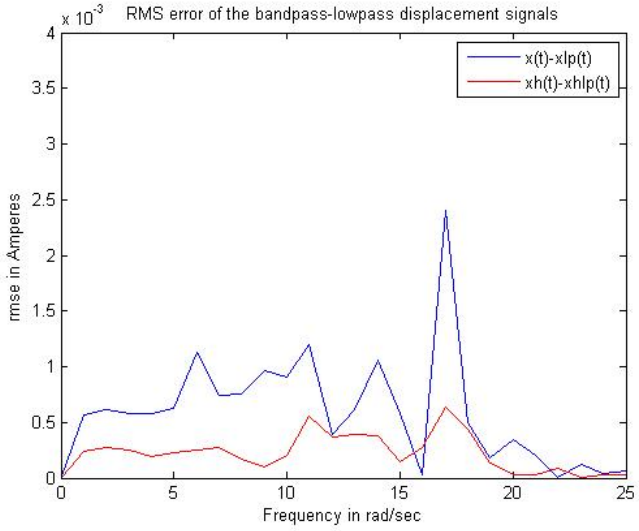

Figure 5.22 RMS error between the band pass and the lowpass displacement signal for a disturbance force excitation

5.7 Ramp excitation

After examining the behavior of the coupled system when excited by a sinusoidal voltage and a sinusoidal disturbance signal of various amplitudes and frequencies, it relationship between the mass displacement, the voltage signal, the disturbance signal and the current signal is still not evident. The next step is to excite the system with a ramp function. This method will clearly depict how the mass behaves when excited by a linearly increasing control voltage or a linearly increasing exogenous disturbance signal.

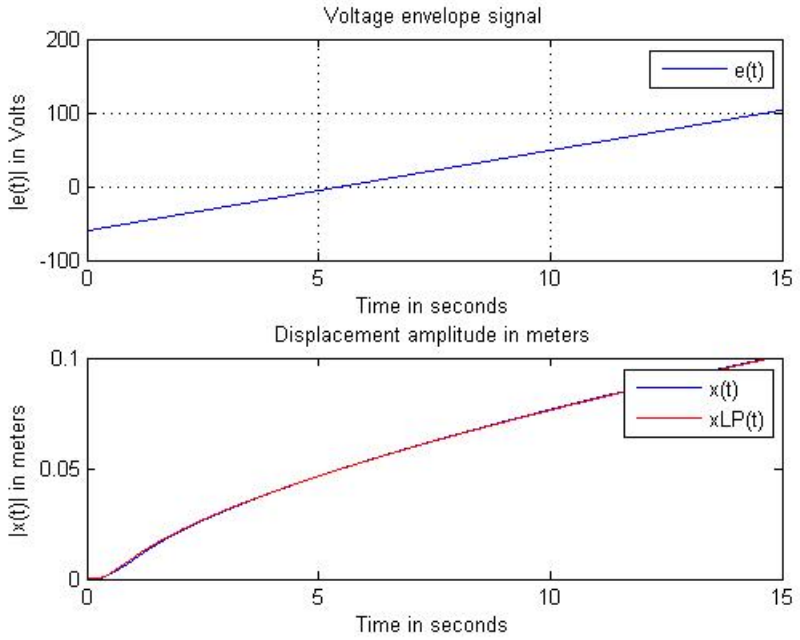

Figure 5.23 Displacement of the mass when excited by a ramp function voltage signal

For a voltage input signal that has the form of a linearly increasing ramp function the band pass and the low pass equivalent system behavior is recorder in figure 5.23. Indeed the non linear response of the mechanical system is seen especially in the region between 0.5 seconds and 5 seconds. What defines this nonlinearity is the velocity of the mass, since it represents the rate of change in the displacement, as it more easily seen in figure

5.24. If the velocity was constant, then we would have a linear response since the input is also linear.

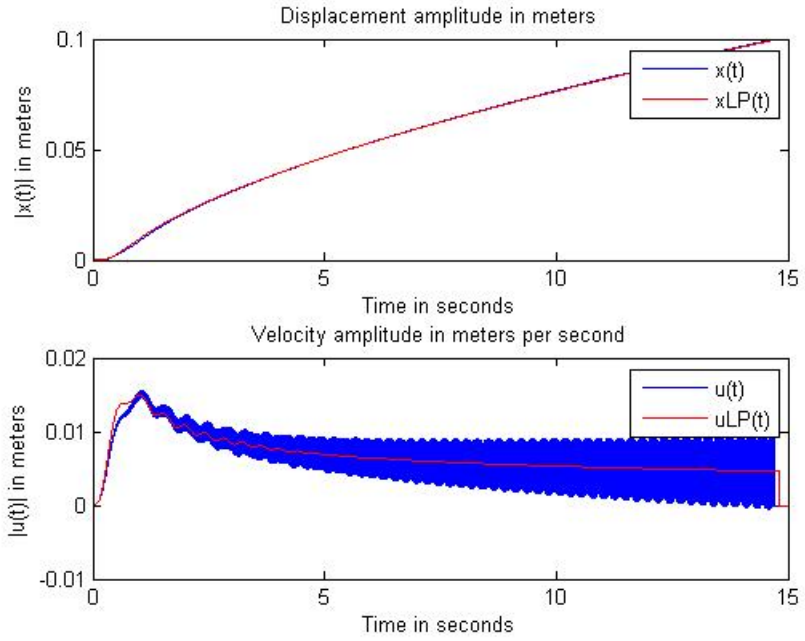

Figure 5.24 Displacement and velocity signals for a ramp control voltage input.

Using the ramp excitation method we can gather information about other important signals as well, such as the behavior of the real and imaginary part of the complex envelope of the current.

After generating the data from these test series it is possible to compare the imaginary part of the current against the displacement signal and against the voltage signal, to determine the effect of the latest to the current. Indeed the nonlinear relationship between those signals is found on figure 5.25:

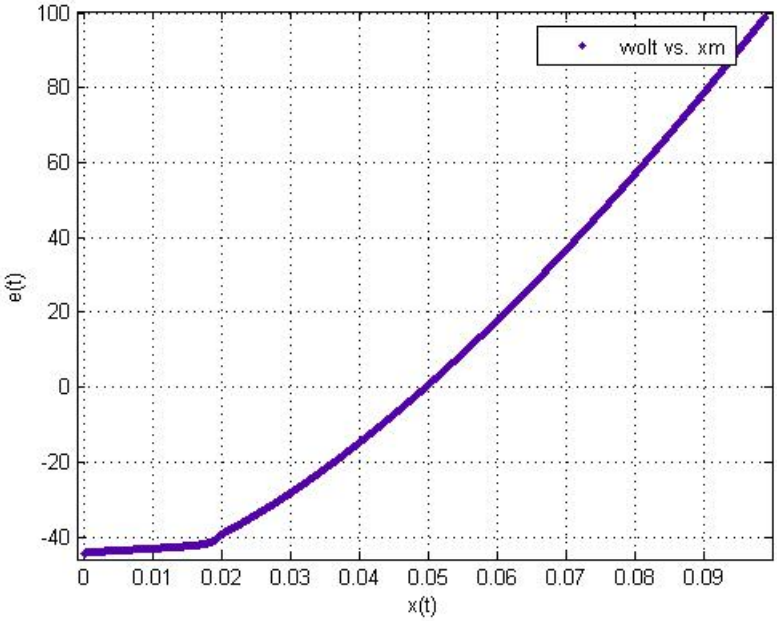

Figure 5.25 Voltage vs displacement (ramp excitation method)

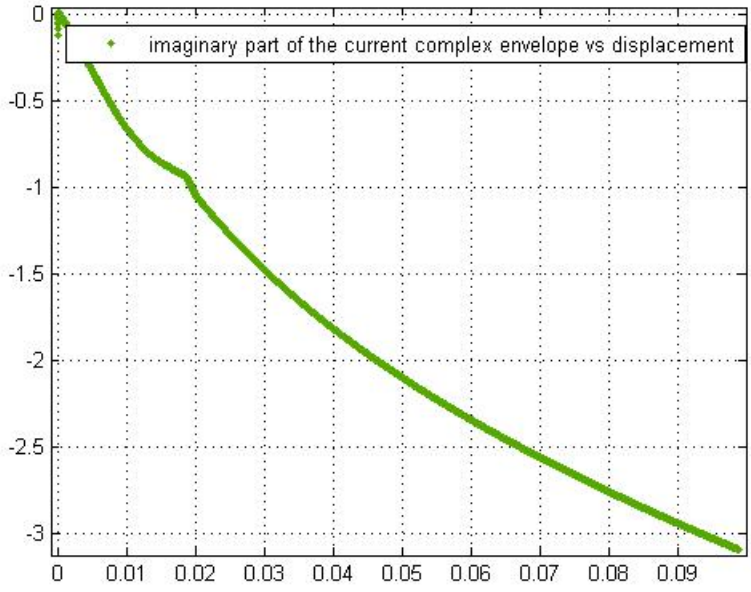

Figure 5.26 Imaginary part of the current complex envelope vs displacement

Figure 5.26 shows the degradation of the imaginary part of the current complex envelope signal for the displacement of the mass. Using the above two graphs we can compose figure 5.27, showing the relationship between the imaginary part of the current and the voltage.

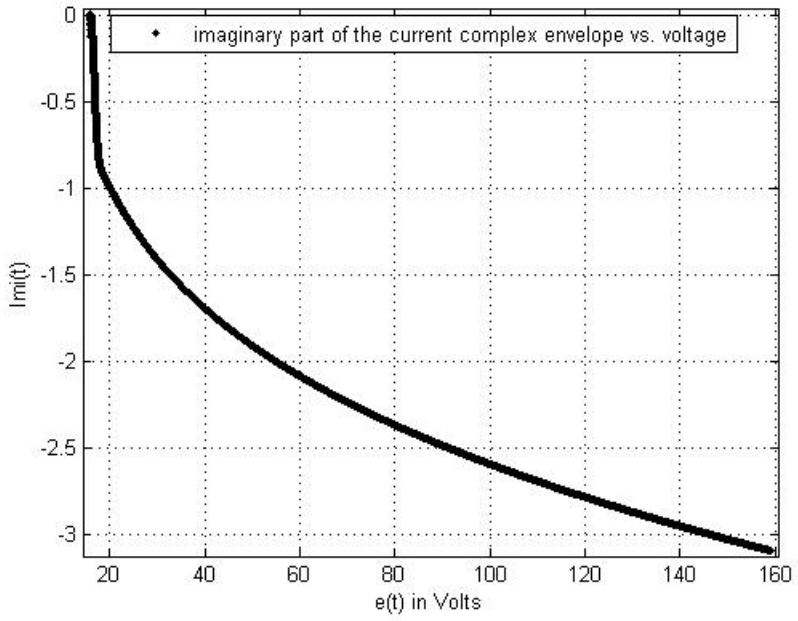

Figure 5.27 Imaginary part of the current complex envelope vs voltage (ramp excitation method)

By performing curve fitting one can obtain a mathematical relationship connecting the voltage and the current, or the voltage and the displacement. A polyonymous function of third degree would be sufficient with 95% confidence levels. Curve fitting allows for two ways to actually control the position of the mass: Provided that there is no disturbance force on the system, by knowing the displacement of the mass, one can use the appropriate relationships described in the graphs above to directly calculate the amount of voltage amplitude that corresponds to that position. The alternative approach is to measure the current through the resistor. Again by using the corresponding mathematical

relationship one would be able to calculate the exact position of the mass based on the imaginary part of the current complex envelope, and then from that calculate the amount of voltage that corresponds to that point.

When an exogenous disturbance force is introduced to the system, one would have to determine the effect of the force on the current, then translate this information to mass position, and then use the above graphs or mathematical relationship to calculate the voltage needed to change the displacement.

5.8 Earnshaw's theorem of static instability

When the system is excited by a linearly increasing disturbance signal the case is a little more complex. The system is oversensitive to the sudden changes that come from the disturbance force, due to the fact that there is a constant electromagnetic force applied to keep the mass at the position 0.05m. This constant magnetic force is also a requirement, since the inductor needs to be run by current for any change in inductance to occur due to the change in the mass position. However the magnetic force coming from the inductor cannot guarantee stability. In fact there are cases where the magnetic force would produce static instability, because of the inverse square law that governs the magnetic force, a phenomenon that is known as elastic buckling or divergence [12]. Samuel Earnshaw, a British mathematician first proved in 1842 that it is impossible for a static set of charges, magnetic and electric dipoles, and steady currents to be in a stable state of equilibrium without any mechanical or other feedback forces to compensate for that. [12]

Indeed this phenomenon can be easily seen in the electromechanical system studied here, when the system is excited with a constant disturbance force that opposes the electromagnetic force and follows the direction of the restoring force of the spring. In this case, the magnitude of the electromagnetic force will be changed due to the displacement of the mass, and it will not be able to compensate for the effect of the disturbance force.

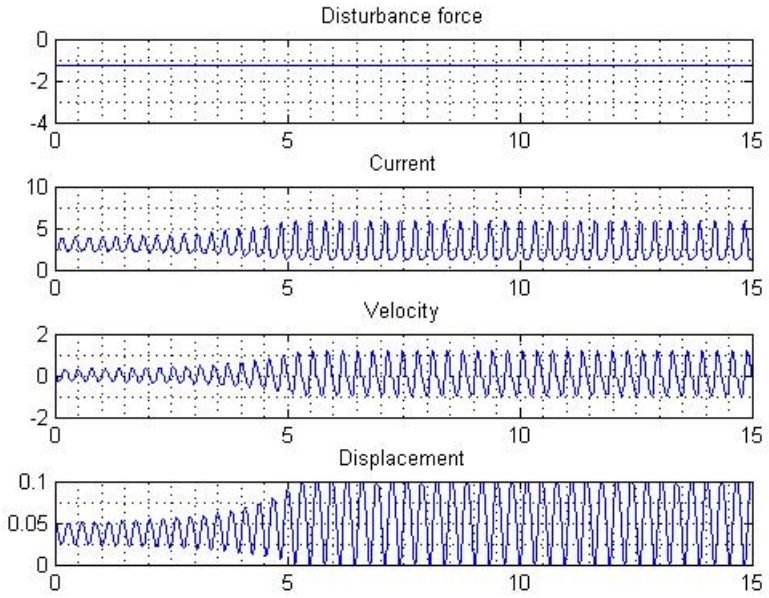

Figure 5.28 A constant disturbance force opposing the electromagnetic magnetic force

The system will then enter a state of constant oscillation, as figure 5.28 above shows for the low pass equivalent model. It is for that reason that feedback control is mandatory in order to operate and stabilize the coupled system, making the analysis of electromechanical systems very important.

6. FRAMEWORK FOR ESTIMATING THE DISPLACEMENT SIGNAL BY MEASURING THE CURRENT SIGNAL

6.1 Overview

This section will propose a framework, by which sensorless control can be applied to control the position of the mass. No position or other sensors will be required to indicate the displacement signal, other than a simple ammeter measuring the current through the resistor in the electrical circuit. Using the readings of the ammeter, the current signal will be appropriately manipulated to estimate the displacement signal for the following two cases:

- System excitation with a DC control voltage signal and a variable exogenous disturbance force.
- System excitation using a variable control signal and a variable exogenous disturbance force signal.

6.2 Estimating the mass position when they system is excited by a DC control voltage signal and a variable disturbance force.

As shown in the previous chapters the displacement of the mass introduces a change in the current of the electrical circuit. Using the signals of the low pass equivalent model, this change can be directly seen in the waveform of the imaginary part of the complex envelope of the current, as figure 6.1 presents.

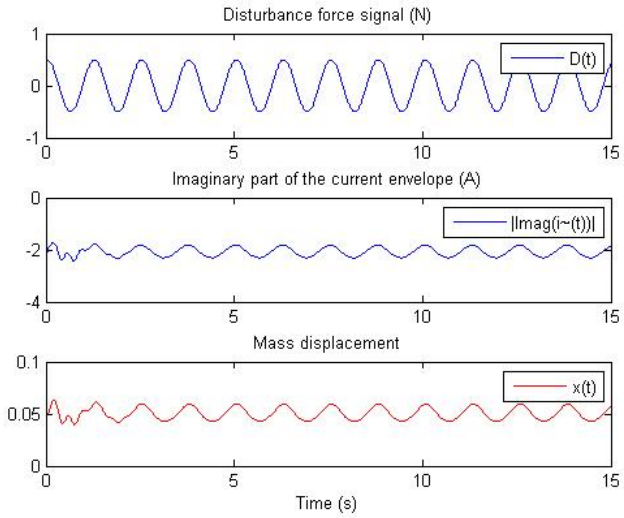

Figure 6.1 The change of the imaginary part of the current complex envelope due to the displacement of the mass

The waveform of the imaginary part of the current envelope will follow closely the displacement of the mass for each frequency and amplitude of the exogenous disturbance force signal. Slight variations will however appear at the peaks of the current signal for higher frequencies mostly due to the nonlinearity of the coupling of the systems. This is easily seen after appropriately manipulating the imaginary part of the current envelope signal to scale it with the actual displacement signal, after the system has been excited with a filtered white noise exogenous disturbance form.

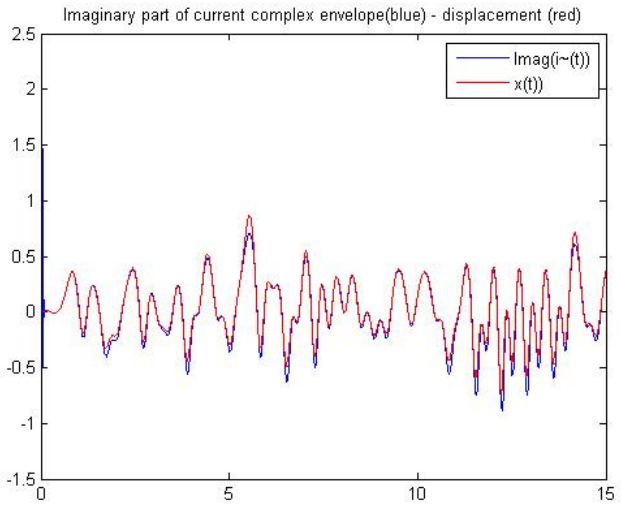

Figure 6.2 The imaginary part of the current envelope estimating the displacement signal when excited by a white noise disturbance force signal.

To compensate for that, a very small nonlinear increasing term can be added to the signal that will estimate the displacement of the mass, that will be depended on the amplitude and frequency of the disturbance signal. The methodology proposed to generate the estimated displacement signal through current measurement is as follows:

1. Excitation of the coupled system using a sinusoidal disturbance force signal of amplitude 0.5N for the frequencies up to 25rad/sec.
2. Recording of the peak-to-peak values of the displacement signal, and the imaginary part of the current complex envelope signal.

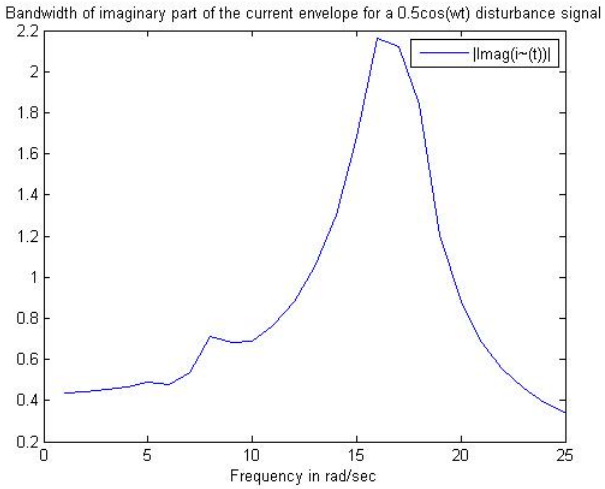

Figure 6.3 Range of imaginary part of the current complex envelope for a 0.5cos(ωt) disturbance signal

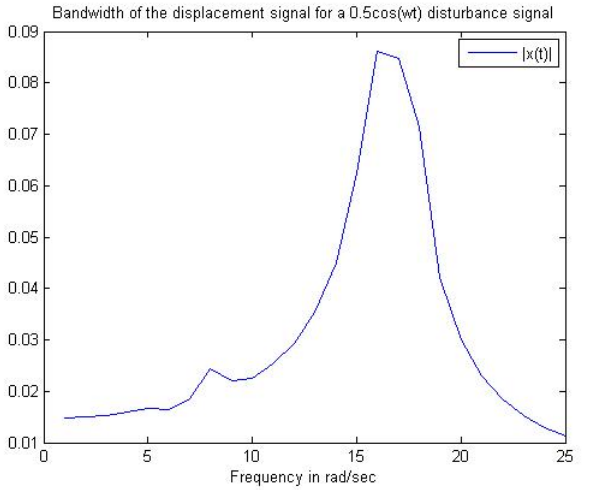

Figure 6.4 Range of the displacement signal for a 0.5cos(ωt) disturbance signal

3. By dividing the signals presented in figure 6.3 and 6.4, the term by which the current signal needs to be multiplied to match in amplitude and estimate the actual displacement signal is obtained:

$$I_{bw}(\omega) = \frac{\left|\max(\mathrm{Im}\,ag(\tilde{i}(t,\omega))) - \min(\mathrm{Im}\,ag(\tilde{i}(t,\omega)))\right|}{\left|\max(x(t,\omega)) - \min(x(t,\omega))\right|}$$

Where:

ω is the frequency of the disturbance force signal

4. Removing the zero frequency (DC) component and estimating the displacement signal using:

$$\hat{x} = \frac{1}{I_{bw}(\omega)}(\text{Imag}(\tilde{i}(t)\text{-}\tilde{I}(0))$$

The following graphs present the estimated displacement signal and the actual displacement signal (after having removed the DC component), for various amplitude and frequencies of a disturbance force signal.

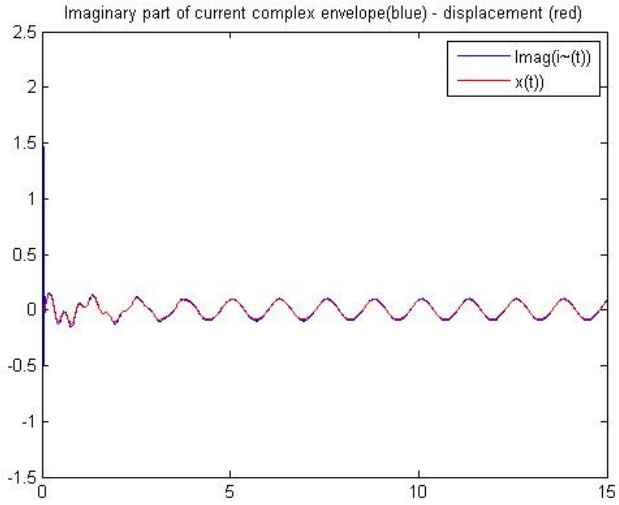

Figure 6.5 Estimated displacement signal for a sinusoidal disturbance force of amplitude 0.2N and frequency 5rad/sec.

It is easily seen that in figure 6.5 the actual displacement signal (blue) peaks a little higher than then estimated signal using the current complex envelope. For the purpose of this study these slight variations will be neglected, but for a more accurate estimation of

the displacement signal a very small nonlinear term should be included as proposed before.

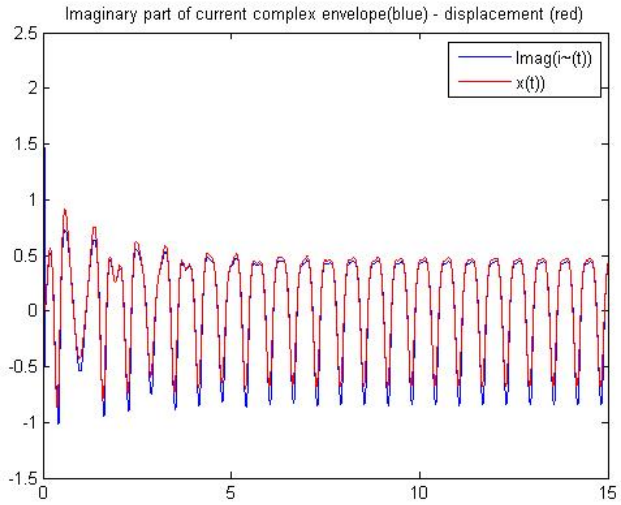

Figure 6.6 Estimated displacement for a sinusoidal disturbance force of amplitude 1N and frequency 10rad/sec.

6.3 Estimating the mass position when they system is excited by a variable control voltage signal and a variable disturbance force signal

The current in the electrical circuit is depended upon the mass position due to the coupling factor L=L0+L1x. However it is also depended on the voltage signal applied to the electrical circuit. The following figure presents the effect of the control voltage signal on the current, and indicates the need to compensate for that effect when estimating the displacement signal. The system is excited with a very slow sinusoidal voltage signal of frequency 2 rad/sec and amplitude 10V. A sinusoidal disturbance force is also apparent of amplitude 0.5N and frequency 5rad/sec.

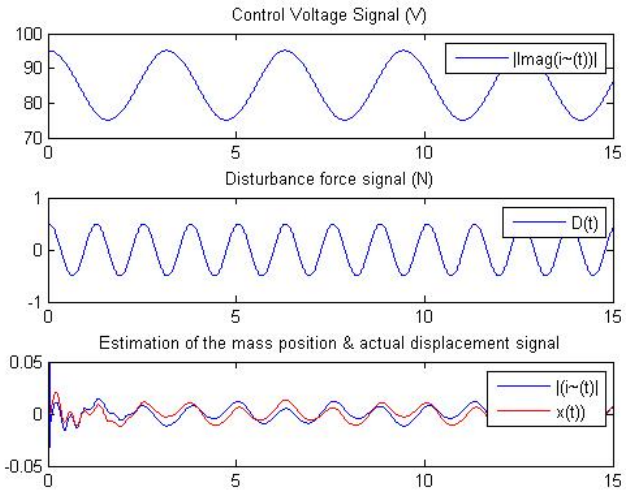

Figure 6.7 Estimation of the displacement signal and the need for compensation for the effect of the control voltage signal

In order to remove the effect of the control voltage signal the following steps were taken:

1. The coupled system was excited with a sinusoidal control voltage signal of amplitude 10Volts for frequencies up to 25rad/sec.
2. The peak-to-peak values of the imaginary part of the current complex envelope and the displacement signal were recorded.
3. From the above the factor I_{bw} was calculated as follows:

$$I_{bw}(\omega) = \frac{\left|\max(\mathrm{Im}\,ag(\tilde{i}(t,\omega))) - \min(\mathrm{Im}\,ag(\tilde{i}(t,\omega)))\right|}{\left|\max(x(t,\omega)) - \min(x(t,\omega))\right|}$$

Where

ω is the frequency of the control voltage signal

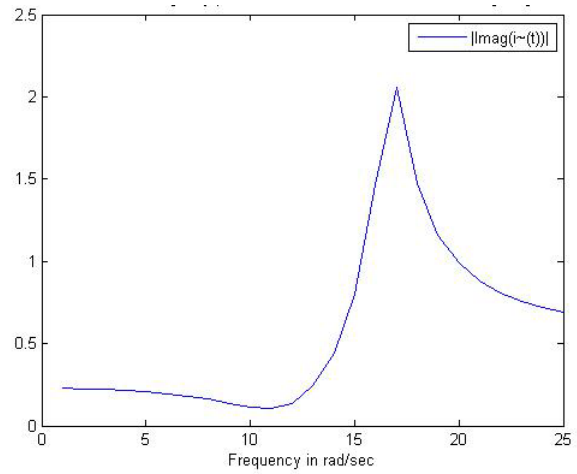

Figure 6.8 Peak-to-peak values of imaginary part of the current envelope for a 10cos(ωt) control voltage

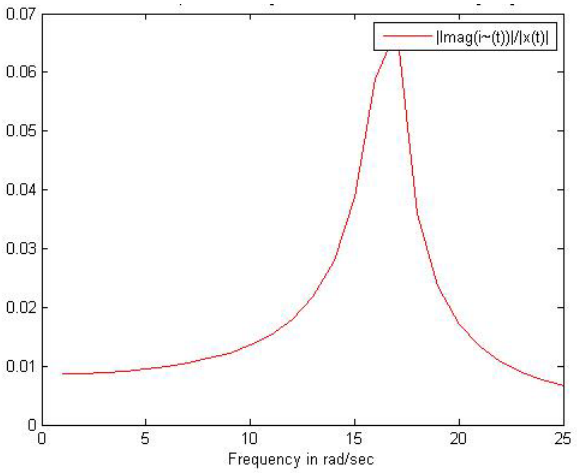

Figure 6.9 Peak-to-peak values of the displacement for a 10cos(ωt) control voltage

4. An additional model was created that represents the behavior electrical sub system when the mass position is constant at x=0.05m. The input of this model is the same sinusoidal control voltage signal that will excite the original coupled electromechanical system. The imaginary part of the current complex envelope is then recorded.

5. The estimated displacement signal is found by:

$$\hat{x} = \frac{1}{I_{bw}(\omega)}(\text{Imag}(\tilde{i}(t)\text{-}\tilde{I}(0)) - \text{Imag}(\tilde{i}_{x=0.05}(t)+\tilde{I}_{x=0.05}(0))$$

Where:

$\text{Imag}(\tilde{i}(t))$ is the imaginary part of the current complex envelope of the coupled electromechanical system.

$\tilde{I}(0)$ is the DC component of the imaginary part of the current envelope due to the DC voltage source applied to maintain the mass to the equilibrium point.

$\text{Imag}(\tilde{i}_{x=0.05}(t)$ is the imaginary part of the current envelope for the new model where the mass position is always kept constant at x=0.05

$\tilde{I}_{x=0.05}(0)$ is the DC component of the imaginary part of the current envelope of the new model.

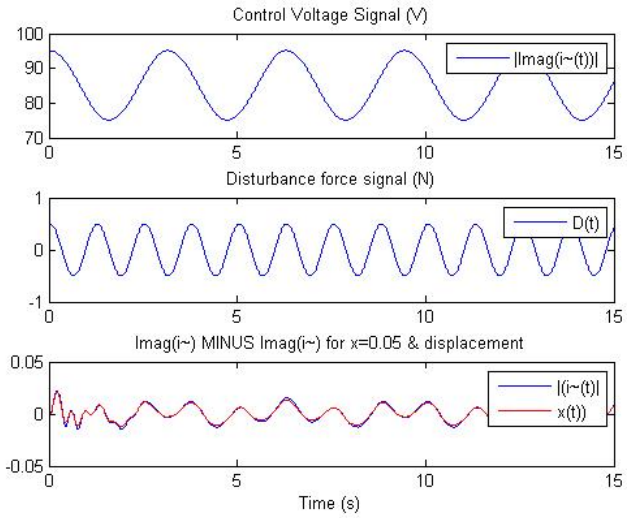

Figure 6.10 Estimation of the displacement signal when taking into account the control voltage signal

In figure 6.10 the coupled system is excited with sinusoidal disturbance signal of the form 0.5cos(5t) and a control voltage signal is also apparent of the form 10cos(2t). It is directly seen that after taking into account the effect of the voltage signal on the imaginary part of the current complex envelope, the estimated signal can now accurately reproduce the displacement of the mass.

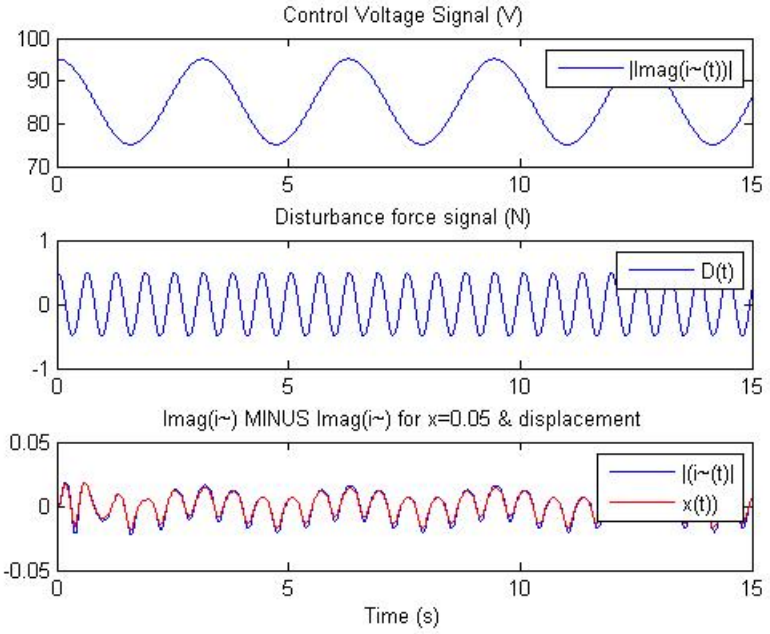

Figure 6.11 Estimation of the displacement signal when taking into account the control voltage signal for a disturbance force of frequency 10rad/sec

Even if the frequency or amplitude of the disturbance force increases, the estimated displacement signal will be able to accurately follow the changes in the mass position, as figure 6.11 shows. However for more accurate estimations, the need for a very small nonlinear term dependent on frequency is still there, as in frequency 15rad/sec the difference in the peaks of the actual displacement signal and the estimated displacement signal using the imaginary part of the current complex envelope is more visible (fig.6.12).

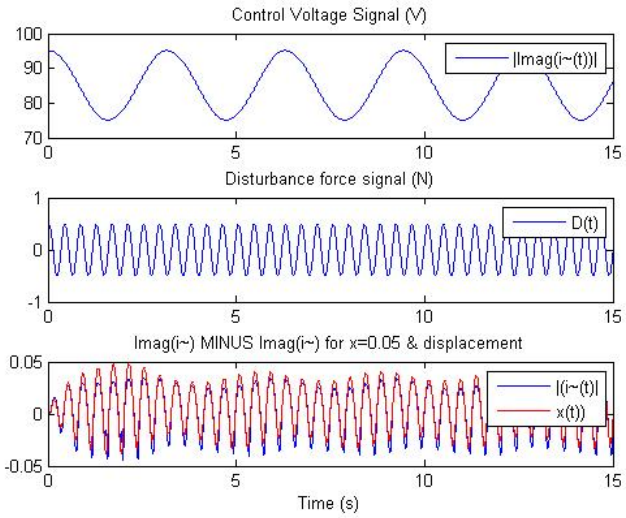

Figure 6.12 Estimation of the displacement signal when taking into account the control voltage signal for a disturbance force of frequency 15rad/sec

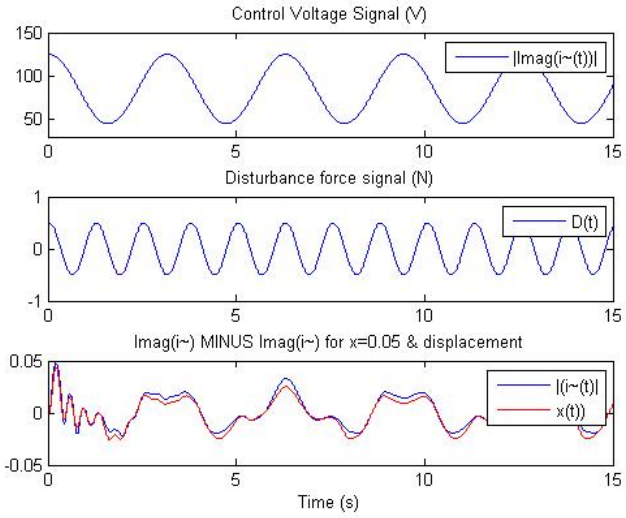

Figure 6.13 Estimation of the displacement signal when taking into account the control voltage signal for a voltage signal of the form 40cos(5t)

The same holds true when for example the control voltage signal is four times as large. A very small nonlinear term is again needed to provide very small corrections to the

amplitude of the estimated displacement signal to allow more accurate estimation, as figure 6.13 clearly indicates.

6.4 Extracting the complex envelope of the current signal in real-time using the band pass model

One of the main advantages of the low pass equivalent model is that only the complex envelope of the band pass signals found in the band pass model are required to simulate the dynamics of the coupled electromechanical system. This allows for direct calculations for estimation of the mass position as shown in the previous section. In reality however the system we have in hand is band pass and for example the current signal that we can measure through the resistor is also band pass. For that reason a methodology is proposed here to extract the low pass complex envelope of the band pass signals using a Hilbert Filter.

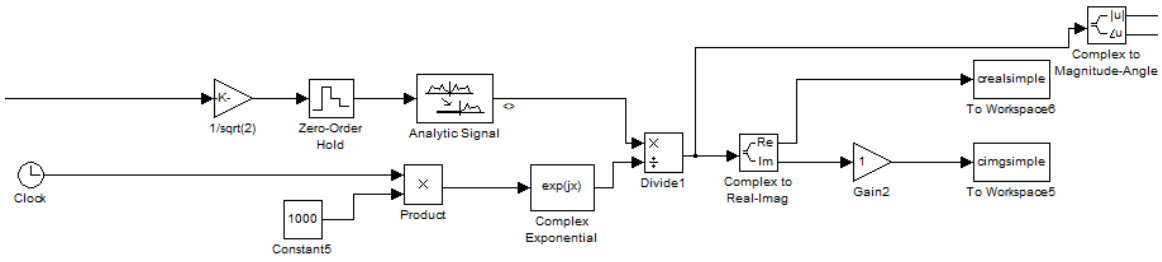

Figure 6.14 Extracting the complex envelope of the band pass current signal using Hilbert Filter

By measuring the current through the resistor in the electrical circuit we obtain a band pass signal containing the high frequency carrier signal modulated by a low frequency envelope. The continuous signal is then sampled using a zero order hold to be converted to discrete form. The analytic signal block is composed by a FIR filter of order that will phase shift the input by 90 degrees, thus providing the complex Hilbert transform of the

real input signal. This signal is then added to the actual input signal effectively creating the complex preenvelope as discussed in section 3.3.1. By dividing the output of the analytic signal block by $\exp(j\omega_{\varepsilon}t)$ the complex envelope of the input is finally obtained. The FIR filter used to produce the Hilbert transform of the input signals will introduce a group phase delay of 50samples, as shown in the next figure.

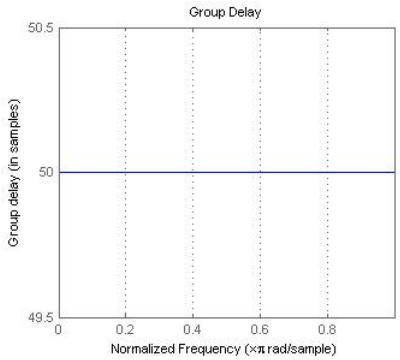

Figure 6.15 Group delay of 50samples of the FIR Hilbert filter

For that reason and to perform comparison of the actual displacement signal with the estimated signal produced by the imaginary part of the current all signals other than the current signal need to be delayed by 50samples in order to compensate for the latency introduced by the FIR filter.

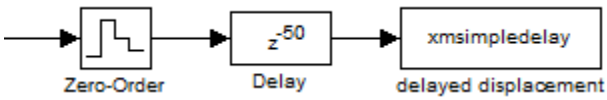

Figure 6.16 Delaying the displacement signal by 50 samples

This can be done easily by sampling the signals and then delaying them by 50samples using the Delay block of Simulink, as figure 6.16 shows.

7. CONCLUSIONS

The coupling of the electromechanical system studied in this document is of high interest due to the nonlinearity introduced by the magnetic force produced by the coil in the electrical circuit that is directly affecting the position of the metallic mass of the mechanical sub system. The change in the position will additionally introduce a change to the inductance of the coil; thus resulting in a change to the current. The signals coming through the electrical circuit contain high frequencies, due to the high frequency carrier signal. The mechanical subsystem however will not be affected at all by those high frequency changes. As it is seen, the mechanical system acts as a filter, filtering out all frequencies higher than double its natural frequency. For that reason it is possible to modulate the high frequency carrier signal by a low pass voltage envelope with low frequencies close to the natural frequencies of the mechanical system. Due to this fact the advantages of the low pass equivalent model presented are directly seen.

In order to simulate the dynamics of the coupling of the system using the band pass model, one would have to use a really high sampling rate, that would be at least two times the highest frequency present on the system, according to the Nyquist theorem. Thus the sampling rate is highly depended upon the frequency of the carrier signal in the electrical circuit. This effectively increases the simulation times needed to produce results and requires high computable power and resources to perform the calculations.

The low pass equivalent model in contrast, is able to fully represent the dynamics of the band pass system, using only the low frequency complex envelopes of the band pass signals. Since the frequencies of those signals are close to the natural frequency of the mechanical sub system, the sampling rate can effectively be very small. Performance issues additionally arise when using Matlab's embedded functions and S functions. Although state-space representation of the differential equations describing the system is a straight forward way to model the dynamics in Simulink the compiler has to be called each time a variable changes (including time) resulting in very slow simulation times. For that reason it is seen that using the basic blocks will provide much faster simulations.

Earnshaw's theorem of static instability is directly observed in the test cases performed in this document. A feedback control system is needed to maintain the stability of the system when the system is excited by various inputs, such as a constant disturbance force with the opposite direction of the magnetic force produced by the coil. In order to implement a feedback control system however, one would need to accurately identify the position of the mass using some kind of a sensor. As proposed here, a sensorless way to identify the displacement of the mass is possible, only through measuring the current in the electrical system. The effect of the displacement of the mass on the current waveform depends upon the frequency of the change of position, as well as the range of the displacement. Additionally the current waveform already includes the effect of the voltage source signal and thus this has to be removed in order to accurately estimate the position of the mass. According to the results presented in this thesis, it is seen that the displacement of the mass is directly related to the imaginary part of the complex envelope

of the current signal. By measuring the change of the peak-to-peak values for a constant amplitude sinusoidal voltage and disturbance force signal for the frequency ranges close to the natural frequency of the coupled system, one can calculate the factor by which the imaginary part of the current envelope signal needs to be multiplied in order to estimate and match the amplitude of the actual displacement signal. In this way using only measurements of the current it is possible to estimate the position of the mass with very small variations. Since the change in the current due to the mass displacement depends not only on the frequency and amplitude of the displacement but also on the frequency and amplitude of the control voltage signal, a very small magnitude nonlinear term would need to be added to the estimated signal to compensate for the small variations appearing in frequencies close to the resonant frequency of the coupled system.

8. APPENDIX

8.1 Matlab source files

8.1.1 Parameters of the system

```
t1=15;
w1=0;
w2=0;
w3=0;
d1=0;
d2=0;
d3=0;
e1=0;
e=0;
d=0;
input=0;
e2=0;
w=0;
m=0.25;
k=25;
b=.5;
c=0.00002;
r=10;
l0=0.05;
l1=0.5;
DC=85.1481;
```

8.1.2 Algorithm for finding the maximum voltage amplitude (mx.m)

```
clear stoixeia
for i=1:26
e=jem(i);
w=tt(i);
ww=tt(i);
simulation;
```

```
clear m1 m2 m3
for l=15000:length(t)

   m1(l-14999)=xm1(l, 1);
   m2(l-14999)=z3(1,2,l);
   m3(l-14999)=xm1(l, 2);
end;


up=max(m1);
low=min(m1);
if i==1
  low=up;
end;
band=abs(up-low);
maxcur=max(m2);
mincur=min(m2);
bandcur=abs(maxcur-mincur);
maxvel=max(m3);
minvel=min(m3);
bandvel=abs(maxvel-minvel);

stoixeia(1, i)=e;
stoixeia(2, i)=up;
stoixeia(3, i)=low;
stoixeia(4, i)=band;
stoixeia(5, i)=maxcur;
stoixeia(6, i)=mincur;
stoixeia(7,i)=bandcur;
stoixeia(8, i)=maxvel;
stoixeia(9, i)=minvel;
stoixeia(10,i)=bandvel;

e=vltglp(i);
simulationLP;
clear m1 m2 m3 m4 m5
for l=15000:length(t)

   m1(l-14999)=xm(l);
   m2(l-14999)=cimg(l);
   m3(l-14999)=creal(l);
   m4(l-14999)=z2(l);
   m5(l-14999)=veloc(l);
end;
up=max(m1);
```

```
low=min(m1);
if i==1
  up=max(m1);
  low=up;
end;
band=abs(up-low);
maxcimg=max(m2);
mincimg=min(m2);
bandcimg=abs(maxcimg-mincimg);
maxcreal=max(m3);
mincreal=min(m3);
bandcreal=abs(maxcreal-mincreal);
maxcur=max(m4);
mincur=min(m4);
bandcur=abs(maxcur-mincur);
maxvel=max(m5);
minvel=min(m5);
bandvel=abs(maxvel-minvel);

stoixeia(11, i)=e;
stoixeia(12, i)=up;
stoixeia(13, i)=low;
stoixeia(14, i)=band;
stoixeia(15, i)=maxcimg;
stoixeia(16, i)=mincimg;
stoixeia(17,i)=bandcimg;
stoixeia(18, i)=maxcreal;
stoixeia(19, i)=mincreal;
stoixeia(20,i)=bandcreal;
stoixeia(21, i)=maxcur;
stoixeia(22, i)=mincur;
stoixeia(23,i)=bandcur;
stoixeia(24, i)=maxvel;
stoixeia(25, i)=minvel;
stoixeia(26,i)=bandvel;


%second with half
e=jem(i)/2;
simulation;
clear m1 m2 m3
for l=15000:length(t)

   m1(l-14999)=xm1(l, 1);
   m2(l-14999)=z3(1,2,l);
```

```
   m3(l-14999)=xm1(l, 2);
end;


up=max(m1);
low=min(m1);
if i==1
  up=max(m1);
  low=up;
end;
band=abs(up-low);
maxcur=max(m2);
mincur=min(m2);
bandcur=abs(maxcur-mincur);
maxvel=max(m3);
minvel=min(m3);
bandvel=abs(maxvel-minvel);

stoixeia(27, i)=e;
stoixeia(28, i)=up;
stoixeia(29, i)=low;
stoixeia(30, i)=band;
stoixeia(31, i)=maxcur;
stoixeia(32, i)=mincur;
stoixeia(33,i)=bandcur;
stoixeia(34, i)=maxvel;
stoixeia(35, i)=minvel;
stoixeia(36,i)=bandvel;

e=vltglp(i)/2;
simulationLP;
clear m1 m2 m3 m4 m5
for l=15000:length(t)

   m1(l-14999)=xm(l);
   m2(l-14999)=cimg(l);
   m3(l-14999)=creal(l);
   m4(l-14999)=z2(l);
   m5(l-14999)=veloc(l);
end;
up=max(m1);
low=min(m1);
if i==1
  up=max(m1);
  low=up;
```

```
end;
band=abs(up-low);
maxcimg=max(m2);
mincimg=min(m2);
bandcimg=abs(maxcimg-mincimg);
maxcreal=max(m3);
mincreal=min(m3);
bandcreal=abs(maxcreal-mincreal);
maxcur=max(m4);
mincur=min(m4);
bandcur=abs(maxcur-mincur);
maxvel=max(m5);
minvel=min(m5);
bandvel=abs(maxvel-minvel);

stoixeia(37, i)=e;
stoixeia(38, i)=up;
stoixeia(39, i)=low;
stoixeia(40, i)=band;
stoixeia(41, i)=maxcimg;
stoixeia(42, i)=mincimg;
stoixeia(43,i)=bandcimg;
stoixeia(44, i)=maxcreal;
stoixeia(45, i)=mincreal;
stoixeia(46,i)=bandcreal;
stoixeia(47, i)=maxcur;
stoixeia(48, i)=mincur;
stoixeia(49,i)=bandcur;
stoixeia(50, i)=maxvel;
stoixeia(51, i)=minvel;
stoixeia(52,i)=bandvel;

times=i
end;
stoixeiabak=stoixeia;
```

8.1.3 Algorithm for finding max disturbance amplitude (mxd.m)

```
clear stoixeiad
tt=0:1:25;
for i=1:26
e=0;ww=0;
```

```
d=distbr(i);
w=tt(i);
simulation;
clear m1 m2 m3
for l=15000:length(t)

   m1(l-14999)=xm1(l, 1);
   m2(l-14999)=z3(1,2,l);
   m3(l-14999)=xm1(l, 2);
end;


up=max(m1);
low=min(m1);
if i==1
  low=up;
end;
band=abs(up-low);
maxcur=max(m2);
mincur=min(m2);
bandcur=abs(maxcur-mincur);
maxvel=max(m3);
minvel=min(m3);
bandvel=abs(maxvel-minvel);

stoixeiad(1, i)=d;
stoixeiad(2, i)=up;
stoixeiad(3, i)=low;
stoixeiad(4, i)=band;
stoixeiad(5, i)=maxcur;
stoixeiad(6, i)=mincur;
stoixeiad(7,i)=bandcur;
stoixeiad(8, i)=maxvel;
stoixeiad(9, i)=minvel;
stoixeiad(10,i)=bandvel;

d=distbrlp(i);
simulationLP;
clear m1 m2 m3 m4 m5
for l=15000:length(t)

   m1(l-14999)=xm(l);
   m2(l-14999)=cimg(l);
   m3(l-14999)=creal(l);
   m4(l-14999)=z2(l);
```

```
   m5(l-14999)=veloc(l);
Dimitriend;
up=max(m1);
low=min(m1);
if i==1
  up=max(m1);
  low=up;
end;
band=abs(up-low);
maxcimg=max(m2);
mincimg=min(m2);
bandcimg=abs(maxcimg-mincimg);
maxcreal=max(m3);
mincreal=min(m3);
bandcreal=abs(maxcreal-mincreal);
maxcur=max(m4);
mincur=min(m4);
bandcur=abs(maxcur-mincur);
maxvel=max(m5);
minvel=min(m5);
bandvel=abs(maxvel-minvel);

stoixeiad(11, i)=d;
stoixeiad(12, i)=up;
stoixeiad(13, i)=low;
stoixeiad(14, i)=band;
stoixeiad(15, i)=maxcimg;
stoixeiad(16, i)=mincimg;
stoixeiad(17,i)=bandcimg;
stoixeiad(18, i)=maxcreal;
stoixeiad(19, i)=mincreal;
stoixeiad(20,i)=bandcreal;
stoixeiad(21, i)=maxcur;
stoixeiad(22, i)=mincur;
stoixeiad(23,i)=bandcur;
stoixeiad(24, i)=maxvel;
stoixeiad(25, i)=minvel;
stoixeiad(26,i)=bandvel;


%second with half
d=distbr(i)/2;
simulation;
clear m1 m2 m3
for l=15000:length(t)
```

```
   m1(l-14999)=xm1(l, 1);
   m2(l-14999)=z3(1,2,l);
   m3(l-14999)=xm1(l, 2);
end;


up=max(m1);
low=min(m1);
if i==1
  up=max(m1);
  low=up;
end;
band=abs(up-low);
maxcur=max(m2);
mincur=min(m2);
bandcur=abs(maxcur-mincur);
maxvel=max(m3);
minvel=min(m3);
bandvel=abs(maxvel-minvel);

stoixeiad(27, i)=d;
stoixeiad(28, i)=up;
stoixeiad(29, i)=low;
stoixeiad(30, i)=band;
stoixeiad(31, i)=maxcur;
stoixeiad(32, i)=mincur;
stoixeiad(33,i)=bandcur;
stoixeiad(34, i)=maxvel;
stoixeiad(35, i)=minvel;
stoixeiad(36,i)=bandvel;

d=distbrlp(i)/2;
simulationLP;
clear m1 m2 m3 m4 m5
for l=15000:length(t)

   m1(l-14999)=xm(l);
   m2(l-14999)=cimg(l);
   m3(l-14999)=creal(l);
   m4(l-14999)=z2(l);
   m5(l-14999)=veloc(l);
end;
up=max(m1);
low=min(m1);
```

```
if i==1
  up=max(m1);
  low=up;
end;
band=abs(up-low);
maxcimg=max(m2);
mincimg=min(m2);
bandcimg=abs(maxcimg-mincimg);
maxcreal=max(m3);
mincreal=min(m3);
bandcreal=abs(maxcreal-mincreal);
maxcur=max(m4);
mincur=min(m4);
bandcur=abs(maxcur-mincur);
maxvel=max(m5);
minvel=min(m5);
bandvel=abs(maxvel-minvel);

stoixeiad(37, i)=d;
stoixeiad(38, i)=up;
stoixeiad(39, i)=low;
stoixeiad(40, i)=band;
stoixeiad(41, i)=maxcimg;
stoixeiad(42, i)=mincimg;
stoixeiad(43,i)=bandcimg;
stoixeiad(44, i)=maxcreal;
stoixeiad(45, i)=mincreal;
stoixeiad(46,i)=bandcreal;
stoixeiad(47, i)=maxcur;
stoixeiad(48, i)=mincur;
stoixeiad(49,i)=bandcur;
stoixeiad(50, i)=maxvel;
stoixeiad(51, i)=minvel;
stoixeiad(52,i)=bandvel;

times=i
end;
stoixeiabakd=stoixeiad;
```

8.1.4 Algorithm for finding the correlation between signals

```
x = cimg-i0;
y = 20*(xm-0.05);
```

```
mx = mean(x)
my = mean(y)
mxy = mean(x.*y)
sqrt( 1/length(t) * sum((x-mx).^2))
sqrt( 1/length(t) * sum((y-my).^2))
cov(x,y,1)
corrcoef(x,y)
```

8.1.5 Algorithm for finding the FFT of the signals

```
Fs = 1/0.00063;                 % Sampling frequency
T = 1/Fs;% Sample time

for i=1:(length(t)-15873)
ak(i)=sht(15873+i);
end;



y=ak;
%%%%%%%%
%clear y
%y=xm(:,1);

L = length(y);                  % Length of signal
t = (0:L-1)*T;              % Time vector

figure(1)

NFFT = 2^(nextpow2(L)+2); % Next power of 2 from length of y
Y = fft(y,NFFT)/L;
f = Fs/2*linspace(0,1,NFFT/2+1);
figure(1)
% Plot single-sided amplitude spectrum.
plot(f,2*abs(Y(1:NFFT/2+1)))
%axis([0  2  0  3])
title('Single-Sided amplitude spectrum of the displacement signal')
xlabel('Frequency (Hz)')
ylabel('|D(f)|')
axis([0  5  0  0.1])
%curent?

%%%%%%% c img
```

```
clear y
y=cimg;
L = length(y);                  % Length of signal
t = (0:L-1)*T;              % Time vector

figure(2)

NFFT = 2^(nextpow2(L)+2); % Next power of 2 from length of y
Y = fft(y,NFFT)/L;
f = Fs/2*linspace(0,1,NFFT/2+1);
figure(3)
% Plot single-sided amplitude spectrum.
plot(f,2*abs(Y(1:NFFT/2+1)))
axis([0  5  0  1])
title('Single-Sided amplitude spectrum of the imaginary current')
xlabel('Frequency (Hz)')
ylabel('|Iim(f)|')
```

8.2 Simulation Results Tables

Table 8.1 Band pass model - Maximum voltage for frequencies 0-12rad/s

Ω	0	1	2	3	4	5	6	7	8	9	10	11	12
E	140	70,4	70,8	67,4	67,4	59,6	64,2	55,8	43,8	52,8	54,4	49	42,6
Xmax	0,099536	0,077123	0,078031	0,07872	0,083978	0,081885	0,076093	0,074196	0,092963	0,092292	0,09459	0,095223	0,094516
Xlow	0,099536	0,007601	0,005401	0,005385	0,006586	0,005796	0,007599	0,00545	0,006043	0,018429	0,011524	0,008861	0,00836
Xbw	0	0,069522	0,07263	0,073335	0,077392	0,076089	0,068494	0,068747	0,08692	0,073864	0,083066	0,086362	0,086155
Imax	4,446133	3,904566	3,895967	3,954374	4,036577	4,026105	4,09846	4,028503	4,701444	4,163664	4,077794	4,166076	4,273275
Ilow	-4,44605	-3,9045	-3,89602	-3,95417	-4,0359	-4,02598	-4,09765	-4,028	-4,7053	-4,16206	-4,08072	-4,16142	-4,2791
Ibw	8,892179	7,809064	7,791982	7,908541	8,072473	8,052083	8,196115	8,056505	9,406743	8,325728	8,158515	8,327492	8,552372
Umax	0,005658	0,036133	0,087035	0,166204	0,295305	0,308819	0,366826	0,396796	0,655039	0,487419	0,52185	0,563491	0,584223
Ulow	-0,00625	-0,03518	-0,07132	-0,11887	-0,20249	-0,195	-0,29243	-0,31703	-0,3815	-0,3551	-0,41507	-0,4624	-0,49053
Ubw	0,01191	0,071312	0,158351	0,285072	0,49779	0,503815	0,659259	0,713829	1,036538	0,842518	0,936916	1,02589	1,074755

Table 8.2 Low pass model - Maximum voltage for frequencies 0-12rad/s

Ω	0	1	2	3	4	5	6	7	8	9	10	11	12
Elp	98,99495	49,78032	50,06316	47,659	47,659	42,14356	45,39626	39,45656	30,97128	37,33524	38,46661	34,64823	30,12275
Xmax	0,099143	0,07689	0,077764	0,078086	0,083532	0,07959	0,075957	0,071433	0,07962	0,091611	0,09294	0,095341	0,091695
Xlow	0,099143	0,008551	0,006582	0,00702	0,006269	0,008895	0,009222	0,008861	0,010288	0,018473	0,012307	0,008329	0,010217
Xbw	0	0,068339	0,071182	0,071066	0,077262	0,070696	0,066735	0,062572	0,069331	0,073138	0,080633	0,087012	0,081477
Imgmx	-3,08601	-0,37706	-0,30348	-0,39828	-0,42129	-0,67694	-0,57413	-0,76956	-1,21689	-1,11165	-0,97688	-0,92584	-1,21233
Iimglw	-3,08661	-2,67979	-2,66979	-2,67624	-2,73291	-2,63309	-2,77258	-2,66213	-2,77134	-2,48952	-2,39212	-2,40911	-2,34743
Iimgbw	0,000599	2,302729	2,366318	2,277965	2,311623	1,956145	2,198453	1,892565	1,554445	1,37787	1,415242	1,48327	1,135107
Irealmx	0,622789	1,025213	1,123518	1,310456	1,787004	1,657143	1,785368	1,874615	2,541385	2,01478	2,117195	2,566506	2,509726
Ireallw	0,622536	0,696725	0,684155	0,66024	0,581682	0,603443	0,569033	0,584559	0,470132	0,44393	0,437482	0,40077	0,40916
Irealbw	0,000253	0,328488	0,439363	0,650216	1,205321	1,0537	1,216335	1,290056	2,071252	1,57085	1,679713	2,165737	2,100566
Imx	3,148813	2,768989	2,761125	2,774781	2,858734	2,757654	2,88229	2,771403	2,959918	2,98404	2,883109	3,093219	3,02468
Ilow	3,148176	0,959436	0,958307	1,15745	1,05789	1,526926	1,314788	1,804912	1,521989	1,443484	1,748658	1,941832	1,92254
Ibw	0,000638	1,809553	1,802819	1,617332	1,800844	1,230728	1,567502	0,966492	1,437928	1,540556	1,134451	1,151387	1,10214
Umax	0,000211	0,033563	0,081703	0,143225	0,293025	0,250981	0,345236	0,339492	0,489753	0,484221	0,504027	0,584493	0,544902
Ulow	-0,00018	-0,03291	-0,06756	-0,10777	-0,19814	-0,17696	-0,27617	-0,28353	-0,32314	-0,34164	-0,39204	-0,44837	-0,45685
Ubw	0,000389	0,066469	0,149268	0,251	0,491165	0,427938	0,621407	0,623023	0,812888	0,825862	0,896071	1,032866	1,00175

Table 8.3 Band pass model - Maximum voltage for frequencies 13-25rad/s

Ω	13	14	15	16	17	18	19	20	21	22	23	24	25
E	34,8	26	16,8	7,8	6,6	16,6	28,2	40,4	53,4	66,4	79,2	92	101,6
Xmax	0,094145	0,093426	0,092829	0,091602	0,090909	0,092325	0,09207	0,092077	0,092307	0,092372	0,092402	0,092438	0,092194
Xlow	0,009692	0,012389	0,015464	0,019089	0,022448	0,025119	0,028604	0,032043	0,035509	0,038972	0,042385	0,045738	0,048555
Xbw	0,084452	0,081037	0,077366	0,072513	0,068461	0,067206	0,063466	0,060034	0,056798	0,0534	0,050017	0,046699	0,043638
Imax	4,525913	4,908107	5,244201	5,548007	5,798193	6,144079	6,367994	6,544848	6,755487	6,908335	7,020998	7,120945	7,148774
Ilow	-4,53059	-4,91071	-5,24285	-5,54149	-5,80439	-6,14461	-6,36327	-6,54295	-6,76136	-6,90452	-7,02209	-7,1157	-7,13882
Ibw	9,056505	9,818821	10,48705	11,0895	11,60258	12,28869	12,73126	13,0878	13,51685	13,81285	14,04309	14,23665	14,28759
Umax	0,606743	0,620325	0,629099	0,623641	0,621709	0,644319	0,641165	0,637093	0,63323	0,624434	0,612332	0,598437	0,580756
Ulow	-0,51742	-0,53372	-0,54625	-0,54785	-0,5533	-0,57605	-0,57815	-0,57947	-0,57954	-0,57526	-0,56771	-0,55723	-0,5423
Ubw	1,124161	1,154043	1,175345	1,171492	1,175012	1,220371	1,219319	1,216562	1,21277	1,199699	1,18004	1,155667	1,123051

Table 8.4 Low pass model - Maximum voltage for frequencies 13-25rad/s

Ω	13	14	15	16	17	18	19	20	21	22	23	24	25
Elp	24,60732	18,38478	11,87939	5,515433	4,666905	11,73797	19,94041	28,56711	37,7595	46,95189	56,00286	65,05382	71,84205
Xmax	0,09159	0,090309	0,088387	0,085123	0,1	0,096448	0,093752	0,092925	0,092737	0,092595	0,092464	0,092431	0,092115
Xlow	0,011955	0,014657	0,018175	0,022803	0,01811	0,023624	0,028097	0,031823	0,03538	0,038886	0,042301	0,045659	0,048478
Xbw	0,079635	0,075651	0,070212	0,06232	0,08189	0,072824	0,065655	0,061102	0,057356	0,053709	0,050164	0,046772	0,043637
Imgmx	-1,54213	-1,64706	-1,53572	-1,43138	-1,10422	-0,97114	-0,82389	-0,65033	-0,46008	-0,26932	-0,08107	0,107711	0,253606
Iimglw	-2,43477	-2,5581	-2,71364	-2,88227	-3,38848	-3,60093	-3,80955	-4,01962	-4,22056	-4,38744	-4,52452	-4,6421	-4,697
Iimgbw	0,892645	0,911047	1,177925	1,45089	2,284258	2,629793	2,985669	3,369292	3,760484	4,118115	4,443452	4,749815	4,950608
Irealmx	2,706711	2,765903	2,703296	2,469061	3,468843	3,039584	2,75836	2,589369	2,456428	2,330247	2,214298	2,109292	2,015184
Ireallw	0,384104	0,364078	0,346239	0,33437	0,216983	0,198073	0,171084	0,13362	0,090768	0,047112	0,003337	-0,0412	-0,07771
Irealbw	2,322607	2,401825	2,357057	2,134691	3,25186	2,841511	2,587277	2,455749	2,36566	2,283136	2,210961	2,150495	2,092895
Imx	3,251195	3,463192	3,639262	3,711957	4,638787	4,624587	4,654577	4,746156	4,854035	4,942058	5,013719	5,076449	5,088985
Ilow	1,803842	1,688105	1,575181	1,470724	1,126085	0,991783	0,842375	0,665127	0,470538	0,275392	0,082777	0,037954	0,064932
Ibw	1,447353	1,775087	2,064081	2,241234	3,512703	3,632805	3,812202	4,08103	4,383497	4,666666	4,930942	5,038495	5,024053
Umax	0,571466	0,573439	0,562694	0,527275	0,768296	0,699523	0,660808	0,645612	0,636269	0,624535	0,610417	0,595696	0,577299
Ulow	-0,48468	-0,49647	-0,49384	-0,47216	-0,65214	-0,6188	-0,5946	-0,58691	-0,583	-0,576	-0,56668	-0,5555	-0,54003
Ubw	1,056149	1,069914	1,056531	0,999438	1,420436	1,318324	1,255404	1,23252	1,219265	1,200537	1,177098	1,151191	1,117326

Table 8.5 Band pass model – Half max voltage for frequencies 0-12rad/s

Ω	0	1	2	3	4	5	6	7	8	9	10	11	12
E	70	35,2	35,4	33,7	33,7	29,8	32,1	27,9	21,9	26,4	27,2	24,5	21,3
Xmax	0,07692	0,064366	0,064598	0,064179	0,064483	0,063561	0,064276	0,062923	0,061343	0,067712	0,069397	0,06961	0,069989
Xlow	0,07692	0,032941	0,03255	0,033072	0,03239	0,033903	0,032005	0,033007	0,034938	0,034049	0,031182	0,030579	0,030284
Xbw	0	0,031425	0,032048	0,031107	0,032093	0,029658	0,03227	0,029916	0,026405	0,033663	0,038215	0,039031	0,039705
Imax	3,906535	3,567758	3,559293	3,530337	3,517786	3,452454	3,48513	3,422772	3,379628	3,339479	3,329075	3,400012	3,545646
Ilow	-3,90651	-3,56767	-3,5594	-3,53032	-3,51776	-3,45256	-3,48493	-3,42292	-3,37951	-3,33944	-3,32884	-3,40035	-3,54605
Ibw	7,81305	7,135425	7,118694	7,060659	7,035544	6,905012	6,970059	6,845696	6,759133	6,678916	6,65791	6,800367	7,091691
Umax	0,003778	0,017962	0,034109	0,048379	0,063998	0,075641	0,112891	0,119849	0,14414	0,182727	0,209387	0,228641	0,250923
Ulow	-0,00407	-0,01806	-0,03428	-0,04833	-0,06611	-0,07215	-0,10669	-0,1134	-0,10269	-0,14088	-0,18367	-0,20774	-0,23122
Ubw	0,007846	0,03602	0,06839	0,096707	0,130111	0,147787	0,219581	0,233251	0,246832	0,323607	0,393062	0,436385	0,482142

Table 8.6 Low pass model – Half max voltage for frequencies 0-12rad/s

Ω	0	1	2	3	4	5	6	7	8	9	10	11	12
Elp	0,076681	0,064198	0,064421	0,064016	0,064296	0,063363	0,064177	0,062866	0,060849	0,067301	0,068954	0,06908	0,069422
Xmax	0,076681	0,033144	0,032775	0,033301	0,03265	0,034164	0,032282	0,033352	0,035311	0,034151	0,031448	0,030923	0,030736
Xlow	0	0,031055	0,031646	0,030715	0,031647	0,029199	0,031895	0,029514	0,025539	0,03315	0,037506	0,038157	0,038685
Xbw	-2,67911	-1,56252	-1,56374	-1,60486	-1,61756	-1,70294	-1,67335	-1,777	-1,8562	-1,78251	-1,83311	-1,92164	-1,97051
Imgmx	-2,67954	-2,41661	-2,41394	-2,39261	-2,38363	-2,33548	-2,35932	-2,31078	-2,26711	-2,17395	-2,16342	-2,15365	-2,18668
Iimglw	0,000429	0,854089	0,850202	0,787752	0,766073	0,632542	0,685974	0,533782	0,410907	0,391436	0,33031	0,232011	0,21617
Iimgbw	0,699009	0,944223	0,955887	0,966557	0,998429	1,003836	1,054807	1,078721	1,108338	1,12861	1,213811	1,290789	1,365959
Irealmx	0,698767	0,752782	0,748934	0,74649	0,74107	0,734463	0,719468	0,724405	0,725306	0,640504	0,615386	0,59725	0,573293
Ireallw	0,000241	0,191441	0,206953	0,220067	0,257359	0,269372	0,335338	0,354316	0,383032	0,488106	0,598425	0,693539	0,792665
Irealbw	2,769216	2,531167	2,527643	2,506797	2,496292	2,450169	2,472126	2,42515	2,390931	2,366576	2,366913	2,415913	2,517285
Imx	2,76874	1,825043	1,831554	1,871312	1,892889	1,968092	1,961109	2,050248	2,051816	2,040461	2,1324	2,137212	2,066462
Ilow	0,000476	0,706124	0,696089	0,635485	0,603403	0,482078	0,511017	0,374902	0,339115	0,326115	0,234513	0,278701	0,450823
Ibw	0,000102	0,015577	0,031454	0,045573	0,060664	0,07188	0,107954	0,114207	0,132856	0,177363	0,202982	0,220939	0,241355
Umax	-0,00012	-0,01544	-0,03148	-0,0456	-0,06274	-0,06952	-0,10228	-0,10895	-0,09958	-0,13426	-0,17695	-0,2007	-0,22327
Ulow	0,000221	0,031017	0,062932	0,091174	0,123403	0,1414	0,210235	0,22316	0,232439	0,311622	0,379934	0,421643	0,464621
Ubw	0,076681	0,064198	0,064421	0,064016	0,064296	0,063363	0,064177	0,062866	0,060849	0,067301	0,068954	0,06908	0,069422

Table 8.7 Band pass model – Half max voltage for frequencies 13-25rad/s

Ω	13	14	15	16	17	18	19	20	21	22	23	24	25
E	17,4	13	8,4	3,9	3,3	8,3	14,1	20,2	26,7	33,2	39,6	46	50,8
Xmax	0,070262	0,070305	0,070324	0,068279	0,064174	0,068778	0,070155	0,070836	0,071488	0,07186	0,072073	0,072286	0,071815
Xlow	0,030471	0,03105	0,031833	0,03427	0,038001	0,035768	0,036134	0,037089	0,038199	0,039524	0,040922	0,04237	0,043759
Xbw	0,039791	0,039255	0,038491	0,034008	0,026173	0,033011	0,034021	0,033747	0,033289	0,032336	0,03115	0,029916	0,028056
Imax	3,722758	3,908935	4,0913	4,150099	4,041749	4,493736	4,758431	4,960676	5,161187	5,323827	5,46504	5,59333	5,651655
Ilow	-3,72329	-3,90799	-4,08943	-4,15074	-4,04194	-4,49357	-4,75796	-4,96	-5,15798	-5,32258	-5,46331	-5,59372	-5,65259
Ibw	7,44605	7,816922	8,180731	8,300835	8,083691	8,987309	9,516392	9,920671	10,31917	10,64641	10,92835	11,18705	11,30425
Umax	0,270512	0,286602	0,30042	0,282305	0,229868	0,308193	0,335754	0,351262	0,363778	0,370592	0,373761	0,375265	0,366537
Ulow	-0,25173	-0,26763	-0,28159	-0,26664	-0,22003	-0,29148	-0,31678	-0,33119	-0,34337	-0,35008	-0,35363	-0,35531	-0,34822
Ubw	0,522246	0,554234	0,58201	0,548941	0,449896	0,59967	0,652533	0,682455	0,707145	0,720669	0,727392	0,730577	0,714754

Table 8.8 Low pass model – Half max voltage for frequencies 13-25rad/s

Ω	13	14	15	16	17	18	19	20	21	22	23	24	25
Elp	0,069536	0,069438	0,069091	0,066777	0,06503	0,069775	0,070787	0,071288	0,071761	0,072039	0,072205	0,072354	0,071852
Xmax	0,031036	0,031735	0,032752	0,035343	0,037314	0,035128	0,035773	0,036855	0,038058	0,039418	0,040852	0,042302	0,043701
Xlow	0,0385	0,037704	0,036339	0,031434	0,027716	0,034647	0,035014	0,034432	0,033703	0,032621	0,031353	0,030052	0,02815
Xbw	-1,90591	-1,82724	-1,74587	-1,69623	-1,65009	-1,44737	-1,31702	-1,19427	-1,06691	-0,94344	-0,82377	-0,70472	-0,61994
Imgmx	-2,26011	-2,35867	-2,46473	-2,52432	-2,57391	-2,83638	-2,99339	-3,13134	-3,26847	-3,39119	-3,50083	-3,60353	-3,65984
Iimglw	0,354194	0,531434	0,718868	0,828086	0,923827	1,389009	1,676371	1,937064	2,201563	2,447745	2,677057	2,898814	3,039901
Iimgbw	1,431621	1,476812	1,505581	1,43451	1,38789	1,630637	1,694462	1,724605	1,7475	1,75443	1,751455	1,744767	1,718285
Irealmx	0,549605	0,526089	0,504197	0,506152	0,505026	0,411458	0,36776	0,329582	0,290448	0,253312	0,21755	0,181815	0,157118
Ireallw	0,882017	0,950723	1,001383	0,928359	0,882864	1,219179	1,326702	1,395023	1,457052	1,501118	1,533904	1,562952	1,561166
Irealbw	2,640118	2,761106	2,873711	2,894933	2,918148	3,261663	3,429042	3,563958	3,694944	3,806327	3,902181	3,990827	4,029909
Imx	1,988015	1,903589	1,818548	1,771177	1,726588	1,505713	1,368524	1,240258	1,10739	0,978872	0,854486	0,730798	0,643084
Ilow	0,652103	0,857516	1,055163	1,123756	1,191561	1,75595	2,060518	2,323699	2,587555	2,827455	3,047695	3,260028	3,386825
Ibw	0,259329	0,272401	0,280712	0,257863	0,240936	0,321021	0,342971	0,355395	0,365513	0,371022	0,373293	0,373777	0,364904
Umax	-0,24121	-0,25511	-0,26383	-0,24483	-0,23027	-0,30308	-0,32352	-0,33534	-0,34535	-0,35102	-0,35362	-0,35472	-0,34703
Ulow	0,500537	0,527515	0,544538	0,502695	0,471208	0,624101	0,666488	0,69074	0,71086	0,722045	0,726914	0,728496	0,711938
Ubw	0,069536	0,069438	0,069091	0,066777	0,06503	0,069775	0,070787	0,071288	0,071761	0,072039	0,072205	0,072354	0,071852

Table 8.9 Band pass model - Maximum disturbance for frequencies 0-12rad/s

Ω	0	1	2	3	4	5	6	7	8	9	10	11	12
D	1,97	1,95	1,9	1,81	1,64	1,58	1,82	1,52	0,97	1,5	1,72	1,41	1,38
Xmax	0,094495	0,094382	0,094472	0,094325	0,094297	0,094432	0,089437	0,094678	0,094306	0,08637	0,087215	0,086336	0,093173
Xlow	0,094495	0,030087	0,030382	0,030558	0,029967	0,02757	0,015746	0,025647	0,023922	0,007853	0,007613	0,013487	0,012916
Xbw	0	0,064295	0,06409	0,063766	0,06433	0,066862	0,073691	0,06903	0,070385	0,078517	0,079602	0,072848	0,080257
Imax	1,764948	4,602845	4,584726	4,528405	4,631327	4,882216	6,224158	5,118446	5,310414	7,068233	7,170102	6,594652	6,669955
Ilow	-1,76495	-4,60282	-4,5847	-4,52842	-4,63073	-4,88209	-6,22234	-5,11608	-5,31358	-7,06817	-7,16731	-6,58977	-6,66821
Ibw	3,529899	9,205663	9,169428	9,056825	9,262054	9,764302	12,4465	10,23453	10,62399	14,1364	14,33741	13,18442	13,33817
Umax	0,000762	0,04092	0,077028	0,115729	0,161342	0,229617	0,616411	0,367949	0,405574	0,813126	0,79655	0,639427	0,666855
Ulow	-0,00082	-0,04049	-0,08172	-0,1266	-0,19978	-0,24842	-0,49895	-0,36143	-0,45561	-0,63637	-0,60989	-0,5097	-0,5347
Ubw	0,001578	0,08141	0,158745	0,242333	0,361124	0,478041	1,115363	0,729383	0,861188	1,449499	1,406442	1,149127	1,201555

Table 8.10 Low pass model - Maximum disturbance for frequencies 0-12rad/s

Ω	0	1	2	3	4	5	6	7	8	9	10	11	12
Dlp	1,9	1,89	1,83	1,75	1,6	1,54	1,77	1,48	0,97	1,49	1,7	1,32	1,35
Xmax	0,092269	0,092342	0,092171	0,092183	0,092453	0,092292	0,093879	0,092093	0,092164	0,091097	0,09189	0,09115	0,092127
Xlow	0,092269	0,030945	0,031191	0,031391	0,031051	0,02863	0,014437	0,02686	0,025607	0,007653	0,007658	0,012175	0,013857
Xbw	0	0,061397	0,060979	0,060792	0,061402	0,063663	0,079441	0,065233	0,066557	0,083444	0,084232	0,078975	0,07827
Imgmx	-1,24651	-1,24561	-1,24762	-1,24752	-1,24414	-1,2461	-1,22666	-1,24854	-1,24749	-1,26042	-1,25062	-1,26006	-1,24805
Iimglw	-1,24653	-2,74488	-2,7359	-2,72873	-2,74202	-2,82937	-3,27802	-2,89209	-2,93529	-3,49455	-3,48942	-3,36477	-3,2907
Iimgbw	2,47E-05	1,49927	1,488284	1,481208	1,497875	1,583272	2,051356	1,643544	1,687798	2,234135	2,238798	2,104712	2,04265
Irealmx	0,270201	1,774229	1,754521	1,73919	1,768859	1,981537	3,910956	2,162048	2,300037	5,072368	5,076631	4,350958	4,013529
Ireallw	0,27019	0,269776	0,270808	0,270599	0,269007	0,269878	0,260878	0,270973	0,270302	0,275765	0,271432	0,27601	0,270675
Irealbw	1,12E-05	1,504453	1,483713	1,468591	1,499853	1,711659	3,650078	1,891075	2,029734	4,796602	4,805199	4,074949	3,742854
Imx	1,275479	3,26825	3,250007	3,235466	3,261365	3,449453	4,811424	3,597703	3,706273	5,467078	5,471093	5,093346	4,874431
Ilow	1,275453	1,274486	1,276671	1,276539	1,272911	1,275014	1,254164	1,277637	1,276505	1,290362	1,279875	1,290005	1,277109
Ibw	2,65E-05	1,993764	1,973336	1,958928	1,988454	2,174439	3,557259	2,320066	2,429768	4,176716	4,191218	3,803341	3,597322
Umax	1,16E-05	0,037901	0,073215	0,108883	0,151529	0,215642	0,699107	0,345144	0,380578	0,891996	0,87276	0,75869	0,675004
Ulow	-1,5E-05	-0,03723	-0,07626	-0,11869	-0,18384	-0,23503	-0,534	-0,34032	-0,42515	-0,66574	-0,6338	-0,57556	-0,52767
Ubw	2,67E-05	0,07513	0,149473	0,227572	0,335365	0,450669	1,233109	0,685466	0,805726	1,557732	1,506564	1,334247	1,202678

Table 8.11 Band pass model - Maximum disturbance for frequencies 13-25rad/s

Ω	13	14	15	16	17	18	19	20	21	22	23	24	25
D	1,1	0,79	0,5	0,23	0,19	0,46	0,78	1,11	1,46	1,84	2,22	2,63	3,03
Xmax	0,093802	0,093846	0,093244	0,092216	0,091334	0,091826	0,091946	0,092052	0,091894	0,092003	0,092089	0,092188	0,091739
Xlow	0,015032	0,017179	0,018603	0,020028	0,021096	0,021346	0,021667	0,022046	0,022243	0,022442	0,022592	0,02275	0,022915
Xbw	0,078769	0,076667	0,07464	0,072188	0,070238	0,07048	0,070279	0,070006	0,06965	0,069561	0,069496	0,069438	0,068824
Imax	6,355185	6,13964	5,913662	5,774348	5,6418	5,572296	5,57418	5,501039	5,497397	5,457546	5,440398	5,420878	5,401118
Ilow	-6,31925	-6,14205	-5,90972	-5,78056	-5,64957	-5,57406	-5,56993	-5,50379	-5,50379	-5,46786	-5,43827	-5,42977	-5,39405
Ibw	12,67443	12,28169	11,82338	11,55491	11,29137	11,14636	11,14411	11,00483	11,00118	10,92541	10,87867	10,85065	10,79517
Umax	0,635355	0,613214	0,610887	0,611432	0,621357	0,653778	0,68391	0,715285	0,741918	0,776377	0,807451	0,842537	0,870151
Ulow	-0,53081	-0,53337	-0,54736	-0,55998	-0,5777	-0,61289	-0,64603	-0,67705	-0,70893	-0,74326	-0,77731	-0,81118	-0,84039
Ubw	1,166161	1,146585	1,158248	1,171412	1,199061	1,266664	1,329937	1,392332	1,450851	1,519634	1,584765	1,653719	1,710539

Table 8.12 Low pass model - Maximum disturbance for frequencies 13-25rad/s

Ω	13	14	15	16	17	18	19	20	21	22	23	24	25
Dlp	1,08	0,78	0,52	0,26	0,16	0,41	0,74	1,09	1,44	1,79	2,19	2,59	2,99
Xmax	0,09231	0,090266	0,091586	0,092268	0,083392	0,090296	0,092807	0,093406	0,092845	0,092257	0,092685	0,092571	0,092301
Xlow	0,016697	0,019005	0,019874	0,020258	0,025418	0,022359	0,021594	0,021668	0,022128	0,022668	0,02257	0,022894	0,023142
Xbw	0,075613	0,071262	0,071713	0,07201	0,057974	0,067937	0,071213	0,071738	0,070718	0,069588	0,070115	0,069677	0,069159
Imgmx	-1,24574	-1,27125	-1,25452	-1,24599	-1,36475	-1,27048	-1,2391	-1,23181	-1,2385	-1,24546	-1,23998	-1,24126	-1,24469
Iimglw	-3,20763	-3,13816	-3,12619	-3,10697	-2,94529	-3,04664	-3,07413	-3,07458	-3,06205	-3,04617	-3,0518	-3,04286	-3,03625
Iimgbw	1,961896	1,866903	1,871676	1,860971	1,580538	1,776166	1,835033	1,84278	1,823555	1,800715	1,811819	1,801601	1,791559
Irealmx	3,531793	3,167396	3,089193	2,983077	2,325517	2,697366	2,799511	2,790364	2,730744	2,662221	2,675675	2,635929	2,606517
Ireallw	0,269555	0,281198	0,273366	0,269385	0,326352	0,280401	0,265925	0,26259	0,265492	0,268411	0,265689	0,266131	0,267713
Irealbw	3,262238	2,886198	2,815826	2,713692	1,999165	2,416965	2,533586	2,527774	2,465252	2,393809	2,409986	2,369798	2,338804
Imx	4,585794	4,337172	4,283315	4,207569	3,721663	4,000734	4,071978	4,062912	4,017836	3,965673	3,972975	3,941346	3,917124
Ilow	1,274618	1,302055	1,284044	1,274888	1,403386	1,301201	1,26747	1,259647	1,266821	1,274296	1,268411	1,269776	1,273416
Ibw	3,311175	3,035117	2,99927	2,932681	2,318277	2,699533	2,804509	2,803265	2,751015	2,691377	2,704565	2,671571	2,643709
Umax	0,611495	0,570084	0,592059	0,610539	0,50525	0,627233	0,690522	0,727255	0,751612	0,770926	0,81301	0,842601	0,867833
Ulow	-0,50786	-0,49993	-0,51989	-0,55628	-0,47874	-0,58889	-0,64897	-0,68938	-0,7158	-0,73947	-0,7781	-0,80766	-0,83857
Ubw	1,11935	1,07001	1,111945	1,166823	0,983992	1,216125	1,339489	1,416636	1,467413	1,510396	1,591114	1,650262	1,706407

Table 8.13 Band pass model – Half max disturbance for frequencies 0-12rad/s

Ω	0	1	2	3	4	5	6	7	8	9	10	11	12
D	0,985	0,975	0,95	0,905	0,82	0,79	0,91	0,76	0,485	0,75	0,86	0,705	0,69
Xmax	0,068278	0,068172	0,067985	0,067643	0,066643	0,067383	0,068843	0,069474	0,065842	0,064535	0,065853	0,067224	0,070926
Xlow	0,068278	0,038196	0,038391	0,038724	0,039343	0,038903	0,037715	0,039044	0,038576	0,02914	0,028361	0,031475	0,029827
Xbw	0	0,029976	0,029594	0,028918	0,027299	0,02848	0,031128	0,03043	0,027266	0,035395	0,037492	0,03575	0,041099
Imax	2,393145	3,905093	3,900445	3,868845	3,825596	3,848613	3,952332	3,850307	3,886872	4,625332	4,817536	4,500977	4,667104
Ilow	-2,39316	-3,90512	-3,90052	-3,86877	-3,82577	-3,84859	-3,95237	-3,85006	-3,88749	-4,62692	-4,81571	-4,50192	-4,66699
Ibw	4,786306	7,810214	7,800965	7,737613	7,651363	7,697199	7,904707	7,700366	7,774367	9,252255	9,633245	9,002898	9,334097
Umax	0,0014	0,017905	0,032795	0,046378	0,053885	0,076358	0,135086	0,138112	0,130414	0,255511	0,266944	0,229836	0,274789
Ulow	-0,00152	-0,01809	-0,03365	-0,04866	-0,06626	-0,09074	-0,15286	-0,15169	-0,17462	-0,26358	-0,25833	-0,22284	-0,26211
Ubw	0,002919	0,035992	0,066447	0,095035	0,12015	0,167095	0,287949	0,289803	0,305037	0,519088	0,525276	0,452681	0,536901

Table 8.14 Low pass model – Half max disturbance for frequencies 0-12rad/s

Ω	0	1	2	3	4	5	6	7	8	9	10	11	12
Dlp	0,067367	0,067374	0,067058	0,066786	0,066014	0,066629	0,067987	0,068537	0,065493	0,064956	0,065209	0,06577	0,069892
Xmax	0,067367	0,038636	0,038879	0,03916	0,039705	0,039299	0,038147	0,039492	0,039104	0,029056	0,028755	0,032858	0,030653
Xlow	0	0,028738	0,028179	0,027626	0,026309	0,02733	0,02984	0,029045	0,026389	0,0359	0,036454	0,032912	0,039239
Xbw	-1,64269	-1,64256	-1,64903	-1,65462	-1,67069	-1,6578	-1,63003	-1,61891	-1,68147	-1,69288	-1,68776	-1,67574	-1,59225
Imgmx	-1,64279	-2,45821	-2,44915	-2,43932	-2,41912	-2,43401	-2,47688	-2,42741	-2,44204	-2,8169	-2,82728	-2,67638	-2,75892
Iimglw	9,68E-05	0,815647	0,800126	0,784705	0,748426	0,776214	0,846851	0,808499	0,760571	1,124013	1,13952	1,000645	1,166675
Iimgbw	0,487745	1,272444	1,25993	1,24571	1,218782	1,239314	1,300628	1,230873	1,251844	1,948846	1,975838	1,635814	1,809165
Irealmx	0,487681	0,48759	0,491798	0,495442	0,506051	0,497447	0,479376	0,47213	0,512963	0,520579	0,517461	0,509305	0,455239
Ireallw	6,32E-05	0,784854	0,768132	0,750268	0,712731	0,741868	0,821253	0,758743	0,738881	1,428267	1,458377	1,126509	1,353926
Irealbw	1,713666	2,768013	2,754211	2,738993	2,708709	2,731155	2,796873	2,721115	2,74323	3,41655	3,440429	3,133208	3,293072
Imx	1,713555	1,713403	1,720805	1,727211	1,745672	1,730856	1,699079	1,686398	1,758069	1,77124	1,765334	1,751477	1,656117
Ilow	0,000111	1,05461	1,033406	1,011783	0,963037	1,000299	1,097794	1,034717	0,985161	1,645309	1,675095	1,381731	1,636955
Ibw	3,94E-05	0,015049	0,029514	0,042601	0,049428	0,071814	0,127947	0,129653	0,125844	0,260019	0,260906	0,206989	0,25945
Umax	-3,2E-05	-0,01526	-0,03012	-0,04472	-0,06141	-0,08457	-0,14696	-0,14246	-0,1655	-0,26916	-0,25371	-0,20279	-0,24878
Ulow	7,11E-05	0,030309	0,059632	0,087323	0,11084	0,15638	0,274911	0,27211	0,291346	0,529182	0,514614	0,40978	0,508231
Ubw	0,067367	0,067374	0,067058	0,066786	0,066014	0,066629	0,067987	0,068537	0,065493	0,064956	0,065209	0,06577	0,069892

Table 8.15 Band pass model – Half max disturbance for frequencies 13-25rad/s

Ω	13	14	15	16	17	18	19	20	21	22	23	24	25
D	0,55	0,395	0,25	0,115	0,095	0,23	0,39	0,555	0,73	0,92	1,11	1,315	1,515
Xmax	0,071513	0,071092	0,070795	0,068412	0,063715	0,067338	0,068415	0,068661	0,068793	0,069048	0,06903	0,069123	0,069027
Xlow	0,030694	0,031735	0,032423	0,03443	0,038077	0,035523	0,034882	0,034812	0,034809	0,034716	0,034785	0,034763	0,034877
Xbw	0,040819	0,039357	0,038372	0,033982	0,025638	0,031815	0,033533	0,033849	0,033984	0,034331	0,034245	0,03436	0,03415
Imax	4,577512	4,476589	4,410576	4,224731	3,925301	4,131668	4,18886	4,191921	4,198086	4,205785	4,199093	4,199212	4,193476
Ilow	-4,57981	-4,4743	-4,40967	-4,22377	-3,92643	-4,132	-4,19132	-4,18989	-4,19785	-4,20647	-4,20109	-4,20289	-4,19301
Ibw	9,157325	8,950888	8,820242	8,448505	7,851734	8,263666	8,380178	8,381813	8,395939	8,412252	8,400178	8,402102	8,386482
Umax	0,283441	0,287163	0,296432	0,277894	0,222001	0,291166	0,323514	0,342938	0,361344	0,382244	0,398459	0,417196	0,43112
Ulow	-0,27082	-0,27683	-0,28715	-0,27098	-0,21836	-0,28518	-0,31673	-0,33629	-0,35437	-0,37509	-0,39149	-0,40961	-0,42429
Ubw	0,554264	0,563988	0,583581	0,548877	0,440359	0,576349	0,640243	0,679226	0,715713	0,757339	0,789952	0,826808	0,855408

Table 8.16 Low pass model – Half max disturbance for frequencies 13-25rad/s

Ω	13	14	15	16	17	18	19	20	21	22	23	24	25
Dlp	0,070347	0,06996	0,070328	0,06924	0,061879	0,066019	0,068004	0,068781	0,068897	0,068781	0,069005	0,069068	0,068944
Xmax	0,031498	0,032556	0,032731	0,033834	0,039465	0,036456	0,03517	0,034756	0,034768	0,034906	0,034819	0,034859	0,034954
Xlow	0,038849	0,037404	0,037598	0,035406	0,022414	0,029563	0,032833	0,034025	0,034129	0,033875	0,034186	0,034209	0,033991
Xbw	-1,58338	-1,59072	-1,58355	-1,60455	-1,76129	-1,66983	-1,62881	-1,61317	-1,61075	-1,61292	-1,60835	-1,60698	-1,60927
Imgmx	-2,72862	-2,68839	-2,68208	-2,64055	-2,42949	-2,54169	-2,59065	-2,60669	-2,60654	-2,60161	-2,60524	-2,60405	-2,60076
Iimglw	1,145235	1,097663	1,098525	1,036	0,668198	0,871859	0,961836	0,993528	0,995791	0,98869	0,996883	0,997067	0,991494
Iimgbw	1,741133	1,66048	1,648533	1,570256	1,235852	1,402521	1,483772	1,512161	1,512598	1,5047	1,511837	1,510581	1,505626
Irealmx	0,449622	0,454065	0,449505	0,462497	0,568192	0,50458	0,477574	0,46744	0,465766	0,466993	0,463951	0,462922	0,464196
Ireallw	1,29151	1,206415	1,199029	1,107759	0,66766	0,897942	1,006197	1,044721	1,046832	1,037707	1,047887	1,047659	1,04143
Irealbw	3,230608	3,15503	3,143076	3,067662	2,724182	2,899753	2,980863	3,008092	3,007693	2,99909	3,005179	3,003017	2,997239
Imx	1,646082	1,654389	1,646266	1,670057	1,850885	1,744647	1,697655	1,679832	1,677076	1,679532	1,674346	1,672772	1,675358
Ilow	1,584525	1,500641	1,49681	1,397605	0,873297	1,155106	1,283208	1,32826	1,330617	1,319558	1,330833	1,330246	1,321881
Ibw	0,266614	0,269936	0,287992	0,287148	0,191713	0,268011	0,314189	0,342506	0,360552	0,374712	0,395293	0,412557	0,426994
Umax	-0,25658	-0,26121	-0,27882	-0,27966	-0,18908	-0,26306	-0,30815	-0,33569	-0,35371	-0,36789	-0,38838	-0,40569	-0,41998
Ulow	0,523191	0,531149	0,566812	0,566806	0,380793	0,531069	0,622341	0,678196	0,714262	0,742599	0,783673	0,818248	0,846977
Ubw	0,070347	0,06996	0,070328	0,06924	0,061879	0,066019	0,068004	0,068781	0,068897	0,068781	0,069005	0,069068	0,068944

9. BIBLIOGRAPHY

[1] Nikolaos I. Xiros, Ioannis T. Georgiou, Analysis of coupled electromechanical oscillators by a band-pass, reduced complexity Volterra method, IMECE2005-81487

[2] Nikolaos I. Xiros, Ioannis T. Georgiou, A combined method for the investigation of coupled bandpass-lowpass nonlinear oscillators based on Hilbert transform and perturbation analysis, IMECE2006-13903

[3] Lecture notes in Mathematical Methods in Ocean Engineering 2, by Dr. Nikolaos I. Xiros

[4] T. Ogunfunmi, Adaptive Nonlinear System Identification, The Volterra and Wiener Model Approaches.

[5] Emmanuel C. Ifeachor, Barrie W. Jervis, Digital Signal Processing a Practical Approach, Second Edition

[6] Schetzen M. The Volterra and Wiener Theories of Nonlinear Systems, John Wiley & Sons, 1980, USA

[7] Katsuhiko Ogata, Modern Control Engineering

[8] Haykin, S., Veen, B.V., Signals And Systems, Wiley, 1999

[9] Proakis JG, Manolakis DG, Digital Signal Processing; Principles, Algorithms and Applications (3rd ed.) Prentice-Hall, 1996, USA.

[10] Haluk Kulah and Khalil Najafi, An electromagnetic micro power generator for low

frequency environmental vibrations.

[11] Massimo Panella, Giuseppe Martinelli - RC distributed circuits for vibration damping in piezo-electromechanical beams.

[12] Mechatronics systems, sensors and actuators: Fundamentals and Modeling, Second Edition, by Robert. H. Bishop, CRC Press

[13] Landa PS. Nonlinear Oscillations and Waves in Dynamical Systems. Kluwer, 1996, The Netherlands.

[14] Doyle FJ, Pearson RK and Ogunnaike BA. Identification and Control Using Volterra Models,. Springer-Verlag (Communications and Control Engineering Series), 2001, UK.

[15] Pacheco RP and Steffen V (Jr.). On the identification of non-linear mechanical systems using orthogonal functions. International Journal of Non-Linear Mechanics, 2004; 39:1147-1159

[16] Lucia DK, Beran PS and Silva WA. Reduced-order modeling: new approaches for computational physics. Progress in Aerospace Sciences, 2004; 40:51-117

[17] Rugh WJ. Nonlinear System Theory; The Volterra/Wiener Approach, The John Hopkings University Press, 1981, USA

[18] Advanced Engineering Mathematics - Michael D. Greenberg, 2nd Ed, Prentice Hall-Inc, 1998

[19] Andrzej M. Pawlak, Sensors and Actuators in mechatronics: Design and applications, CRC Press, 2007

[20] John R. Brauer, Magnetic sensors and actuators, John Wiley and Sons, 2006

[21] Harry L.Trietley, Transducers in mechanical and electronic design, CRC Press, 1986

[22] Richard M. Crowder, Electric drives and electromechanical systems, Elsevier, 2006

[23] Shanmugam, KS. Digital and analog communication systems, John Wiley and Sons, 1979

[24] Osita D. I. Nwokah, Yildirim Hurmuzlu, The mechanical systems design handbook, Modelling, measurement, and control, CRC Press, 2002

[25] I. Boldea, S. A. Nasar, Linear electric actuators and generators, Cambridge University Press, 1997